Atomic Energy Control Board
P.O. Box 1046
Ottawa, Canada
K1P 5S9

Commission de contrôle de l'énergie atomique
C.P. 1046
Ottawa, Canada
K1P 5S9

INFO-0156

CANDU FUEL BEHAVIOUR DURING LARGE BREAK LOSS-OF-COOLANT POWER TRANSIENTS

by

V.J. Langman
IDEA Research

A research report prepared for the
Atomic Energy Control Board
Ottawa, Canada

March, 1985

Canada

Research report

CANDU FUEL BEHAVIOUR DURING LARGE BREAK LOSS-OF-COOLANT POWER TRANSIENTS

ABSTRACT

An assessment of the thermal/mechanical behaviour of CANDU fuel during large break loss-of-coolant overpower transients is summarized. The assessment includes a review of the world in-reactor test data on fuel behaviour in power transients, an ELESIM-II (MOD9)/ELOCA MK2 computer analysis of CANDU fuel behaviour as a function of overpower severity and heat removal conditions and a brief discussion of some of the mechanisms that may influence CANDU fuel behaviour during overpower transients. Recommendations are provided for limits on the increase of axial peak, radial average fuel enthalpy to prevent sheath failure, loss of fuel geometry and loss of pressure tube integrity.

RÉSUMÉ

Le présent rapport évalue brièvement le comportement thermomécanique du combustible CANDU lors de transitoires de surpuissance en cas de perte de fluide caloporteur due à une large brèche. Il contient une revue de résultats d'essais internationaux à l'intérieur d'un réacteur sur le comportement du combustible lors de transitoires de surpuissance. Il contient également une analyse du comportement du combustible CANDU en fonction du niveau de surpuissance et des conditions de transfert de chaleur, à l'aide des codes ELESIM-II (MOD9) et ELOCA(MK2), et une brève discussion sur quelques mécanismes qui pourraient déterminer le comportement du combustible CANDU en cas de surpuissance. Le rapport fait des recommandations sur les limites d'augmentation du pic axial, sur l'enthalpie radiale moyenne pour préserver l'intégrité de la gaine, sur les pertes d'intégrité géometrique du combustible et sur les pertes d'intégrité des tubes de force.

DISCLAIMER

The Atomic Energy Control Board is not responsible for the accuracy of the statements made or opinions expressed in this publication and neither the Board nor the author assumes liability with respect to any damage or loss incurred as a result of the use made of the information contained in the publication.

CANDU FUEL BEHAVIOUR DURING LARGE BREAK LOSS-OF-COOLANT POWER TRANSIENTS

EXECUTIVE SUMMARY

During the first few seconds of a large break loss-of-coolant accident (LOCA) the fuel in a CANDU reactor will experience a power excursion, prior to the effective action of the reactor shutdown systems, due to the positive reactivity coefficient associated with the voiding of the primary heat transport system (PHTS). Fuel response to a power transient will depend on the magnitude and duration of the power excursion and the rate of blowdown heat removal from the fuel (i.e. the net energy deposition in the fuel) and the initial fuel conditions.

This report addresses CANDU fuel behaviour during large break LOCA power transients. Estimates are made of the fuel conditions which lead to sheath failure, loss of fuel geometry and loss of pressure tube integrity.

The majority of experimental data available on fuel behaviour during rapid power transients is for Light Water Reactor (LWR) fuel under Reactivity Initiated Accident (RIA) and Operational Transient (OPTRAN) conditions. The LWR test fuel design and RIA and OPTRAN power transient conditions vary significantly from the CANDU fuel design and LOCA power transients. The detailed technical assessment of the world test data concludes that it is impossible to directly apply LWR RIA and OPTRAN fuel behaviour test data to the behaviour of CANDU fuel during a large break LOCA power transient.

The computer codes ELESIM-II(MOD9) and ELOCA MK2 are used to evaluate CANDU 37 element design fuel behaviour for selected combinations of fuel overpower transients and heat removal conditions. The adiabatic heat addition associated with these overpower transients varies from 110 to 946 J/g of UO_2 for initial element linear powers of 30 and 55 kW/m respectively. The LOCA heat removal conditions are characterised by sheath-to-coolant heat transfer coefficients of 50.0, 5.0, 1.5, 0.5 and 0.1 $kW/m^2 °C$ coincident with channel depressurisation.

CANDU FUEL BEHAVIOUR DURING LARGE BREAK LOSS-OF-COOLANT POWER TRANSIENTS

EXECUTIVE SUMMARY

The results of the computer analysis indicate that early sheath failure (i.e. in the first 10 seconds of a LOCA) is not probable for power transients typical of CANDU large break LOCA's (i.e. overpower factors of approximately two) for the range of heat removal conditions studied. For transients with overpower factors much higher (i.e. factors of five or more) than expected for CANDU large break LOCA's two general types of sheath failure are possible. Low ductility sheath failures could occur due to pellet-clad interaction (PCI) if the sheath remains well cooled during the first few seconds of the LOCA. If the sheath starts to heatup during the first few seconds of the LOCA low ductility, PCI-type failures are not probable because increased sheath temperature helps to anneal the sheath and remove the initial internal stress. For degraded heat removal conditions sheath failure due to localised strain or embrittlement is possible.

The ELOCA MK2 computer code does not take into account the following mechanisms which may affect fuel behaviour during a large break LOCA power transient: i) the potential for the Zircaloy/uranium dioxide interaction on the inner sheath surface; ii) the potential for hydrogen generated from the exothermic Zircaloy-steam reaction to be absorbed into the zirconium dioxide layer or the underlying Zircaloy; iii) the potential for the zirconium dioxide layer and the oxygen absorbed in the underlying Zircaloy to affect sheath deformation; and iv) the potential for transient gas release and consequent fuel swelling. The potential effects of these mechanisms, along with fuel melting and relocation, and fuel/coolant interaction, on CANDU fuel behaviour during large break LOCA overpower transients are briefly discussed.

The prediction of the thermal/mechanical behaviour of CANDU fuel during the first 10 seconds of a large break LOCA is extremely complex. Computer models are not available at present which could take into account all the important fuel behaviour mechanisms for a wide range of overpower and heat removal transients. In the absence of more complete, mechanistic treatments of CANDU fuel behaviour during large break LOCA overpower transients recommendations are made for limits on the increase in axial peak, radial average fuel enthalpy for the onset of PCI-related sheath failures, sheath failure due to localised sheath melting, loss of fuel geometry and loss of pressure tube integrity. These limits are 150, 250 to 400, 600 to 800, and 800 to 1000 J/g of UO_2 respectively. The low value in each enthalpy increase range can be applied to initial element linear powers greater than or equal to 50 kW/m. The high value is for linear powers less than or equal to 30 kW/m.

CANDU FUEL BEHAVIOUR DURING
LARGE BREAK LOSS-OF-COOLANT POWER TRANSIENTS

TABLE OF CONTENTS

ABSTRACT.....i

EXECUTIVE SUMMARY.....ii

A. INTRODUCTION.....1

B. FUEL CONDITIONS.....4

1. CANDU LOCA Power Transients.....4
2. LWR RIA Power Transients.....5
3. LWR OPTRAN Power Transients.....6

C. REVIEW OF EXPERIMENTAL DATA.....7

1. RIA Related.....8

1.1 PBF Tests.....8

1.1.1 Pellet-Clad Mechanical Interaction.....9
1.1.2 Sheath Plastic Deformation and Melting.....9
1.1.3 Fuel Swelling and Thermal Failure.....10
1.1.4 Sheath Oxidation and Embrittlement.....10
1.1.5 Molten Fuel-Coolant Interaction.....11
1.1.6 PBF Test Recommendations.....11

1.2 NSRR Tests.....11

1.2.1 Failure Mechanisms for Standard NSRR Elements.12
1.2.2 Effect of Fuel Element Design Variations.....12
1.2.3 Effect of Coolant Environment Variations.....13
1.2.4 Effect of Waterlogged Fuel.....13
1.2.5 NSRR Recommendations.....13

1.3 SPERT and TREAT Tests.....14

2. OPTRAN Tests.....15

3. CANDU LOCA Test in the PBF.....16

D. EVALUATION OF CANDU FUEL BEHAVIOUR.....17

1. Initial Conditions.....17
2. LOCA Boundary Conditions.....18
3. ELOCA MK2 Results.....18

E. FUEL BEHAVIOUR MECHANISMS.....21

1. Sheath Oxidation and Embrittlement.....21
2. The Zr/UO_2 Interaction.....23
3. Transient Gas Release and Fuel Swelling.....24
4. Fuel Melting and Relocation.....25
5. Fuel/Coolant Interaction.....26

F. RECOMMENDATIONS.....27

1. Sheath Failure.....27
2. Loss of Fuel Geometry.....28
3. Loss of Fuel Channel Integrity.....28

G. REFERENCES.....29

TABLES

FIGURES

APPENDIX I : ELOCA MK2 Fuel Behaviour Predictions

CANDU FUEL BEHAVIOUR DURING LARGE BREAK LOSS-OF-COOLANT POWER TRANSIENTS

A. INTRODUCTION

During the first few seconds of a large break LOCA the fuel in a CANDU reactor will experience a power excursion, prior to the effective action of the reactor shutdown systems, due to the positive reactivity coefficient associated with the voiding of the PHTS. Fuel response to a power transient will depend on the magnitude and duration of the power excursion and the rate of blowdown heat removal from the fuel (i.e. the net energy deposition in the fuel) and the initial fuel conditions. The fuel response to a power excursion could be:

1. negligible fuel/sheath overheating with no sheath failure;

2. central fuel heatup with negligible sheath overheating which could cause non-ductile sheath failure:

3. moderate fuel/sheath overheating with consequent sheath failure but no loss of fuel geometry and no additional fission product release beyond the pre-transient free inventory;

4. severe fuel/sheath overheating with consequent sheath failure, loss of fuel geometry and/or additional fission product release beyond the pre-transient free inventory but no resultant pressure pulse in the fuel channel and no pressure tube overheating due to thermal/mechanical interaction between the fuel and the pressure tube; or

5. very severe fuel/sheath overheating with consequent sheath failure, loss of fuel geometry, additional fission product release beyond the pre-transient free inventory, a pressure pulse in the fuel channel and/or pressure tube overheating due to thermal/mechanical interaction between the fuel and the pressure tube and/or the occurence of an energetic fuel/coolant interaction.

Any version of the latter scenario could result in pressure tube and/or fuel channel (i.e. pressure tube and calandria tube) failure.

Assessments of CANDU fuel behaviour during large break LOCA power transients and reviews of the experimental information available on fuel behaviour during rapid power excursions have been presented (1,2,3). In these assessments the primary focus has been the effect of fuel behaviour during rapid power excursions on the integrity of the pressure tubes. However, since the issue of these reports new information has become available.

A. INTRODUCTION (Continued)

In the Special Power Excursion Reactor Test (SPERT) and Transient Reactor Test (TREAT) experiments reviewed in references 1,2 and 3 the total energy deposition into the fuel was considerably greater than the resultant peak axial, radial average fuel enthalpy (i.e. stored energy). The difference was due to non-negligible heat transfer from the fuel to the coolant during the power transient and because of the relatively large fraction (i.e. 10 to 25 per cent) of the total energy deposition which was due to delayed fissions and therefore had little influence on fuel element behaviour during the power pulse because it was deposited late in the transient (i.e. most of the delayed fission energy is deposited after the fuel elements have rewet). The assessment of fuel behaviour in references 1,2, and 3 was related to total energy deposition rather than maximum fuel enthalpy.

Data on the behaviour, during RIA conditions, of previously irradiated single elements and fuel clusters over a relatively wide range of coolant conditions has been generated from the experimental programs in the Power Burst Facility (PBF) and the Nuclear Safety Research Reactor (NSRR).

Data on fuel behaviour during OPTRAN's, where the fuel power is expected to increase at much slower rates and to much lower values than in RIA's, has been generated from a test series in the PBF.

The CANDU LOCA fuel behaviour test in the PBF has been completed where pre-irradiated CANDU fuel elements of the 37 element design were subjected to simultaneous power pulse and LOCA blowdown conditions.

The objective of the work discussed in this report is to assess CANDU fuel behaviour during large break LOCA power transients. Criteria for CANDU fuel are provided which define the fuel/fuel channel behaviour limits of sheath failure, loss of fuel geometry, and loss of pressure tube integrity.

The expected fuel conditions during CANDU LOCA power transients, LWR RIA power transients and LWR OPTRAN power transients are discussed in Section B of this report.

A. INTRODUCTION (Continued)

A critical review of the available experimental information on fuel behaviour during rapid power excursions was performed and is presented in Section C of this report. However, most of the available information is for light water reactor (LWR) fuel behaviour during RIA's. It is impossible to directly apply LWR RIA and OPTRAN fuel behaviour data to the prediction of CANDU fuel behaviour during large break LOCA power excursions because of the many differences between LWR and CANDU fuel designs and between RIA's, OPTRAN's and LOCA power excursions.

The results of an evaluation of CANDU fuel behaviour during LOCA power transients are presented in Section D of this report. The computer codes ELESIM-II(MOD9)(4) and ELOCA MK2(5) were used to predict CANDU fuel behaviour for a range of power transients and heat removal scenarios. The results of these predictions helped in the estimate of the fuel and thermohydraulic conditions which would lead to sheath failure, loss of fuel geometry and loss of channel integrity in a LOCA power transient.

Mechanisms which are not modelled in ELOCA MK2 but which could affect CANDU fuel behaviour during LOCA power transients are identified and discussed in Section E of this report. These mechanisms include the effect of oxidation and potential hydrogen absorption on sheath deformation, the high temperature interaction between Zircaloy and uranium dioxide (Zr/UO_2), transient gas release and fuel swelling, the relocation of molten fuel and the potential for energetic fuel/coolant interaction (FCI).

Finally, in Section F recommendations of the fuel and thermohydraulic conditions in large break LOCA power transients which could result in sheath failure, loss of bundle geometry and pressure tube failure are provided for CANDU fuel. These recommendations are based on the author's assessment of the information discussed in Sections C, D and E of this report.

B. FUEL CONDITIONS

1. CANDU LOCA Power Transients

At the beginning of a CANDU LOCA power transient the fuel is operating at full power under nucleate boiling heat removal conditions. The temperature distribution across the diameter of a fuel element is approximately parabolic with the maximum fuel temperature at the centre of the element. Typical centre, average and surface fuel temperatures as predicted by ELESIM-II(MOD9) are given as a function of element linear power for the 37 and 28 element fuel designs in Tables 1 and 2 respectively. For the same linear power, the fuel temperatures and enthalpies for the 28 element fuel design are lower than those for the 37 element design because there is more fuel weight per unit length for the 28 element design.

During the first seconds of a large break LOCA transient the system pressure decreases, heat transfer from the fuel to the coolant starts to degrade and the neutronic power increases. In a typical, large break LOCA the element power can increase by a factor of two or three in less than two seconds. After two or three seconds the element power decreases rapidly due to the effective action of the shutdown system. Some heat transfer from the fuel to the coolant will occur during the power transient because its time duration is on the order of seconds. Examples of large break LOCA power transients are shown in Figure 1. The magnitude of overpower transient 'A' is more typical of CANDU large break LOCA's than transient 'C'.

The transient behaviour of the temperature distribution across the diameter of a fuel element is dependent on the timing and extent of heat removal from the fuel element for a given neutronic power transient. If the rate of heat removal remains high then the central fuel temperature will increase more than the surface fuel temperature. If the rate of heat removal from the fuel decreases rapidly then the surface fuel temperature will increase more than the central fuel temperature. In either case, however, the maximum fuel temperature occurs at the centre of the fuel element. Thus, if fuel melting occurs it will occur at the centre of the fuel element. An example of the transient behaviour of the fuel temperature distribution across the diameter of an element is shown in Figure 2 for the case where heat transfer from the fuel to the coolant degrades very rapidly in the LOCA.

Under normal operating conditions the fuel sheath of a CANDU element is collapsed onto the fuel stack. During a LOCA the sheath may lift off the fuel if the element internal pressure exceeds the coolant pressure while the sheath temperature is elevated and sheath strength is consequently reduced. During the first few seconds of a LOCA sheath liftoff can only occur for the higher powered, high burnup elements which have a substantial internal gas pressure (i.e. approximately 5 MPa or greater). Later in a LOCA when the system pressure is low, lower powered elements may also experience sheath liftoff.

B. FUEL CONDITIONS (Continued)

2. LWR RIA Power Transients

All the RIA tests in the PBF were conducted with coolant conditions representative of hot-startup conditions for a Boiling Water Reactor (BWR). At the beginning of a RIA power transient from hot-startup conditions the fuel element power is approximately zero. The fuel and coolant temperatures are equal at approximately 540 K. The system pressure increases from 6.5 MPa to approximately 8.4 MPa during an RIA transient. As shown in Figure 1, RIA power transients have extremely large magnitudes and extremely short durations. The maximum element linear power attained in the RIA power transient shown in Figure 1 is a factor of 400 greater than that for LOCA power transient 'A'. However, the time duration of a RIA power transient is less than 50 milliseconds which is much less than that of LOCA power transients.

An RIA can be divided into two time periods during which different mechanisms dominate fuel behaviour. During the first time period the fuel element is thermally isolated from the coolant and fuel heatup due to the neutronic power transient is the dominant mechanism that controls fuel behaviour. In the second period the temperature of the fuel sheath determines fuel behaviour.

In the initial period of a RIA the fuel heats up, thermally expands and consequently closes the initial gap between the fuel and the sheath. The initial gap size is on the order of 60 to 70 microns. The fuel temperature distribution across the pellet diameter peaks near the fuel surface because of the self-shielding effect of the enriched fuel. This self-shielding results in a larger power density in the outer regions of the fuel pellet which causes higher fuel temperatures near the fuel surface. As shown in Figure 3 the peak temperature occurs away from the fuel surface because some heat is transferred from the pellet surface to the sheath/coolant during the transient.

The closure of the fuel/sheath gap results in very large sheath stresses which can cause sheath failure due to high strain rate brittle fracture or tearing, or local plastic deformation. The sheath remains cold (i.e. approximately 600 K) during this period and if sheath failures occur they are characterised by angular fractures. The sheath strain rate and temperature determine if the sheath fails or plastically deforms without failure.

The fuel continues to heatup and may melt depending on the energy of the power transient. Since the peak fuel temperature occurs just inside the fuel surface, fuel melting may result in rapid sheath failure by melting.

B. FUEL CONDITIONS (Continued)

Film boiling on the outer surface of the sheath begins at approximately the same time as the peak fuel enthalpy occurs. The onset of film boiling at approximately 25 milliseconds into the RIA terminates the period when fuel heatup dominates fuel behaviour. The sheath temperature becomes the dominant factor for fuel behaviour during the second period of the RIA. High sheath temperatures can result in oxidation, thickening and thinning and sheath melting. Peak sheath temperatures are attained 1 to 3 seconds after the time of maximum fuel power.

The RIA transient is over when the sheath rewets. Rewet times are in the range of 3 to 25 seconds for the PBF RIA tests.

3. LWR OPTRAN Power Transients

The OPTRAN test series in the PBF was performed to investigate BWR fuel behaviour during the most severe anticipated operational transients with and without shutdown. In BWR's many operational transients involve a loss of heat sink with a consequent rise in system pressure, collapse of steam bubbles in the two-phase coolant and a consequent rapid increase in fuel element power. The power transients in the PBF OPTRAN tests are shown in Figure 4. These power transients are more characteristic of CANDU LOCA power transients than RIA power transients. In the most severe PBF OPTRAN tests the fuel element power was increased by as much as an order of magnitude over a period of 1 to 2 seconds.

At the beginning of an OPTRAN the fuel is at full power with rapid two-phase heat removal. Thus, as at the beginning of a CANDU LOCA, the temperature distribution across the diameter of the fuel element is parabolic. During an OPTRAN the rate of heat removal may or may not degrade for a brief period of time depending on the magnitude and duration of the power transient. Thus, the rate of heat removal during a BWR OPTRAN may be greater than during the initial seconds of a CANDU LOCA. The initial fuel-sheath gap may or may not close depending on the magnitude and duration of the overpower transient.

C. REVIEW OF EXPERIMENTAL DATA

The majority of experimental data available on fuel behaviour during rapid power transients is for LWR fuel under RIA conditions. The LWR test fuel design and RIA power transient conditions vary considerably from CANDU fuel and LOCA power transients.

For example, the LWR test fuel design used in the RIA tests and the CANDU fuel design have the following differences which may affect fuel behaviour in rapid power excursions:

1. the U-235 enrichments of the LWR test fuels are in the range 5 to 20 per cent whereas CANDU fuel is 0.7 per cent;

2. the LWR test fuel is smaller in diameter than CANDU fuel;

3. the LWR test fuel has a thicker fuel sheath than CANDU fuel;

4. the CANDU fuel sheath has bearing pads and/or spacers and associated heat-treated zones whereas the LWR test fuel does not;

5. the orientation of the LWR test fuel is vertical whereas CANDU fuel is horizontal;

6. the elements of a CANDU fuel bundle have a complex radial flux distribution which is the result of the flux depression in the fuel bundle being superimposed on the flux depression associated with the element itself whereas the LWR test fuel generally has simple single element flux distributions;

7. the fuel sheath of the LWR test fuel is free-standing under normal operating conditions which results in there being a gap between the fuel and the sheath whereas the CANDU fuel sheath collapses under normal operating conditions resulting in there being no fuel/sheath gap; and

8. the void volume of the LWR test fuel is much larger than in CANDU fuel.

Also RIA power transients are different from those in CANDU LOCA's in the following respects, which may effect fuel behaviour in rapid power excursions:

1. the initial fuel power in the RIA tests is zero whereas CANDU fuel is at full power at the beginning of a LOCA;

2. the initial fuel temperature distribution is relatively flat in the RIA tests whereas it is parabolic in CANDU fuel at power;

3. the initial volume averaged fuel temperature is much lower in the RIA tests than for CANDU fuel at power;

C. REVIEW OF EXPERIMENTAL DATA (Continued)

4. the rate of power rise in the RIA tests is more rapid than for CANDU LOCA power pulses; and

5. the duration of the power excursion in the RIA tests is shorter than for CANDU LOCA power pulses.

A critical review of the pertinent experimental and analytical work on fuel behaviour during rapid power excursions has been completed and the results are discussed in the following subsections. It is concluded that the results of the LWR RIA and OPTRAN tests cannot be directly applied to the behaviour of CANDU fuel during large break LOCA power transients.

1. RIA Related

1.1 PBF Tests

Seven in-reactor RIA tests have been completed in the PBF at Idaho Nuclear Engineering Laboratories (INEL). The results of these tests are summarised in references 6 through 9 inclusive. Note that the information presented in references 7 and 8 is very similar. Detailed discussions of the fuel behaviour of the various tests are presented in references 6 and 10 through 15 inclusive. References 13 through 15 inclusive all discuss RIA-ST-4 which was the PBF RIA test with the highest energy deposition and consequently the most severe fuel behaviour. It is believed that an energetic FCI occurred during RIA-ST-4.

A summary of the PBF RIA test results is given in Table 3. All tests were performed on fuel with enrichments greater than 5 wt% U-235 in total U. At such a high enrichment self-shielding will cause the maximum energy deposition to occur near the fuel surface. The maximum burnup of the elements tested was approximately 130 MWh/kgU. At the beginning of a RIA test the coolant temperature, pressure and flow per element were approximately 540 K, 6.5 MPa and 0.085 l/s respectively for the single element tests. The flow per element was increased to approximately 0.14 l/s for the 9 element cluster test RIA 1-4. The fuel enthalpies given in Table 3 are mainly due to the RIA power transient as the fuel is initially at zero power. In all tests approximately 25% of the total energy deposited by the RIA power transients is removed by the surrounding coolant.

The fuel behaviour results of the PBF RIA tests are summarised in Table 4. In only one case (i.e. RIA 1-2, fuel element 802-3) did a radial average, peak fuel enthalpy of less than 200 cal/g of UO_2 result in sheath failure. From the results of the RIA tests in the PBF the principal fuel failure mechanisms have been identified and are discussed in order of occurrence in a RIA in the following subsections.

C. REVIEW OF EXPERIMENTAL DATA (Continued)

1.1.1 Pellet-Clad Mechanical Interaction (PCI)

Under normal operating conditions there is a 60-70 micron gap between the fuel and sheath in the PWR fuel design. Very early in a RIA power transient the fuel thermally expands and comes into contact with the sheath. At this time in the transient film boiling has not occurred and therefore the sheath is still relatively cool. Sheath failure can occur due to fracturing or tearing of the alpha-phase Zircaloy sheath due to high strain rate deformation caused by PCI.

PCI resulted in sheath failure for fuel element 802-3 of RIA 1-2 and all but the centre element of the 3 x 3 cluster in RIA 1-4. In RIA 1-2, 802-3 was the only fuel element that was not opened prior to the test. Therefore, 802-3 still had its original fission product inventory at an internal pressure of approximately 0.1 MPa. The three elements opened prior to the RIA test did not fail. Element 802-3 failed due to 22 small, longitudinal cracks which are thought to have occurred very early in the transient when the radial average, peak fuel enthalpy was approximately 140 cal/g.

In test RIA 1-4 all nine fuel elements were left intact prior to testing. The oxide layer thickness on the crack surfaces of the eight peripheral elements which experienced sheath failure was very similar to that on the outer surface of the sheath. The similarity in thicknesses indicates that the sheaths failed at low temperature before the onset of film boiling. An example of a PCI sheath failure from test RIA 1-4 is shown in Figure 5.

1.1.2 Sheath Plastic Deformation and Melting

Sheath wall thickness variations and melting occurred on all the elements of RIA 1-1 and all the peripheral elements of RIA 1-4. Sheath wall thickness variations are thought to be produced by plastic deformation due to the stresses imposed on the sheath by the rapid expansion of the fuel and by coolant pressure pulses. Sheaths are particularly susceptible to plastic deformation at high temperatures early in a RIA transient prior to significant oxidation. An example of sheath wall thickness variations from RIA 1-1 is shown in Figure 6. Sheath wall thickness variations resulted in enhanced embrittlement and sheath fracture in the thinner regions as shown in Figure 6.

Extensive fuel/sheath intermixing occurred when molten and solid UO_2 contacted the sheath as shown in Figures 7 and 8 for test RIA 1-1. Fuel/sheath intermixing modes included UO_2 dissolution by molten Zircaloy and the reduction of UO_2 by Zircaloy to form a low melting point Zr/U eutectic. The Zircaloy sheath will melt at temperatures between 2100 K (the beta phase Zircaloy melting temperature) and 2973 K (the melting temperature of zirconium dioxide).

C. REVIEW OF EXPERIMENTAL DATA (Continued)

Sheath melting due to fuel/sheath contact also occurred and in conjunction with Zr/UO_2 interaction produced localised fuel relocation. Molten UO_2 generally solidified on contact with the sheath. An example of sheath melting due to fuel/sheath contact is shown in Figure 9. The globule of UO_2 and Zircaloy shown in Figure 9 is thought to be from material that slumped down from a higher axial location.

1.1.3 Fuel Swelling and Thermal Failure

Fission product induced swelling of molten or nearly molten fuel resulted in sheath failure and complete blockage of the coolant flow shrouds for elements 801-1 and 801-2 in test RIA 1-1. The prior molten fuel in the blockage region was highly porous. This high fuel porosity was attributed to the release, coalescence and expansion of gaseous and volatile fission products during the RIA transient. Similar regions of highly porous fuel were also observed in the peripheral elements of test RIA 1-4. However, overall fuel swelling in test RIA 1-4 was much less than in test RIA 1-1. It is thought that fuel swelling only becomes significant at fuel enthalpies greater than 280 cal/g of UO_2 and/or under conditions of more degraded heat removal. In test RIA 1-4 the radial average, peak fuel enthalpy was near 280 cal/g of UO_2, however, the coolant flow per element was almost twice that of the single element tests. Also the fuel in test RIA 1-4 rewet in approximately 6 to 9 seconds from the start of the transient which is shorter than the 9 to 15 second rewet times for test RIA 1-1.

1.1.4 Sheath Oxidation and Embrittlement

Fuel elements experience a period of film boiling after the power transient in a RIA. Consequent high sheath temperatures can result in sheath oxidation and embrittlement. The sheath can become heavily oxidised from the Zr/UO_2 interaction on the inside surface and the Zircaloy-steam reaction on the outside surface. In some tests the oxidation process consumed all of the beta phase material in regions of sheath thinning, leaving only brittle oxygen stabilised alpha Zircaloy and zirconium dioxide.

The single element RIA tests in the PBF experienced longer periods of film boiling than the 9 element cluster test RIA 1-4. Thus, the fuel elements of RIA 1-4 experienced localised oxidation and embrittlement and remained relatively intact after rewet. The thermal stresses induced by rewet resulted in extensive fuel element fracturing and fragmentation in many of the single element tests which experienced longer times in film boiling. In test RIA 1-1 the unirradiated and irradiated elements experienced 35% and 65% fragmentation respectively due to a radial average, peak fuel enthalpy of 285 cal/g of UO_2.

C. REVIEW OF EXPERIMENTAL DATA (Continued)

1.1.5 Molten Fuel-Coolant Interaction (FCI)

In test RIA ST-4 a single unirradiated, 20% enriched UO_2 fuel element in a Zircaloy flow shroud was subjected to a total energy deposition of 695 cal/g of UO_2 (13, 14, 15). The radially-averaged, peak fuel enthalpy at the time of fuel element failure was 350 cal/g of UO_2. An extensive amount of molten debris was produced (i.e. 386 g which is greater than 50% of the total element UO_2 and Zircaloy). This debris was expelled into the coolant and against the shroud wall. A frozen layer 0.7 mm thick of previously molten UO_2 and Zircaloy formed on the Zircaloy shroud tube which was initially water cooled on the outside surface. Film boiling occurred on the outside surface of the flow shroud, however, due to the initial low temperature of the flow shroud it did not melt. Fine fragmentation of the molten debris released on element failure caused an energetic fuel-coolant interaction which resulted in a coolant pressure of 35 MPa and a coolant temperature in excess of 940 K.

1.1.6 PBF Test Recommendations

The results of the single element tests in the PBF indicate that radial average, peak fuel enthalpies less than 230 cal/g of UO_2 will not cause severe element damage and loss of fuel geometry. However, from the results of cluster test RIA 1-4, where fuel cooling was enhanced, a value of 265 cal/g of UO_2 is indicated. Loss of fuel element geometry occurs at fuel enthalpies of 285 cal/g of UO_2 or more. Extensive fuel fragmentation and melting occurs for radially-averaged, peak fuel enthalpies in excess of 300-350 cal/g of UO_2.

1.2 NSRR Tests

Over 560 RIA tests have been performed on unirradiated fuel elements in the NSRR reactor. The results of these tests are documented in references 16 through 21 inclusive. The NSRR standard fuel element design specifications are given in Table 5 along with the fuel design parameter variations that were studied in the NSRR RIA tests. Note the fuel enrichment is quite high at 10% and will result in significant self-shielding. In the majority of tests the fuel elements were in stagnant water at room temperature and atmospheric pressure. However, tests have been performed under high pressure (i.e. up to 16 MPa), high temperature (i.e. up to 305°C) conditions in stagnant water. Also low pressure (i.e. 1.1 MPa), low temperature (i.e. 100 - 150 °C) tests have been performed with forced circulation with flow velocities in the range 3 to 6 m/s. The NSRR test results are discussed briefly in the following subsections.

C. REVIEW OF EXPERIMENTAL DATA (Continued)

1.2.1 Failure Mechanisms for Standard NSRR Elements

Unirradiated, Pressurised Water Reactor (PWR) standard design (refer to Table 5) fuel elements were subjected to energy depositions ranging from 40 to 540 cal/g of UO_2 under conditions of atmospheric pressure and ambient temperature in stagnant water. In these tests two fuel failure mechanisms were observed depending on the fuel enthalpy level attained. These were sheath melting or brittle failure and molten UO_2 failure. The post-test appearance of the fuel elements as a function of energy deposition is shown in Figure 10. The radial average, peak fuel enthalpies will be lower than the energy deposition values because some of the energy deposited is transferred to the surrounding coolant during the transient.

At radial average, peak fuel enthalpies greater than 200 cal/g of UO_2 the surface of the fuel approaches the melting temperature. Pellet thermal expansion results in fuel/sheath contact which can result in sheath melting, thinning and/or oxidation on the inner surface. Film boiling results in sheath oxidation on the outer surface. Sheath failure can occur due to PCI cracks, localised melting and/or embrittlement on rewet. This fuel behaviour is consistent with the results of the PBF tests.

At radial average, peak fuel enthalpies greater than 300 cal/g of UO_2 (i.e. total energy depositions greater than 380 cal/g of UO_2) there can be gross fuel melting and/or partial vaporisation of the UO_2 with a consequent rapid increase in the internal element pressure. Fuel fragmentation, fuel expulsion into the coolant and molten FCI can result in the generation of pressure pulses in the coolant.

1.2.2 Effect of Fuel Element Design Variations

Among the fuel design variations examined (refer to Table 5) the initial internal element pressure had the most effect on the fuel failure mechanism. For energy depositions as low as 160 cal/g of UO_2, an initial internal pressure of 3.0 MPa resulted in high temperature sheath deformation and burst-type failure. It should be noted, however, that the external coolant pressure in these tests was atmospheric. The post-test appearance of the pre-pressurised elements is shown in Figure 11 as a function of total energy deposition.

Fuel enrichment was also observed to affect the failure threshold as shown in Figure 12. Increased enrichment results in more self-shielding which causes higher power peaking at the surface of the fuel. Therefore, for the same energy deposition transient, the surface fuel temperature increases more as enrichment increases.

C. REVIEW OF EXPERIMENTAL DATA (Continued)

A reduction in sheath thickness from 620 to 400 microns resulted in a reduction in the energy deposition to cause fuel failure from 260 to approximately 220 cal/g of UO_2.

The effects of the various fuel design variations on the fuel failure threshold in a RIA are summarised in Figure 13.

1.2.3 Effect of Coolant Environment Variations

At atmospheric pressure an increase in subcooling or flow velocity was observed to result in enhanced film boiling heat transfer, lower maximum sheath temperatures, reduced times in film boiling and therefore an increased fuel failure threshold in terms of total energy deposition. At high coolant pressures the beneficial effect of subcooling on sheath temperature was not evident as it was at atmospheric pressure.

It is apparent that higher pressure and coolant flow can enhance heat removal from the fuel and therefore reduce the radial average, peak fuel enthalpy reached for a given total energy deposition.

1.2.4 Effect of Waterlogged Fuel

Waterlogged fuel elements failed due to low temperature sheath deformation and burst at energy deposition levels of 100 to 130 cal/g of UO_2. The sheath ruptures were large openings and fuel was expelled into the coolant. Water vaporisation resulted in peak fuel element internal pressures in excess of 100 MPa prior to sheath failure. On sheath failure large (i.e. up to 10 MPa), sharp pressure pulses occurred in the coolant. Interaction between solid fuel fragments and the coolant resulted in secondary pressure pulses in the coolant up to 6 MPa in magnitude. An example of the pressure pulses generated by the failure of a waterlogged fuel element is given in Figure 14. The magnitude of the first pressure pulse as a function of water content in the fuel-sheath gap and the total energy deposition is shown in Figure 15.

1.2.5 NSRR Recommendations

The Japanese Atomic Energy Commission have established as licensing guidelines that: i) in a high frequency RIA the radially-averaged peak fuel enthalpy should not exceed 170 cal/g of UO_2 in order to avoid failure by sheath melting; and ii) for a low frequency, worst-case RIA the radially-averaged, peak fuel enthalpy should not exceed 230 cal/g of UO_2 in order to avoid damage to the pressure vessel.

The NSRR results are thought to show that these guidelines are conservative with respect to observed fuel behaviour in RIA transients in the NSRR.

C. REVIEW OF EXPERIMENTAL DATA (Continued)

1.3 SPERT and TREAT Tests

Many RIA tests have been performed on single elements and small clusters of fuel elements in the SPERT and TREAT test programs. All of these tests were performed under stagnant coolant conditions of atmospheric pressure and ambient temperature (i.e. 300 K), with zero initial element power. Typical fuel behaviour results from these tests are given in Figure 16 as a function of total energy deposition and radially-averaged, peak fuel enthalpy in cal/g of UO_2. The results of the SPERT and TREAT tests are summarised in reference 7 and discussed in detail in reference 21. The fuel failure mechanisms and thresholds observed in the SPERT and TREAT tests are consistent with the NSRR test results.

For tests on previously unirradiated SPXM fuel (i.e. Zircaloy-2 clad, 356 micron wall thickness, 0.559 cm UO_2 pellet diameter, 10.5 wt% enrichment) in SPERT the following fuel behaviour was observed. The consequences of unirradiated element failure were insignificant for radially-averaged, peak fuel enthalpies less than 240 cal/g of UO_2. Fuel elements fragmented at enthalpies greater than 240 cal/g of UO_2, however, coolant pressure pulses were small with nuclear-to-mechanical energy conversions less than 1% of the total energy deposited. Prompt fuel dispersion was observed at enthalpies greater than 275 cal/ g of UO_2. For radially-averaged, peak fuel enthalpies in excess of 400 cal/g of UO_2 the consequences were more severe. Coolant pressure pulses up to 12 MPa were observed with nuclear-to-mechanical energy conversions of nearly 3%.

In tests with previously irradiated fuel elements, failures occurred at lower enthalpy values than for fresh fuel tests. The failure threshold for previously irradiated elements seemed to be relatively independent of burnup as shown in Figure 17.

C. REVIEW OF EXPERIMENTAL DATA (Continued)

2. OPTRAN Tests

The test program to investigate fuel behaviour during operational transients in the PBF was in the final planning stages at the time of the accident in TMI-2. Since the TMI-2 accident the emphasis of the test program in the PBF has switched to severe core damage fuel behaviour. As a result only two OPTRAN tests were performed (22).

Four overpower transients of increasing severity were performed with four previously irradiated BWR fuel elements in test OPTRAN 1-1. After the first overpower transient two of the fuel elements were removed for post-test examination and replaced with two other previously irradiated fuel elements. In the OPTRAN 1-2 test two previously irradiated fuel elements were subjected to one overpower transient. The overpower transients for OPTRAN tests 1-1 and 1-2 are shown in Figure 4. The burnups of the test elements were in the range of 120 - 550 MWh/kgU as given in Table 6.

There were no fuel element failures in OPTRAN tests 1-1 and 1-2. In OPTRAN test 1-1 the fuel elements did not experience film boiling. The transient release of fission gas was less than 0.5%. The maximum hoop strains remained below the elastic/plastic limit and there was no evidence of incipient PCI defects (i.e. small cracks in the inner sheath surface).

In OPTRAN 1-2 the fuel elements experienced film boiling which resulted in localised, peak sheath temperatures of approximately 1200 K. In the localised regions of sheath overheating there was no evidence of sheath deformation or oxygen embrittlement. Maximum hoop strains were again below the elastic/plastic limit. However, transient fission gas release, at approximately 2%, was greater than in OPTRAN 1-1. One incipient crack, which was 20% of the sheath thickness, was observed and is the only evidence of PCI induced sheath damage. This crack did not occur in a region of film boiling.

C. REVIEW OF EXPERIMENTAL DATA (Continued)

3. CANDU LOCA Test in the PBF (23)

Four (three previously irradiated, one unirradiated) CANDU fuel elements of the 37 element design have been tested in the PBF under LOCA conditions (i.e. simultaneous blowdown and power pulse). At least one of these elements failed. This test represents the only in-reactor information on the behaviour of CANDU fuel during a rapid, albeit modest in the case of the PBF test, power excursion.

The initial conditions of the fuel elements tested are given in Table 7. The overpower, depressurisation and coolant flow transients for the test are shown in Figures 18, 19 and 20 respectively. The adiabatic increase in fuel enthalpy during the first two seconds of the transient is less than 30 cal/g of UO_2. The depressurisation is similar to that expected in a large break LOCA in a CANDU reactor. The coolant flow during the test was effectively zero.

Measured sheath temperatures remained in the 1000 to 1200K range for a time period of approximately 100 seconds. The fuel centre temperature increased slightly due to the power transient as shown in Figure 21. At approximately 20 - 40 seconds into the transient the internal element pressures exceeded the system pressure and the driving force for sheath diametral expansion was available. The axially localised, maximum average diametral sheath strain observed was approximately 20%.

Sheath failure occurred later in the transient and the failure mechanism was not associated with the power transient.

D. EVALUATION OF CANDU FUEL BEHAVIOUR

Calculations of CANDU fuel thermal/mechanical behaviour during rapid power excursions were performed using the ELOCA MKII computer code. A case by case review of the results of these calculations is given in Appendix I.

These calculations were performed for the CANDU 37 element fuel design to study the effect on fuel behaviour of the following parameters: i) characteristics of the power excursion; ii) heat removal from the fuel; and iii) power/burnup history of the fuel. The following aspects of fuel behaviour are of interest: i) fuel/sheath temperature transients; ii) the radial distribution of fuel temperature transients; iii) the fuel/sheath interfacial pressure and heat transfer co-efficient transients; iv) fuel thermal expansion; v) the extent of fuel melting; vi) sheath strain; and vii) sheath oxidation. An overview of the results of these ELOCA MK2 calculations is presented in the following sections.

1. Initial Conditions

The ELESIM-II(MOD9) computer code was used to predict initial fuel conditions for the CANDU 37 and 28 element fuel designs for element linear powers of 55, 50 and 30 kW/m. The element linear powers were assumed to remain constant to an average fuel burnup of 170 MWh/kgU. The fuel conditions at 170 MWh/kgU are given for element linear powers of 55, 50 and 30 kW/m for the CANDU 37 and 28 element designs in Tables 1 and 2 respectively. For equal element linear powers, the fuel temperatures for the 37 element fuel design are slightly higher than those for the 28 element fuel design. As a result, internal gas pressures are also higher for the 37 element design than for the 28 element design for a given element linear power. The reason for these differences is that there is more fuel weight per unit length in the 28 element design than in the 37 element design.

The initial fuel enthalpies given in Tables 1 and 2 were taken from Figure 22. Figure 22 was derived using the UO_2 specific heat capacity temperature dependence from MATPRO-11 (24) shown in Figure 23. ELOCA MK2 calculations are only performed for the 37 element fuel design. The predicted fuel behaviour of the 37 element design will bound the fuel behaviour of the 28 element design for the same LOCA boundary conditions and initial element linear power because: i) for a given element linear power the initial fuel temperatures and enthalpies are greater for the 37 element design; and ii) for a given normalised power transient the adiabatic heat addition is greater for the 37 element design.

D. EVALUATION OF CANDU FUEL BEHAVIOUR (Continued)

2. LOCA Boundary Conditions

The power transients used in the ELOCA MK2 fuel behaviour calculations are summarised in Table 8 and shown on semi-log and linear scales in Figures 24 and 25 respectively. The adiabatic heat addition as a function of initial element linear power is given in Table 9 for power transients 'A' through 'E' for the 37-element fuel design.

Power transient 'A' is typical of those predicted for large break LOCA's in CANDU reactors. Power transients 'B' through 'E' are not typical for CANDU large break LOCA's but are used in the ELOCA MK2 calculations to investigate fuel behaviour as a function of power transient severity.

The coolant boundary conditions which characterise the heat removal transients used in the ELOCA MK2 fuel behaviour calculations are given in Tables 10 through 14 inclusive. The coolant boundary conditions range from rapid heat removal (i.e. transient '1'), to moderate heat removal (i.e. transients '2' and '5') to degraded heat removal (i.e. transients '3' and '4') during the first 10 seconds of a large break LOCA.

ELOCA MK2 calculations are only performed for the first 10 seconds of the large break LOCA transients because that is when the power transients have some influence on fuel behaviour. With effective shutdown, after 10 seconds the predicted fuel behaviour is not controlled by the power transient but by the coolant boundary conditions.

3. ELOCA MK2 Results

ELOCA MK2 calculations were performed for the 37 element fuel design, for the combinations of initial element linear power, power transient and heat removal transient listed in Table 15. In all cases the initial fuel conditions were those at a burnup of 170 MWh/kgU as given in Table 1. The cases are summarised in a matrix format in Table 16. Power transient severity increases from 'A' to 'E' while heat removal decreases from transient '1' to '4'.

The maximum central, average and surface fuel temperatures as predicted by ELOCA MK2 in the first 10 seconds of the LOCA transients are given in Tables 17, 18 and 19 for initial element linear powers of 55, 50 and 30 kW/m respectively. The times at which the maximums occur are also given in Tables 17, 18 and 19. The maximum central fuel temperature is controlled by the severity of the power transient. The nature of the heat removal transient has little or no affect on the maximum central fuel temperature because the thermal time constant of the fuel (i.e. approximately 10 seconds) is relatively long compared to the duration of the power transients.

D. EVALUATION OF CANDU FUEL BEHAVIOUR (Continued)

The maximum average and surface fuel temperatures are more affected by the nature of the heat removal transients. The maximum average and surface fuel temperatures increase as the rate of heat removal from fuel degrades. This effect is more pronounced for the surface than the average fuel temperature. The maximum fuel temperatures decrease as the initial element linear power decreases. Fuel melting is predicted to occur at the centre of the fuel element only in cases 125 and 128.

The fuel enthalpies corresponding to the maximum central, average and surface fuel temperatures are given in Tables 20, 21 and 22 for initial element linear powers of 55, 50 and 30 kW/m respectively. All fuel enthalpies as a function of temperature are taken from Figure 22. The increments in fuel enthalpy corresponding to the increases in maximum central, average and surface fuel temperatures are given in Tables 23, 24 and 25 for initial element linear powers of 55, 50 and 30 kW/m respectively. The maximum average fuel enthalpy was 1060 J/g of UO_2 or 253 cal/g of UO_2 for case 128. The maximum increase in average fuel enthalpy was 690 J/g of UO_2 or 165 cal/g of UO_2 for case 128.

The amount of heat removed from the fuel as a function of power transient and coolant boundary conditions is given in Tables 26, 27 and 28 for initial element linear powers of 55, 50 and 30 kW/m respectively. During the first 10 seconds of the LOCA transients studied the heat removed from the fuel ranged from 14 to 65 per cent of the potential adiabatic heat addition (refer to Table 9).

Some of the ELOCA MK2 fuel behaviour predictions are summarised in Table 29 for the cases studied. Maximum sheath temperatures increased as the heat removal during the transient decreased. During the first 10 seconds of a large break LOCA transient the heat liberated due to the exothermic Zircaloy-steam reaction mainly affects the rate of sheath and fuel surface temperature heatup.

The ELOCA MK2 computer code does not take into account the following mechanisms which may affect fuel behaviour during a large break LOCA: i) the potential for the Zr/UO_2 interaction on the inner sheath surface; ii) the potential for hydrogen generated from the exothermic Zircaloy-steam reaction to be absorbed into the zirconium dioxide (ZrO_2) layer or the underlying Zircaloy; iii) the potential for the ZrO_2 layer and the oxygen absorbed in the underlying Zircaloy to affect sheath deformation; and iv) the potential for transient gas release and consequent fuel swelling.

D. EVALUATION OF CANDU FUEL BEHAVIOUR (Continued)

Judgements have been made, and are summarised in Table 30, as to whether on not these mechanisms could affect the ELOCA MK2 fuel behaviour predictions of the cases studied. The judgements summarised in Table 30 are based on the following 'guidelines': i) at sheath temperatures below the Zircaloy melting point the Zr/UO_2 interaction can only occur if there is a 0.5 to 1.0 MPa interfacial pressure between the fuel and the sheath; ii) above the Zircaloy melting point negligible interfacial pressure is required for the Zr/UO_2 interaction to occur; iii) hydrogen will only be absorbed if the oxidation reaction is proceeding very rapidly under low flow conditions; iv) oxidation could affect sheath deformation if the oxide layer is greater than 20 microns in thickness and the total sheath strain is greater than approximately 1 to 2 per cent; and v) transient gas release fractions of <10%, 10-50% and >50% can occur for peak fuel temperatures in the ranges of 2200-2500K, 2500-2700K and >2700K respectively.

An assessment of whether or not sheath failure could occur during the first 10 seconds of a large break LOCA transient for the cases studied is summarised in Table 31. Sheath failure is not probable for power transient 'A' under the conditions of degraded cooling that were studied (i.e. heat removal transients '5', '3' and '4'). Also, power transient 'A' is not severe enough to cause low ductility sheath failures due to PCI.

For higher powered elements, low ductility, PCI-type sheath failures could occur for power transients 'B', 'D', 'C' and 'E' if the sheath remains well cooled during the first few seconds of the LOCA transient. If the sheath starts to heatup during the first few seconds of the transient low ductility, PCI-type failures are not probable. For power transients 'B', 'D' and 'C' sheath failure due to localised strain or embrittlement is possible for higher powered elements if the heat removal conditions are severely enough degraded (i.e. transient '4'). For power transient 'E' sheath failure due to localised strain or embrittlement is possible even with a less severe degradation in heat removal (i.e. transient '5').

Selected mechanisms of interest to CANDU fuel behaviour during large break LOCA power transients which are not modelled in ELOCA MK2 are briefly discussed in Section E of this report.

E. FUEL BEHAVIOUR MECHANISMS

1. Sheath Oxidation and Embrittlement

The effect of oxidation on sheath deformation behaviour in a steam environment is illustrated in Figure 26 (25). At elevated temperatures the sheath surface reacts with a steam environment to form a layer of ZrO_2, hydrogen and heat. At temperatures greater than 900 to 1000°C an oxygen stabilised alpha zirconium layer forms beneath the ZrO_2 layer. Zircaloy sheath strength can increase due to solution hardening by the oxygen that diffuses into the sheath to form the ZrO_2 and oxygen stabilised alpha-Zr layers.

At elevated temperatures if the sheath experiences sufficient tensile stress due to the internal gas pressure exceeding the surrounding coolant pressure then the sheath will begin to creep. The ZrO_2 layer develops microscopic cracks at an overall sheath strain of approximately 2 per cent. Initially the oxide cracks may not penetrate the oxygen stabilised alpha-Zr layer. The oxide cracks provide relatively free paths for oxygen to react with the exposed metal at the crack tips to form a fresh uncracked oxide layer. This fresh layer eventually cracks and the sequence is repeated. The process is referred to as stress-assisted local oxygen penetration (25). If the crack penetration rate is greater than the radial velocity of the alpha/beta interface the crack will eventually penetrate the oxygen stabilised alpha-Zr layer to the base metal. Necking of the beta-phase base metal may eventually lead to sheath failure. Maximum circumferential sheath strain at burst is shown in Figure 27 as a function of burst temperature and sheath heatup rate for a range of internal pressures in a steam environment. For sheath heatup rates of 25 and 100 K/s burst strains are greater than 10% for burst temperatures less than approximately 1500K to 1600K. For sheath heatup rates of 5K/s burst strains can be less than 10 per cent. Sheath strain data for sheath temperatures greater than 1600K could only be obtained for lower internal gas pressures (i.e. 0.34 MPa). At this low internal gas pressure burst did not occur and sheath strains remained below 10 per cent for all heatup rates due to the oxygen strengthening of the sheath.

Of the ELOCA MK2 cases discussed in Section D, oxidation may affect the prediction of the timing and magnitude of sheath deformation for cases 105, 106, 110, 111, 112, 113, 118, 119, 122, 123, 128, 129, 130 (refer to Table 30). In cases 105, 106, 110, and 111 the total sheath strain at 10 seconds is less than 2 per cent and is probably too low to cause cracks in the oxide layer. For these cases oxidation strengthening may reduce the amount of strain predicted by ELOCA MK2. Sheath failure is not expected.

E. FUEL BEHAVIOUR MECHANISMS (Continued)

In cases 112, 113, 118, 119, 122, 123, and 129 sheath temperatures are near melting and sheath strains are in the 2 to 3 per cent range. For these cases oxide cracks may form which would promote sheath failure which is already possible due to localised melting. In cases 128 and 130 the sheath temperature is greater than 1500K but less than sheath melting. In case 128 the ELOCA MK2 sheath strain prediction exceeds 4 per cent for a maximum sheath temperature of 1744K. Oxidation strengthening may reduce the magnitude of the predicted strain in case 128. The formation of oxide cracks will enhance the possibility of sheath failure for case 128. In case 130 oxidation strengthening may reduce the ELOCA MK2 predicted sheath strain. However, the overall strain is too low for oxide cracks to result in sheath failure for case 130.

Chung at Argonne National Laboratory has observed a reduction in the Zircaloy oxidation rate at elevated temperatures in hydrogen-steam mixtures at relatively low flow velocities (26). Chung's experiments indicate that the reduction in oxidation rate is not due solely to a gas phase diffusion limitation at low flow velocities but is also due to the presence of significant amounts of hydrogen in the oxide layer. At low flow velocities the Japanese have also observed hydrogen present in significant quantities in the Zircaloy base metal. The presence of hydrogen in the oxide layer may affect the conditions under which oxide cracks will form. The presence of hydrogen in the Zircaloy base metal will reduce sheath ductility (27).

In ELOCA MK2 cases where the sheath temperature is predicted to reach near melting the oxidation rate may be rapid enough to generate a high hydrogen fraction environment near the sheath surface for low flow conditions. For these cases (i.e. cases 112, 113, 118, 119, 122, 123, and 129) hydrogen absorption into the oxide or base metal layers is a possibility.

The absorption of oxygen and/or hydrogen into the sheath reduces sheath ductility and can result in embrittlement failures due to the thermal stresses induced by rewet. The Zr/UO_2 reaction that can occur on the sheath inner surface is potentially a major contributor to sheath embrittlement. The $ZrUO_2$ reaction is discussed in the next section.

E. FUEL BEHAVIOUR MECHANISMS (Continued)

2. The Zr/UO_2 Interaction

A detailed summary of the work on the chemical reaction between Zircaloy-4 fuel sheaths and UO_2 fuel pellets is provided in reference 28. The extent to which the Zr/UO_2 reaction occurs depends mainly on whether good contact exists between the Zircaloy sheath and the UO_2 fuel pellets for sheath temperatures below melting. If the interfacial pressure between the sheath and the fuel is greater than approximately 1.0 MPa then the Zr/UO_2 reaction will occur. The Zircaloy reduces the UO_2 to form oxygen-stabilised alpha zirconium and uranium metal. A (U,Zr) alloy rich in uranium is formed when the uranium reacts with low oxygen content Zircaloy. The (U,Zr) alloy is found between two oxygen-stabilised alpha zirconium layers. The (U,Zr) alloy has a melting point of approximately 1150°C. The positions and metallurgical appearances of the reaction layers are shown in Figure 28.

The Zr/UO_2 reaction on the inner sheath surface occurs as rapidly as the Zircaloy-steam reaction on the outer surface of the sheath for sheath temperatures in excess of 1100°C. Therefore, single-sided throughwall oxidation times and 'embrittlement times' can be reduced by a factor of four. For temperatures of approximately 1400°C the rate of the Zr/UO_2 reaction is independent of interfacial pressure for pressures greater than 1.0 MPa. For temperatures of approximately 1700°C the rate of the Zr/UO_2 reaction is independent of interfacial pressure for pressures greater than 0.5 MPa. Above the sheath melting temperature of 1760°C only fuel/sheath contact is required for a Zr/UO_2 interaction to occur. The rate of formation of the reaction layers as a function of temperature is shown in Figure 29.

The Zr/UO_2 reaction may occur in ELOCA MK2 cases 106, 111, 117, 124 and 130 because the sheath temperature exceeds 1100°C when the fuel/sheath interfacial pressure is greater than 1.0 MPa. The Zr/UO_2 reaction will probably not occur for temperatures less than sheath melting if the sheath lifts off the fuel prior to sheath temperatures exceeding 1100°C because of the low fuel/sheath interfacial pressure. After sheath liftoff the fuel will only be in very light contact (i.e. fuel pellet weight only) with the sheath along the bottom of the fuel stack. Molten Zircaloy may locally dissolve some UO_2 in cases 112, 113, 118, 119, 122, 123 and 129 even though sheath liftoff has occurred in most cases.

E. FUEL BEHAVIOUR MECHANISMS (Continued)

3. Transient Gas Release and Fuel Swelling

An increase in fuel temperature during an overpower transient can lead to the additional release of fission products from the fuel to the free inventory. An increase in fuel temperature can also result in an increase in fuel volume (i.e. fuel swelling) due to solid and/or gaseous fission products.

A detailed analysis of transient gas release and fuel swelling for CANDU fuel during large break LOCA power transients is beyond the scope of this work. There is no Canadian-derived computer model presently available to predict transient gas release and fuel swelling in transients for CANDU fuel. Preliminary results from the FASTGRASS-VFP computer code on transient fission product release from CANDU fuel at elevated temperatures have been obtained and are applied to large break LOCA power transients.

FASTGRASS-VFP (29-33) is a mechanistic computer model for predicting the behaviour of fission gas and volatile fission products (VFPs) in UO_2 fuel during steady state and transient conditions. FASTGRASS-VFP accounts for processes which determine the distribution of fission products within the fuel during normal operating conditions and the timing and extent of transient fission product release. These processes include fission product generation; gas bubble nucleation and re-solution; bubble migration and coalescence; the chemical reaction between Iodine, Cesium and fuel; channel formation on grain faces; interlinked porosity on grain edges; fuel microcracking; and grain boundary sweeping of gas bubbles due to transient grain growth. Fission products released from the fuel reach the fuel pellet surface by successively migrating from the grain interiors to grain faces and then to grain edges. Once fission products reach the grain edge tunnels they are transported through a network of interconnected tunnels and as-fabricated porosity to the fuel surface. FASTGRASS-VFP also predicts the extent of fuel swelling associated with transient fission product behaviour.

During a large break LOCA power transient the factors which will affect the timing and extent of transient fission product release from CANDU fuel include re-solution during the overpower transient; the temperature gradient across the fuel radius; the peak fuel temperature attained; and the rate of fuel heatup. Transient release fractions from FASTGRASS-VFP are shown in Figure 30 as a function of fuel temperature for a case where the fuel is irradiated to a burnup of 170 MWh/kgU at a temperature of 1400°K (i.e. typical of a 40 kW/m linear power); the transient heatup rate is 5 K/s; the radial temperature gradient is 1300 K/cm during steady state and the transient; and there is no re-solution during the transient (i.e. no fission power during the transient).

E. FUEL BEHAVIOUR MECHANISMS (Continued)

From the results shown in Figure 30 the following approximations are made for transient release fractions as a function of fuel temperature in large break LOCA power transients: i) less than 10 per cent of the bound inventory for peak fuel temperatures in the range 2200K to 2500K; ii) greater than 10 per cent but less than 50 per cent for peak fuel temperatures in the range 2500K to 2700K; and iii) greater than 50 per cent for peak fuel temperatures greater than 2700K. The fuel heatup rate may be greater, the radial fuel temperature gradient may be less and the amount of re-solution will be greater for a large break LOCA power transient than for the case shown in Figure 30. As a result, transient fission product release fractions as a function of peak fuel temperature should be less for a large break LOCA power transient than those shown in Figure 30.

Transient fission product release and fuel swelling could affect the following aspects of the prediction of CANDU fuel behaviour during a large break LOCA power transient: i) the timing and extent of fuel expansion; ii) the fuel thermal conductivity and therefore the fuel temperature transient; iii) the internal gas pressure transient; and iv) sheath stress and the potential for sheath liftoff

4. Fuel Melting and Relocation

UO_2 fuel melts at a temperature of 3113K. The fuel enthalpy at the onset of melting is approximately 1200 J/g of UO_2 or just under 300 cal/g of UO_2. If it occurs, fuel melting will first occur at the centre of the fuel in a large break LOCA overpower transient. Any fission products in the fuel region that melts will probably be released. Molten fuel may be pushed through radial cracks in the fuel towards the pellet surface by a localised buildup of gas pressure in the central portion of fuel and/or by the stresses induced by the volume expansion associated with fuel melting. However, the extent of fuel melting and localised gas pressure buildup required to cause this radial movement of molten fuel is not known. In-reactor results on post-dryout fuel behaviour indicate that for sheath temperatures less than the melting point of Zircaloy-4 (i.e. 1760°C) central fuel melting to approximately 40 to 50 per cent of the pellet radius will not result in the radial movement of molten fuel for relatively low burnup (i.e. less than 40 MWh/kgU) CANDU fuel of the 37 element design (34).

At higher burnups fission-gas-induced molten fuel foaming may occur (35). Fission gas bubbles trapped in molten fuel can lead to fuel swelling and potentially molten fuel foaming. Fuel foaming is an agglomeration of fission gas bubbles separated from each other by a network of thin liquid UO_2 films. For longer term fuel overheating transients a foamed fuel condition is precluded by the rapid destruction of the liquid UO_2 films, bubble coalescence and the subsequent escape of the bubbles from the molten fuel region.

E. FUEL BEHAVIOUR MECHANISMS (Continued)

5. Fuel/Coolant Interaction

There has been a large amount of experimental and analytical work performed on molten fuel/coolant (MFCI) reactions of which reference 36 represents a recent assessment of intermediate scale (i.e. 5 to 20 kg of molten fuel simulant) experiments. MFCIs are thought to involve the following stages: i) molten fuel mixing with the coolant (i.e. water); ii) triggering of the explosion; iii) propagation of the explosion through the fuel/coolant mixture producing high pressure coolant vapor; and iv) expansion of the explosion products producing mechanical work. A detailed assessment of MFCIs is beyond the scope of this work.

The following factors will reduce the potential for a MFCI during a large break LOCA power transient: i) since fuel melting initiates at the centre of the fuel pellet extensive fuel melting would probably be required before molten fuel could possibly come into contact with the surrounding coolant; ii) the energy deposition required to cause extensive fuel melting is large compared to that due to a typical CANDU overpower transients; iii) the coolant in a fuel channel changes from subcooled water to saturated or superheated steam quite early in a large break LOCA; and iv) the system pressure remains quite high (i.e. greater than 5 MPa) during the overpower period of a large break LOCA.

F. RECOMMENDATIONS

The prediction of the thermal/mechanical behaviour of CANDU fuel during the first 10 seconds of a large break LOCA is extremely complex. Computer models are not available at present which could take into account all the important fuel behaviour mechanisms for a wide range of overpower and heat removal transients.

Fuel enthalpy limits for the onset of sheath failure, loss of fuel geometry and loss of channel integrity are presented in the following subsections. The author's selection of these limits is based on the information discussed in Sections B, C, D and E of this report. Until more complete, mechanistic predictions of CANDU fuel behaviour during large break LOCA overpower transients are available these enthalpy limits should act as conservative guidelines.

1. Sheath Failure

If the fuel sheath remains well cooled (i.e. less than 700K) during the first few seconds of a large break LOCA power transient then an increase in axial peak, radial average fuel enthalpy of approximately 150 J/g of UO_2 or more could result in PCI-related sheath failures. The overpower transient must peak at a normalised power factor of 5 or more to obtain the required increase in fuel enthalpy to cause PCI-related sheath failures because of the rapid heat removal (i.e. approximately 50% or more of the energy deposition in the power transient) associated with keeping the sheath temperatures cool. This 150 J/g of UO_2 limit is based on the results of ELOCA MK2 cases 114, 115, 125, 126 and 127 as discussed in Section D of this report. If the sheath heats up by approximately 300K during the first few seconds of the transient then PCI-related sheath failures will probably not occur.

For conditions of severely degraded heat removal, sheath failure due to localised sheath melting can occur if the surface fuel temperature exceeds the sheath melting temperature. For CANDU fuel with initial linear powers of 50 kW/m or more an increase in axial peak, radial average fuel enthalpy of 250 J/g of UO_2 or more can result in localised sheath melting under severely degraded heat removal conditions. This limit is based on the results of cases 112 and 113. For CANDU fuel with initial linear powers of 30 kW/m or less an increase in axial peak, radial average fuel enthalpy of 400 J/g of UO_2 or more may result in localised sheath melting under severely degraded heat removal conditions based on an extrapolation of the results of case 124. For CANDU fuel with initial linear powers between 30 and 50 kW/m the axial peak, radial average increase in fuel enthalpy that could result in localised sheath melting under severely degraded heat removal conditions can be estimated by a linear interpolation between 250 and 400 J/g of UO_2.

F. RECOMMENDATIONS (Continued)

2. Loss of Fuel Geometry

Loss of fuel geometry is assumed to occur when gross sheath melting occurs in conjunction with the onset of central fuel melting. For CANDU fuel with initial linear powers of 50 kW/m or more an increase in axial peak, radial average fuel enthalpy of 600 J/g of UO_2 or more can result in loss of fuel geometry under degraded heat removal conditions. This limit is based on the results of cases 128 and 129. For CANDU fuel with initial linear powers of 30 kW/m or less an increase in axial peak, radial average fuel enthalpy of 800 J/g of UO_2 or more may result in loss of fuel geometry under degraded heat removal conditions based on an extrapolation of the results of case 130. For CANDU fuel with initial linear powers between 30 and 50 kW/m the axial peak, radial average increase in fuel enthalpy that could result in loss of fuel geometry under degraded heat removal conditions can be estimated by a linear interpolation between 600 and 800 J/g of UO_2.

3. Loss of Fuel Channel Integrity

It is assumed that fuel channel integrity cannot be guaranteed if gross fuel melting occurs under degraded heat transfer conditions. For CANDU fuel with initial linear powers of 50 kW/m or more an increase in axial peak, radial average fuel enthalpy of 800 J/g of UO_2 or more can result in complete fuel melting under degraded heat removal conditions. For CANDU fuel with initial linear powers of 30 kW/m or less an increase in axial peak, radial average fuel enthalpy of 1000 J/g of UO_2 or more may result in complete fuel melting under degraded heat removal conditions. For CANDU fuel with initial linear powers between 30 and 50 kW/m the axial peak, radial average increase in fuel enthalpy that could result in complete fuel melting under degraded heat removal conditions can be estimated by a linear interpolation between 800 and 1000 J/g of UO_2. The onset of complete fuel vaporisation could occur for increases in axial peak, radial average fuel enthalpies of 1100 and 1300 J/g of UO_2 for initial element linear powers of 50 kW/m or greater and 30 kW/m or less respectively.

G. REFERENCES

1. BRS 75/13, Bruce A Generating Station, "Loss-of-Coolant Accident with One Shutdown System Assumed Unavailable", October 1975.

2. 30 RS-5, Pickering Generating Station 'B', "Power Transient Following Loss of Coolant with One Shutdown System Assumed Unavailable", March 1979.

3. M. Cormier, "A Review of Experiments on Fuel Behaviour During a Power Pulse", TDAI-194, October 1980.

4. M. J. Notley, "ELESIM, A Computer Code for Predicting the Performance of Nuclear Fuel Elements", Nuc. Tech., 44, p 445-450, August 1979.

5. H.E. Sills, "ELOCA, Fuel Element Behaviour During High Temperature Transients", AECL-6357, March 1979.

6. B.A. Cook and Z.R. Martinson, "Reactivity Initiated Accident Test Series Test RIA 1-4 Fuel Behaviour Report", NUREG/CR-3938, EGG-2336, September 1984.

7. P.E. MacDonald et al, "Assessment of Light Water Reactor Fuel Damage During a Reactivity Initiated Accident" , CSNI Specialist Meeting on 'Safety Aspects of Fuel Behaviour in Off-Normal and Accident Conditions' , Espoo, Finland, September 1-4 1980.

8. P.E. MacDonald et al., "Assessment of Light-Water-Reactor Fuel Damage During a Reactivity-Initiated Accident", Nuclear Safety, 21, 5 (September-October 1980).

9. R.K. McCardell et al, "Damage and Failure of Previously Irradiated Fuel Rods During a Reactivity Initiated Accident", ANS/ENS Topical Meeting on 'Reactor Safety Aspects of Fuel Behaviour', Sun Valley, Idaho, August 2-6 1981.

10. R.S. Semken et al., "Reactivity Initiated Accident Test Series, RIA Scoping Tests Fuel Behaviour Report", NUREG/CR-1360, EGG-2024 (April 1980).

11. S.L. Seiffert et al., "Reactivity Initiated Accident Test Series, Test RIA-1 (Radial Average Fuel Enthalpy of 285 cal/g) Fuel Behaviour Report", NUREG/CR-1465, EGG-2040 (September 1980).

12. B.A. Cooke et al., "Reactivity Initiated Accident Test Series, Test RIA 1-2 Fuel Behaviour Report", NUREG/CR-1842, EGG-2073 (January 1981).

13. M.S. El-Genk, "Molten Fuel-Coolant Interaction Occurring During a Severe Reactivity Initiated Accident Experiment", NUREG/CR-1900, March 1981.

G. REFERENCES (Continued)

14. M.S. El-Genk and R.L. Moore, "Transient Debris Freezing and Potential Wall Melting During a Severe Reactivity Initiated Accident Experiment", Nuc. Tech., 53, June 1981.

15. M.S. El-Genk et al, "Fragmentation of Molten Debris During a Molten Fuel-Coolant Interaction", J.Nuc.Mat., 113, 1983.

16. S. Shiozawa, "An Examination of the Standard Fuel Behaviour in NSRR Experiments", JAERI-M 7267, August 1977.

17. T. Fujishiro et al, "A Study on Pressure Generation Caused by Actual Fuel Failures in the NSRR Experiment", paper FCI4/26, 4th CSNI Specialist Meeting on 'Fuel-Coolant Interaction in Nuclear Reactor Safety', Bournemouth, U.K., April 2-5, 1979.

18. M. Ishikawa et al, "RIA Fuel Behaviours in the NSRR Tests", CSNI Specialist Meeting on 'Safety Aspects of Fuel Behaviour in Off-Normal and Accident Conditions' , Espoo, Finland, September 1-4 1980.

19. S. Kobayashi et al, "RIA Fuel Behaviour Under High Pressure and High Temperature Coolant Conditions", ANS/ENS Topical Meeting on 'Reactor Safety Aspects of Fuel Behaviour', Sun Valley, Idaho, August 2-6 1981.

20. M. Ishikawa et al, "A Study of Coolability Based on Practical Fuel Failure Behaviour", ANS/ENS Topical Meeting on 'Reactor Safety Aspects of Fuel Behaviour', Sun Valley, Idaho, August 2-6 1981.

21. T. Fujishiro et al, "Light Water Reactor Fuel Response During Reactivity Initiated Accident Experiments", NUREG/CR-0269, TREE-1237, August 1978.

22. S.A. Ploger, "The PBF OPTRAN Experiment Results", NUREG/CP-0048, Volume 3, 11th Water Reactor Safety Research Information Meeting, Gaithersburg, October 24-28, 1983.

23. Technical discussions with Ontario Hydro and AECL staff on the CANDU LOCA test in the PBF.

24. D.A. Hagrman et al, "MATPRO-Version 11 (Revision 1) A Handbook of Materials Properties For Use in the Analysis of Light Water Reactor Fuel Rod Behaviour", NUREG/CR-0497, February 1980.

25. S. Sagat et al., "Deformation and Failure of Zircaloy Fuel Sheaths Under LOCA Conditions", AECL-7754, October 1982.

26. H.M. Chung and G.R. Thomas, "High-Temperature Oxidation of Zircaloy in Hydrogen-Steam Mixtures", ASTM STP 824, pp. 793 - 809, 1984.

G. REFERENCES (Continued)

27. T. Furuta et al., "Ductility Loss of Zircaloy Cladding by Inner-Surface Oxidation During High Temperature Transient", J. Nuc. Mat., 18, pp. 802 - 810, October 1981.

28. P. Hofmann, D.K. Kerwin-Peck, "UO_2/Zircaloy-4 Chemical Interactions and Reaction Kinetics from 1000 to 1700°C Under Isothermal Conditions - Final Report", KfK-3552, November 1983.

29. J. Rest, "The Mechanistic Prediction of Fission Gas, Iodine and Cesium Release From LWR Fuel Under Degraded-Core Accident Conditions", Topical Meeting on 'Fission Product Behaviour and Source Term Research', Snowbird, Utah, July 15-19, 1984.

30. J. Rest, "An Improved Model For Fission Product Behaviour in Nuclear Fuel Under Normal and Accident Conditions", J. Nuc. Mat., 120, pp. 195-212, 1984.

31. J. Rest, "Evaluation of Volatile and Gaseous Fission Product Behaviour in Water Reactor Fuel Under Normal and Severe Core Accident Conditions", Nuc. Tech., 61, April 1983.

32. J. Rest, "The Prediction of Transient Fission-Gas Release and Fuel Microcracking Under Severe Core Accident Conditions", Nuc. Tech., 56, March 1982.

33. J. Rest and S.M. Gehl, "The Mechanistic Prediction of Transient Fission-Gas Release From LWR Fuel", Nuc. Eng. and Design, 56, pp. 233-256, 1980.

34. V.J. Langman et al., "Recent CANDU Transient Fuel Behaviour Data From Research Reactor Irradiations", AECL-7415, May 1982.

35. A.W. Cronenberg et al."Fuel Foaming and Collapse During Light Water Reactor Core Meltdown Accidents", Nuc. Tech., 67, November 1984.

36. M.L. Corradini, "Molten Fuel/Coolant Interactions : Recent Analysis of Experiments", Nuc. Sc. and Eng., 86, 1984.

Table 1
Fuel Element Initial Conditions
As Predicted From ELESIM-II(MOD9)
For ELOCA MK2 Calculations

37 Element Fuel Design
Burnup = 170 MWh/kgU

Element Linear Power (kW/m)	Fuel Temperature (K) Centre	Average	Surface	Final Gas Press (MPa)	Fuel Enthalpy J/g , (cal/g) Centre	Average	Surface
55	2026	1304	721	7.3	630 (150)	370 (88)	185 (44)
50	1811	1192	688	3.5	540 (129)	340 (81)	180 (43)
30	1129	851	600	0.6	310 (74)	225 (54)	150 (36)

Table 2
Fuel Element Initial Conditions
As Predicted From ELESIM-II(MOD9)
For ELOCA MK2 Calculations

28 Element Fuel Design
Burnup = 170 MWh/kgU

Element Linear Power (kW/m)	Fuel Temperature (K) Centre	Average	Surface	Final Gas Press (MPa)	Fuel Enthalpy J/g , (cal/g) Centre	Average	Surface
55	1999	1283	704	6.7	610 (146)	365 (87)	180 (43)
50	1793	1178	678	3.4	530 (126)	330 (79)	175 (42)
30	1122	845	594	0.4	305 (73)	225 (54)	150 (36)

Table 3
Summary of RIA Tests in the PBF

Test	Test Rod Type	Fuel Enrichment (% U-235)	Burnup (MWd/MTU)	Power (kW/ft)	Maximum Clad Surface Temperature (°F)	Maximum Local Fuel Enthalpy (cal/gm)	Comments
RIA-1 Series I	[illegible]	9.6	[illegible]	[illegible]	[illegible]	[illegible]	[illegible]
RIA-1 Series II	[illegible]	9.6	[illegible]	[illegible]	[illegible]	[illegible]	[illegible]
RIA-1	[illegible]	9.6	[illegible]	[illegible]	[illegible]	[illegible]	[illegible]
RIA-1	[illegible]	9.6	[illegible]	[illegible]	[illegible]	[illegible]	[illegible]
RIA-1	[illegible]	9%	[illegible]	[illegible]	[illegible]	[illegible]	[illegible]
RIA	[illegible]	9.6	40,000	[illegible]	565	280	150
	[illegible]	9.6	[illegible]	[illegible]	[illegible]	140	110
RIA-1	[illegible]	9.6	40,000	[illegible]	565	280	150
RIA-1	[illegible]	9.6	40,000	[illegible]	[illegible]	[illegible]	[illegible]

[illegible]

[illegible]

[illegible]

Table 4
Fuel Failure Modes for
RIA Tests in the PBF

Test	Rod Number	Burnup (MWd/tU)	Radial Average Peak Fuel Enthalpy (cal g UO2)	Comments
RIA-ST-1 Burst 1	ST-1	0	185	Did not fail
RIA-ST-1 Burst 2	ST-1	0	250	Failure; oxidation of cladding, wall thickness variations, cladding embrittlement and fragmentation
RIA-ST-2	ST-2	0	260	Failure; oxidation of cladding, wall thickness variations, cladding embrittlement and fragmentation
RIA-ST-3	ST-3	0	225	Did not fail
RIA-ST-4	ST-4	0	350	Completely destroyed
RIA 1-1	801-1	4000	285	Failure; flow blockage
	801-2	4000	285	Failure; flow blockage
	801-3	0	285	Failure; flow blockage after transient
	801-5	0	285	Failure; flow blockage after transient
RIA 1-2	802-1	5000	185	Did not fail
	802-2	5000	185	Did not fail
	802-3	5000	185	Failure; many high-strain-rate cracks
	802-4	5000	185	Did not fail
RIA 1-4	804-1	5300	277	Failure by high-strain-rate cracks and melt through
	804-3	5300	277	Failure by high-strain-rate cracks and melt through
	804-4	5300	255	Failure by high-strain-rate cracks and melt through
	804-5	5300	234	Failure by molten fuel from adjacent rods
	804-6	5300	255	Failure by high-strain-rate cracks and melt through
	804-7	5300	277	Failure by high-strain-rate cracks and melt through
	804-8	5300	255	Failure by high-strain-rate cracks and melt through
	804-9	5300	277	Failure by high-strain-rate cracks and melt through
	804-10	5300	255	Failure by high-strain-rate cracks and melt through

Table 5
Design Characteristics of NSRR
RIA Test Fuel Elements

Items	Standard Fuel Rod (Zry)		Stainless Steel Clad Fuel Rod
	Specification	Remarks(*)	
UO_2 Pellet			
Diameter	9.29 mm	9.38, 9.29 and 9.09 mm	9.34 mm
Length	10.0 mm	-	10.0 mm
Density	95 %T.D.	-	95 %T.D.
enrichment	10 %	2.6, 5, 10 and 20 %	10 %
Shape	Chamfered	Chamfered, Flat and Dished	Chamfered
Cladding			
Material	Zry-4 (Stress-relieved)	Stress-relieved, Cold-worked and Fully-annealed	SST 304
Wall Thickness	0.62 mm	0.62 and 0.40 mm	0.40 mm
Pin			
Diameter	10.92 mm	-	10.33 mm
Pellet-cladding Gap	0.095 mm	0.050, 0.095 and 0.190mm	
Element			
Overall Length	365 mm	-	279 mm
Fuelled Length	135 mm	40, 70, 135 and 280 mm	135 mm
Weight of Fuel Pellets	96.3 g	-	99.4 g
Number of Fuel Pellets	14		14
Fission Gas	He 1 atm	0.1, 1, 3.5, 7, 9, 13, 21, 31 and 41 atm	He 1 atm.
		He, Ne, A	

Note (*) Parameters in Fuel Design Variation Tests

Table 6
OPTRAN Fuel Element Burnups

OPTRAN Rod Gas Analyses

Rod #	Burnup in GWd/t	Total Gas in Std cm^3	Atomic %		
			He	Kr	Xe
901-1	13.5	13.4	97.5	0.24	1 83
901-2	5 0	37.9	99.3	0.07	0.51
901-3	22.75	13.4	96.6	0.33	2.79
901-4	5.1	35.1	97.4	0.15	0.77
901-5	12.1	13.3	94.6	0.53	4 14
901-6	15 4	12.8	94 7	0 44	3 40
902-2	9 6	19 3	77 8	2 56	19 43
902-4	8 0	15.7	82.7	1 94	14 84

Table 7
Fuel Element Characteristics
For CANDU LOCA Test in the PBF

Element Number	Preirradiated	Pressure Transducer	Fuel Centerline Thermocouple	Back-fill Pressure (MPa)
BA-01	YES[a]	NO	NO	0.44
BA-03	YES	NO	NO	0.40[b]
BA-05	YES	YES	NO	1.09
BA-07	NO	YES	YES	0.52

(a) Irradiated to 5000 MWd/t at 54 kW/m
(b) Estimated based on BA-02 measurements

Table 8
Normalised Power Transients Used In
ELOCA MK2 Calculations

Time (s)	Power Transient Identifier				
	A	B	C	D	E
0.0	1.000	1.000	1.000	1.000	1.000
0.2	1.050	1.050	1.050	1.050	1.050
0.3	1.120	1.210	1.310	1.210	1.310
0.4	1.210	1.530	1.840	1.530	1.840
0.7	1.630	3.000	4.800	3.000	4.800
1.0	2.000	4.500	8.300	4.500	8.300
1.3	2.200	5.000	10.000	5.000	10.000
1.5	2.000	4.400	9.000	4.800	9.700
1.7	1.400	3.400	7.000	4.400	9.300
1.9	0.400	1.500	4.000	3.800	8.500
2.0	0.340	0.340	0.340	3.500	8.000
2.5	0.250	0.250	0.250	1.800	5.600
3.0	0.220	0.220	0.220	0.400	3.000
4.0	0.185	0.185	0.185	0.185	0.520
5.0	0.170	0.170	0.170	0.170	0.230
7.0	0.150	0.150	0.150	0.150	0.150
10.0	0.130	0.130	0.130	0.130	0.130

Table 9
Adiabatic Heat Addition
To 37 Element Fuel Design
Due to Power Transients

Legend:
NN : J/g of UO_2
(NN) : cal/g of UO_2

Power Transients	Element Linear Power (kW/m)		
	55	50	30
A	201 (48)	183 (44)	110 (26)
B	336 (80)	305 (73)	183 (44)
D	437 (104)	397 (95)	238 (57)
C	559 (133)	508 (121)	305 (73)
E	946 (226)	860 (205)	516 (123)

Table 10
Heat Removal Conditions 1
For ELOCA MK2 Calculations

Time (s)	Pressure (MPa)	Sheath-to-Coolant Heat Transfer Coefficient (kW/m2K)	Coolant Temperature (K)
0.0	10.0	50.0	550
0.1	9.9	50.0	550
1.0	9.3	50.0	550
2.0	8.8	50.0	550
3.0	8.3	50.0	550
4.0	7.6	50.0	550
5.0	7.2	50.0	550
7.5	5.6	50.0	550
10.0	5.3	50.0	550

Table 11
Heat Removal Conditions 2
For ELOCA MK2 Calculations

Time (s)	Pressure (MPa)	Sheath-to-Coolant Heat Transfer Coefficient (kW/m2K)	Coolant Temperature (K)
0.0	10.0	5.0	550
0.1	9.9	5.0	560
1.0	9.3	5.0	650
2.0	8.8	5.0	750
3.0	8.3	5.0	850
4.0	7.6	5.0	950
5.0	7.2	5.0	1050
7.5	5.6	5.0	1050
10.0	5.3	5.0	1050

Table 12
Heat Removal Conditions 3
For ELOCA MK2 Calculations

Time (s)	Pressure (MPa)	Sheath-to-Coolant Heat Transfer Coefficient (kW/m2K)	Coolant Temperature (K)
0.0	10.0	50.0	550
0.1	9.9	0.5	560
1.0	9.3	0.5	650
2.0	8.8	0.5	750
3.0	8.3	0.5	850
4.0	7.6	0.5	950
5.0	7.2	0.5	1050
7.5	5.6	0.5	1050
10.0	5.3	0.5	1050

Table 13
Heat Removal Conditions 4
For ELOCA MK2 Calculations

Time (s)	Pressure (MPa)	Sheath-to-Coolant Heat Transfer Coefficient (kW/m2K)	Coolant Temperature (K)
0.0	10.0	50.0	550
0.1	9.9	0.1	570
1.0	9.3	0.1	750
2.0	8.8	0.1	950
3.0	8.3	0.1	1150
4.0	7.6	0.1	1350
5.0	7.2	0.1	1550
7.5	5.6	0.1	1550
10.0	5.3	0.1	1550

Table 14
Heat Removal Conditions 5
For ELOCA MK2 Calculations

Time (s)	Pressure (MPa)	Sheath-to-Coolant Heat Transfer Coefficient (kW/m2K)	Coolant Temperature (K)
0.0	10.0	50.0	550
0.1	9.9	1.5	560
1.0	9.3	1.5	650
2.0	8.8	1.5	750
3.0	8.3	1.5	850
4.0	7.6	1.5	950
5.0	7.2	1.5	1050
7.5	5.6	1.5	1050
10.0	5.3	1.5	1050

Table 15
Power Transients and
Heat Removal Conditions
For ELOCA MK2 Calculations

Case Identifier	Element Power (kW/m)	Power Transient Identifier	Heat Removal Conditions
101	55	A	5
102	50	A	5
103	55	A	3
104	50	A	3
105	55	A	4
106	50	A	4
107	30	A	4
108	55	B	2
109	50	B	2
110	55	B	3
111	50	B	3
112	55	B	4
113	50	B	4
114	55	D	1
115	50	D	1
116	55	D	5
117	50	D	5
118	55	D	4
119	50	D	4
120	55	C	2
121	50	C	2
122	55	C	3
123	50	C	3
124	30	C	3
125	55	E	1
126	50	E	1
127	30	E	1
128	55	E	5
129	50	E	5
130	30	E	5

Table 16
Power Transients and
Heat Removal Conditions
For ELOCA MK2 Calculations

Case Identifier-Element Linear Power (kW/m)

Power Transients	Heat Removal Conditions 1	2	5	3	4
A			101-55 102-50	103-55 104-50	105-55 106-50 107-30
B		108-55 109-50		110-55 111-50	112-55 113-50
D	114-55 115-50		116-55 117-50		118-55 119-50
C		120-55 121-50		122-55 123-50 124-30	
E	125-55 126-50 127-30		128-55 129-50 130-30		

Table 17
Maximum Transient Fuel Temperatures
From ELOCA MK2 Calculations
For 55 kW/m Linear Power Cases

Case Identifier
Maximum Central Fuel Temperature (K), Time (s)
Maximum Average Fuel Temperature (K), Time (s)
Maximum Surface Fuel Temperature (K), Time (s)

Power Transients	Heat Removal Conditions 1	2	5	3	4
A			101 2136,1.8 1564,2.0 1389,10.	103 2136,1.8 1642,10. 1528,10.	105 2136,1.8 1773,10. 1749,10.
B		108 2397,1.9 1811,1.9 1415,10.		110 2397,1.9 1934,6.6 1761,10.	112 2397,1.9 2023,5.1 1954,5.1 (1)
D	114 2540,2.8 1792,2.4 849,1.9		116 2543,2.8 2120,2.9 1732,8.3		118 2543,2.8 2211,2.9 2023,2.9 (1)
C		120 2762,2.0 2301,2.0 1666,1.9		122 2762,2.0 2417,2.0 2169,3.4 (1)	
E	125 3113,2.9 2440,2.9 1040,1.8		128 3113,2.9 2918,3.7 2554,3.4		

(1) Maximum at time which ELOCA calculation terminates due to too large a sheath strain increment.

Table 18
Maximum Transient Fuel Temperatures
From ELOCA MK2 Calculations
For 50 kW/m Linear Power Cases

Case Identifier
Maximum Central Fuel Temperature (K)
Maximum Average Fuel Temperature (K)
Maximum Surface Fuel Temperature (K)

Power Transients	Heat Removal Conditions 1	2	5	3	4
A			102 1922,1.8 1434,1.9 1227,9.2	104 1922,1.8 1490,10. 1388,10.	106 1922,1.8 1628,10. 1615,10.
B		109 2187,1.9 1666,1.9 1102,1.8		111 2187,1.9 1765,2.4 1579,9.8	113 2187,1.9 1970,10. 2023,10.
D	115 2337,2.8 1645,2.4 802,1.8		117 2341,2.8 1916,2.8 1451,2.8		119 2341,2.8 2122,4.6 2125,4.6 (1)
C		121 2567,2.0 2091,1.9 1306,1.9		123 2567,2.0 2244,3.3 2035,5.6	
E	126 2996,3.9 2272,2.9 967,2.1		129 2944,2.9 2651,2.9 2182,2.9 (1)		

(1) Maximum at time which ELOCA calculation terminates due to too large a sheath strain increment.

Table 19
Maximum Transient Fuel Temperatures
From ELOCA MK2 Calculations
For 30 kW/m Linear Power Cases

Case Identifier
Maximum Central Fuel Temperature (K)
Maximum Average Fuel Temperature (K)
Maximum Surface Fuel Temperature (K)

Power Transients	Heat Removal Conditions 1	2	5	3	4
A					107 1207,1.8 1153,10. 1161,10.
B					
D					
C				124 1718,2.0 1542,2.0 1406,7.1	
E	127 2154,3.9 1554,2.9 724,2.0		130 2175,4.5 1923,3.5 1525,3.4		

Table 20
Maximum Fuel Enthalpy
From ELOCA MK2 Calculations
For 55 kW/m Linear Power Cases

Case Identifier
Maximum Central Fuel Enthalpy (J/g)
Maximum Average Fuel Enthalpy (J/g)
Maximum Surface Fuel Enthalpy (J/g)

Power Transients	Heat Removal Conditions 1	2	5	3	4
A			101 660 455 400	103 660 480 445	105 660 525 515
B		108 770 540 410		110 770 585 520	112 770 620 590 (1)
D	114 840 530 225		116 840 655 510		118 840 695 620 (1)
C		120 960 730 490		122 960 780 675 (1)	
E	125 1200 795 285 (2)		128 1200 1060 845 (2)		

(1) Maximum at time which ELOCA calculation terminates due to too large a sheath strain increment.

(2) Maximum central fuel enthalpy may be larger than 1200J/g but is less than 1470J/g.

Table 21
Maximum Fuel Enthalpy
From ELOCA MK2 Calculations
For 50 kW/m Linear Power Cases

Case Identifier
Maximum Central Fuel Enthalpy (J/g)
Maximum Average Fuel Enthalpy (J/g)
Maximum Surface Fuel Enthalpy (J/g)

Power Transients	Heat Removal Conditions 1	2	5	3	4
A			102/575 415 345	104/575 435 400	106/575 475 470
B		109/680 490 300		111/680 520 460	113/680 600 620
D	115/745 480 210		117/750 575 420		119/750 655 655 (1)
C		121/855 645 370		123/855 705 625	
E	126/1110 720 265		129/1070 900 680 (1)		

(1) Maximum at time which ELOCA calculation terminates due to too large a sheath strain increment.

Table 22
Maximum Fuel Enthalpy
From ELOCA MK2 Calculations
For 30 kW/m Linear Power Cases

Case Identifier
Maximum Central Fuel Enthalpy (J/g)
Maximum Average Fuel Enthalpy (J/g)
Maximum Surface Fuel Enthalpy (J/g)

Power Transients	Heat Removal Conditions					
	1	2	5	3	4
A					107 340 320 325
B					
D					
C				124 505 450 405	
E	127 670 455 190		130 675 575 445		

Table 23
Increase in Fuel Enthalpy
From ELOCA MK2 Calculations
For 55 kW/m Linear Power Cases

Case Identifier
Increase in Central Fuel Enthalpy (J/g)
Increase in Average Fuel Enthalpy (J/g)
Increase in Surface Fuel Enthalpy (J/g)

Power Transients	Heat Removal Conditions 1	2	5	3	4
A			101 30 85 215	103 30 110 260	105 30 155 330
B		108 140 170 225		110 140 215 335	112 140 250 405
D	114 210 160 40		116 210 285 325		118 210 325 435
C		120 330 360 305		122 330 410 490	
E	125 570 425 100		128 570 690 660		

Table 24
Increase in Fuel Enthalpy
From ELOCA MK2 Calculations
For 50 kW/m Linear Power Cases

Case Identifier
Increase in Central Fuel Enthalpy (J/g)
Increase in Average Fuel Enthalpy (J/g)
Increase in Surface Fuel Enthalpy (J/g)

Power Transients	Heat Removal Conditions 1	2	5	3	4
A			102 35 75 165	104 35 95 220	106 35 135 290
B		109 140 150 120		111 140 180 280	113 140 260 440
D	115 205 140 30		117 210 235 240		119 210 315 475
C		121 315 305 190		123 315 365 445	
E	126 570 380 85		129 530 560 500		

Table 25
Increase in Fuel Enthalpy
From ELOCA MK2 Calculations
For 30 kW/m Linear Power Cases

Case Identifier
Increase in Central Fuel Enthalpy (J/g)
Increase in Average Fuel Enthalpy (J/g)
Increase in Surface Fuel Enthalpy (J/g)

Power Transients	Heat Removal Conditions 1	2	5	3	4
A					107 30 95 175
B					
D					
C				124 195 225 255	
E	127 360 230 40		130 365 350 295		

Table 26
Heat Removal From Fuel
From ELOCA MK2 Calculations
For 55 kW/m Linear Power Cases

Case Identifier
Average Heat Removal From Fuel (J/g of UO_2)
Heat Removal as Percentage of Adiabatic Heat Addition
(Refer to Table 9)

Power Transients	Heat Removal Conditions 1	2	5	3	4
A			101 116 58%	103 91 45%	105 46 23%
B		108 166 49%		110 121 36%	112 86 26%
D	114 277 64%		116 152 35%		118 112 26%
C		120 199 36%		122 149 27%	
E	125 512 55%		128 256 27%		

Table 27
Heat Removal From Fuel
From ELOCA MK2 Calculations
For 50 kW/m Linear Power Cases

Case Identifier
Average Heat Removal From Fuel (J/g of UO_2)
Heat Removal as Percentage of Adiabatic Heat Addition
(Refer to Table 9)

Power Transients	Heat Removal Conditions 1	2	5	3	4
A			102 108 59%	104 88 48%	106 48 26%
B		109 155 51%		111 125 41%	113 45 15%
D	115 257 65%		117 162 41%		119 82 21%
C		121 203 40%		123 143 28%	
E	126 480 56%		129 300 35%		

Table 28
Heat Removal From Fuel
From ELOCA MK2 Calculations
For 30 kW/m Linear Power Cases

Case Identifier
Average Heat Removal From Fuel (J/g of UO_2)
Heat Removal as Percentage of Adiabatic Heat Addition
(Refer to Table 9)

Power Transients	Heat Removal Conditions 1	2	5	3	4
A					107 15 14%
B					
D					
C				124 80 26%	
E	127 286 55%		130 166 32%		

Table 29
Summary of ELOCA MK2
Fuel Behaviour Predictions

(1) Heat liberated due to the exothermic Zircaloy/steam reaction (J/g of UO_2) : 6.4 kJ/g of Zr reacted.
(2) Maximum value.
(3) Interfacial pressure between fuel and sheath at time of maximum sheath temperature.
NA Not available.

Case	Maximum Sheath Temp(K)	Oxide Layer (um)	MWR Heat (1)	Sheath Strain (%)(2)	Athermal Strain (%) (2)	IntP(3) (MPa)
101	1198	6	2.6	0.97	0.00	0.00
102	1215	6	2.6	0.48	0.00	0.38
103	1374	13	5.7	1.24	0.00	0.00
104	1382	13	5.7	0.51	0.00	0.22
105	1755	40	17.7	1.59	0.00	0.00
106	1615	26	11.5	0.57	0.00	0.00
107	1162	4	1.8	0.05	0.00	4.74
108	1126	4	1.8	1.23	0.00	0.00
109	1143	4	1.8	0.89	0.00	0.94
110	1547	28	12.4	1.94	0.00	0.00
111	1561	30	13.2	0.97	0.00	4.17
112	2087	NA	NA	1.75	0.00	0.00
113	2047	95	41.8	1.24	0.00	0.00
114	639	1	0.4	1.22	0.44	0.00
115	633	1	0.4	1.00	0.32	0.00
116	1360	12	5.3	2.10	0.00	0.00
117	1435	17	7.5	1.25	0.00	1.78
118	2063	31	13.7	2.05	0.00	0.00
119	2126	80	34.5	1.44	0.00	1.00
120	1169	5	2.2	2.26	0.00	0.00
121	1219	6	2.6	1.63	0.00	0.00
122	2076	51	22.4	2.51	0.00	0.00
123	2025	144	63.2	1.91	0.00	0.14
124	1403	17	7.5	0.46	0.00	4.60
125	694	1	0.4	2.58	1.91	17.60
126	684	1	0.4	2.25	1.46	22.26
127	644	1	0.4	0.75	0.40	31.65
128	1744	46	20.3	4.19	0.00	0.00
129	2182	41	18.1	2.74	0.00	0.00
130	1517	21	9.3	1.12	0.00	6.50

Table 30
Mechanisms Which Could
Affect Predictions of Fuel
Behaviour Made With ELOCA MK2

(1) Potential for Zr/UO2 interaction on inner sheath surface?
(2) Potential for hydrogen absorption into ZrO2 layer or Zr?
(3) Potential for oxidation to affect sheath deformation?
(4) Transient gas release - L : little (i.e. < 10%)
M : moderate (i.e. > 10% and < 50%)
G : gross (i.e. > 50%)

Case	Zr/UO2 Reaction? (1)	Hydrogen in Oxide or Zirc? (2)	Oxid'n Effect? (3)	Transient Gas Release? (4)		
				Centre	Average	Surface
101	No	No	No	No	No	No
102	No	No	No	No	No	No
103	No	No	No	No	No	No
104	No	No	No	No	No	No
105	No	No	Yes	No	No	No
106	Yes	No	Yes	No	No	No
107	No	No	No	No	No	No
108	No	No	No	L	No	No
109	No	No	No	No	No	No
110	No	No	Yes	L	No	No
111	Yes	No	Yes	No	No	No
112	Yes	Yes	Yes	L	No	No
113	Yes	Yes	Yes	No	No	No
114	No	No	No	M	No	No
115	No	No	No	L	No	No
116	No	No	No	M	No	No
117	Yes	No	No	L	No	No
118	Yes	Yes	Yes	M	L	No
119	Yes	Yes	Yes	L	No	No
120	No	No	No	G	L	No
121	No	No	No	M	No	No
122	Yes	Yes	Yes	G	L	No
123	Yes	Yes	Yes	M	L	No
124	Yes	No	No	No	No	No
125	No	No	No	G	L	No
126	No	No	No	G	L	No
127	No	No	No	No	No	No
128	No	No	Yes	G	G	M
129	Yes	Yes	Yes	G	M	No
130	Yes	No	Yes	No	No	No

Table 31
Overview of Fuel Behaviour As A Function of Power Transient And Heat Removal Conditions For ELOCA MK2 Calculations

Case Identifier(Fuel Behaviour)

Power Transients	Heat Removal Conditions 1	2	5	3	4
A			101(1) 102(1)	103(1) 104(1)	105(2) 106(2) 107(1)
B		108(1) 109(1)		110(2) 111(2)	112(3) 113(3)
D	114(4) 115(4)		116(1) 117(1)		118(3) 119(3)
C		120(1) 121(1)		122(3) 123(3) 124(1)	
E	125(4) (5) 126(4) 127(4)		128(5) (6) 129(3) 130(1) (7)		

(1) : Slight oxidation and sheath strain, sheath intact.
(2) : Oxide layer < 20um, total sheath strain < 2%, sheath failure not probable.
(3) : Sheath failure possible due to localised melting or overstrain under oxide crack.
(4) : Possible non-ductile sheath failure.
(5) : Central fuel melting present.
(6) : Local overstrain failure under oxide crack possible.
(7) : Sheath embrittled, failure on rewet possible.

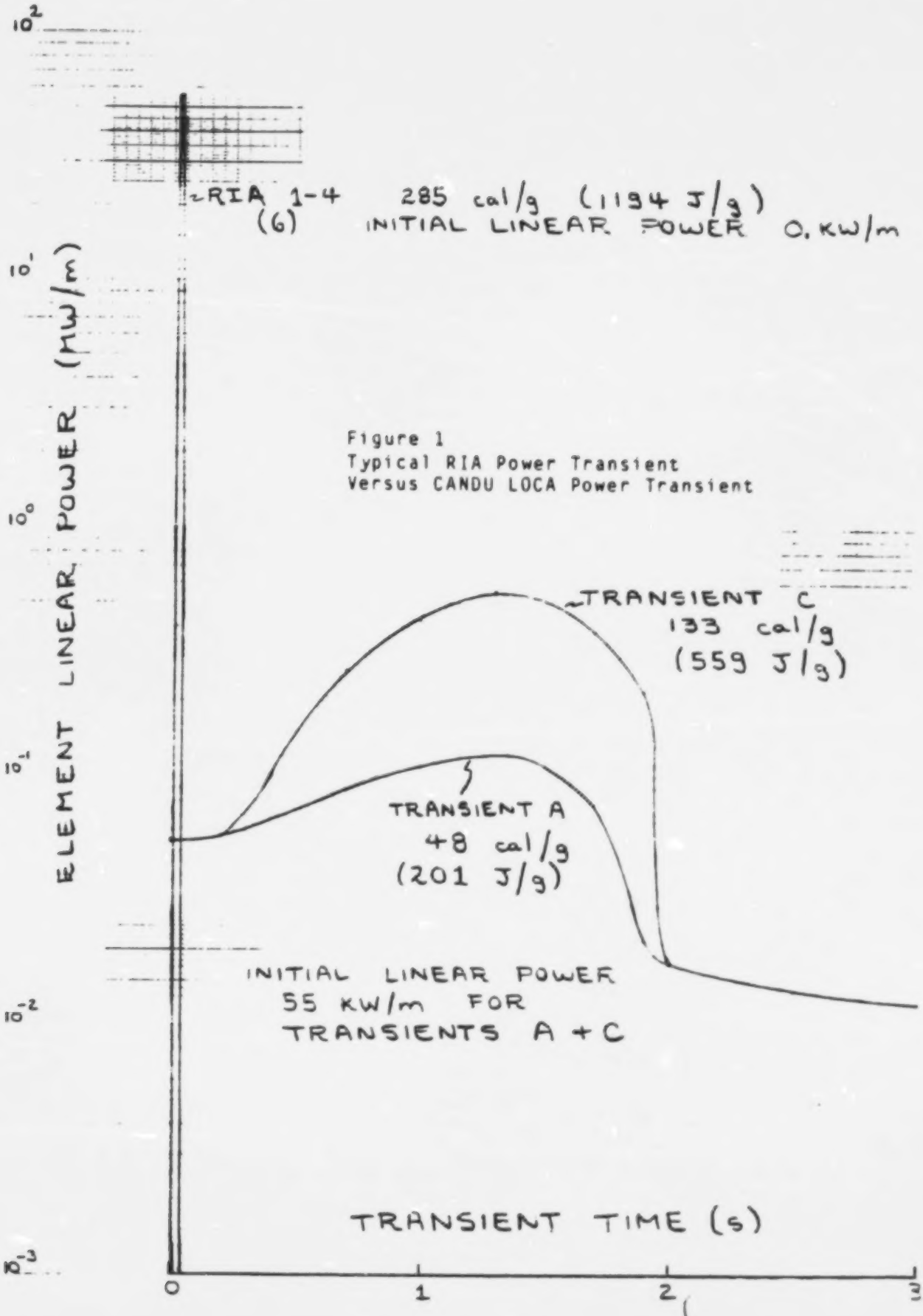

Figure 1
Typical RIA Power Transient
Versus CANDU LOCA Power Transient

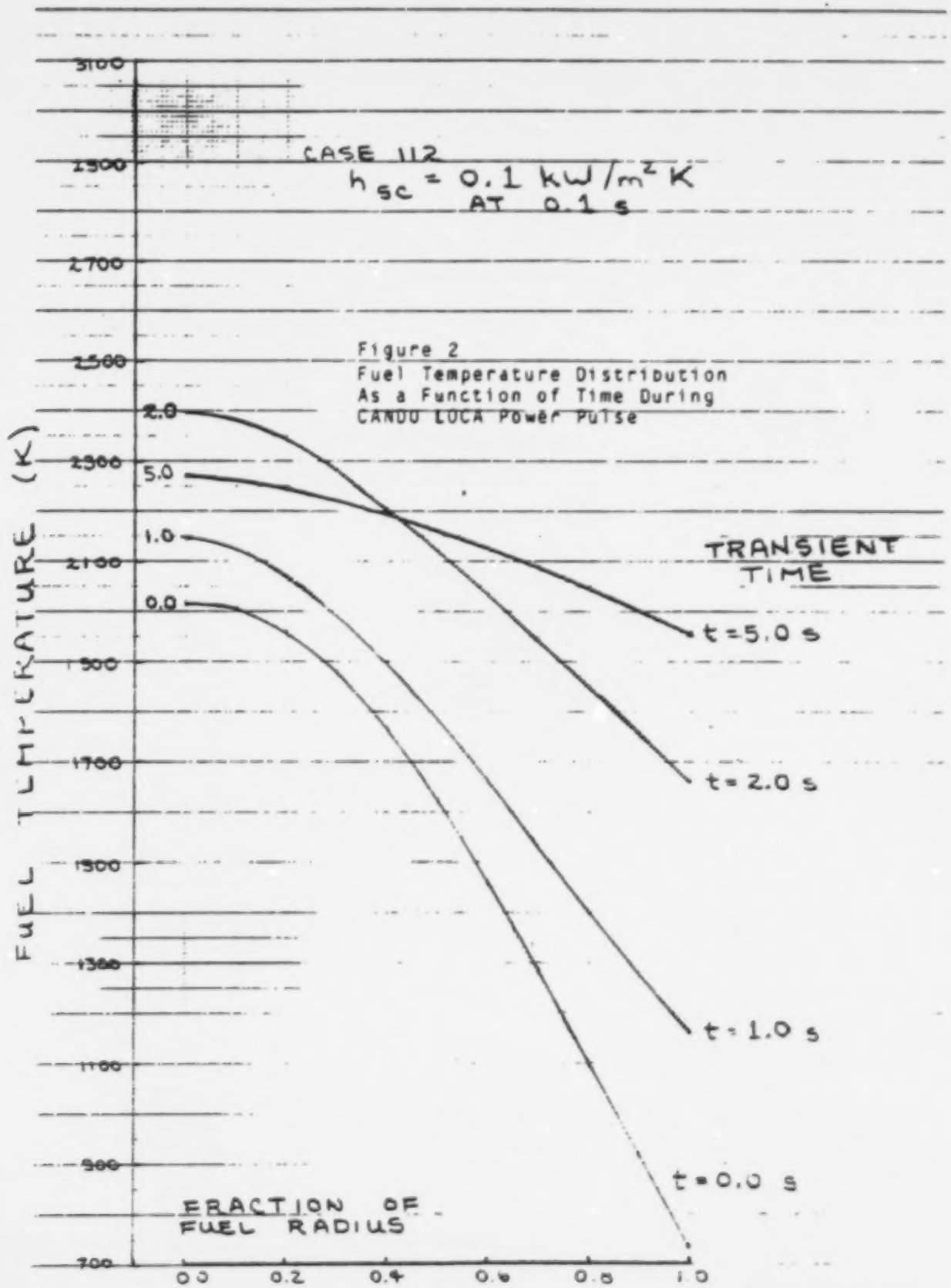

Figure 2
Fuel Temperature Distribution
As a Function of Time During
CANDU LOCA Power Pulse

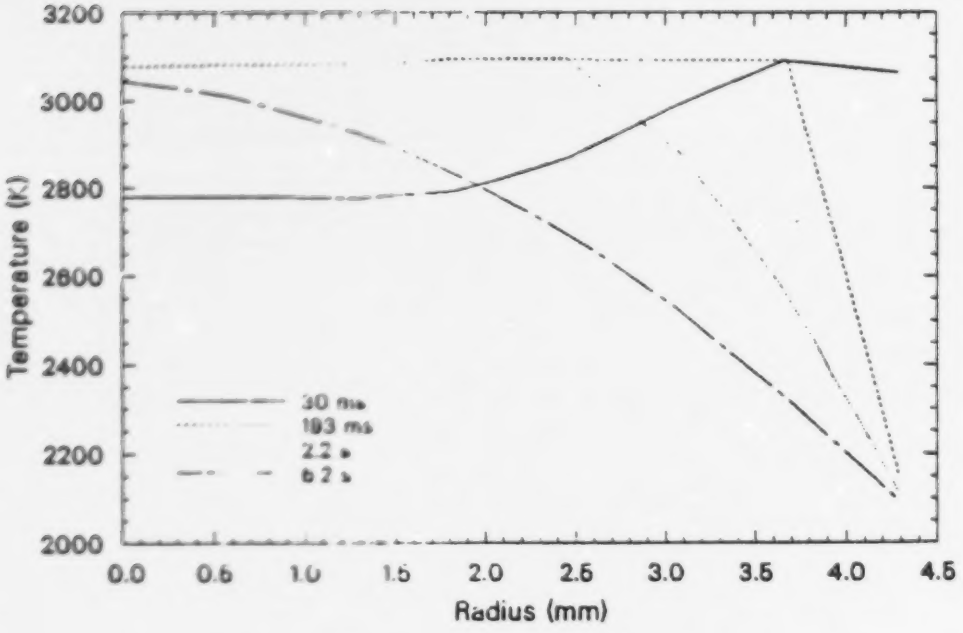

Figure 3
Temperature Distribution at
Various Times During a RIA

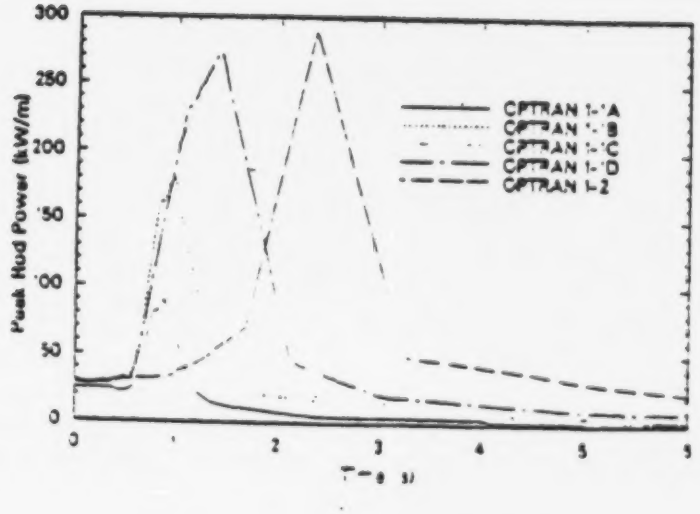

Figure 4
Power Transients for
OPTRAN Tests in the PBF

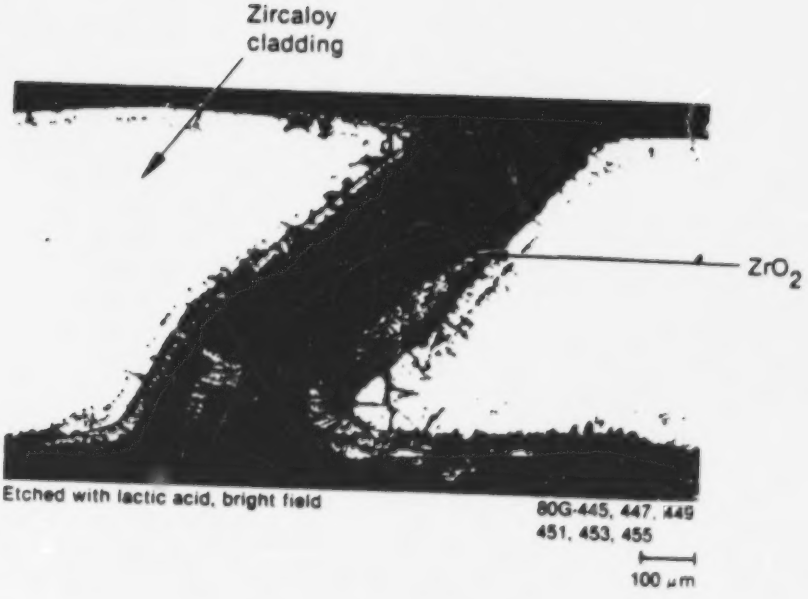

Figure 5
Non-ductile, PCI-type
Sheath Failure

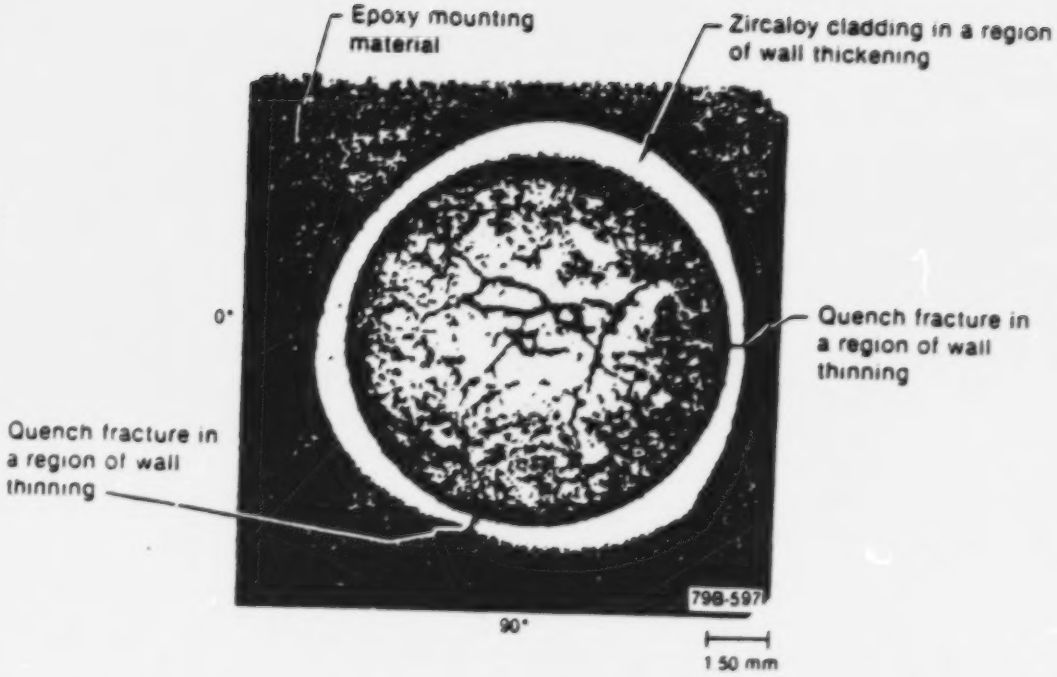
Epoxy mounting material
Zircaloy cladding in a region of wall thickening
0°
Quench fracture in a region of wall thinning
Quench fracture in a region of wall thinning
798-597
90°
1 50 mm

Figure 6
Sheath Thickness Variations
From RIA Test 1-1, Element 801-5

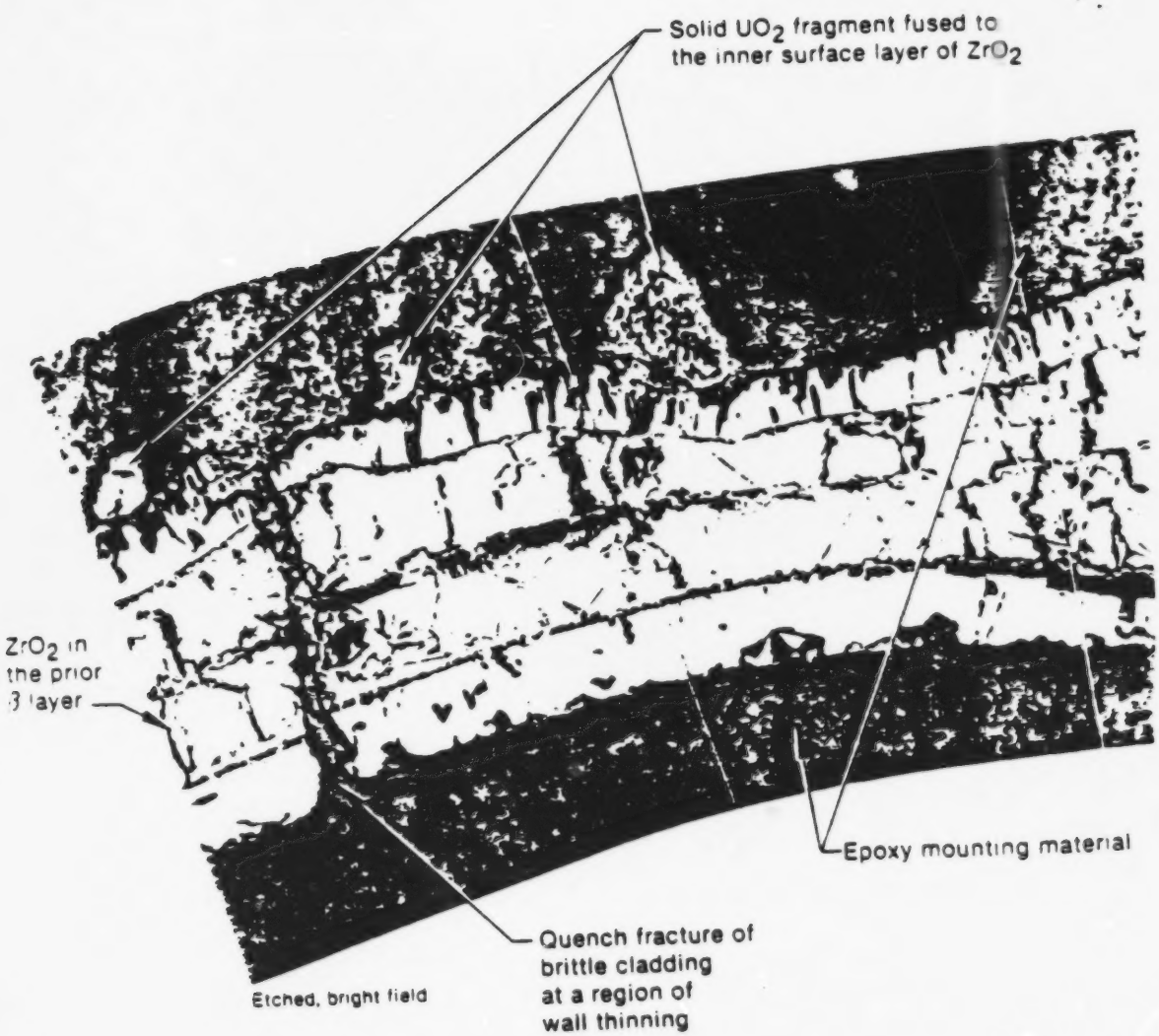
Solid UO_2 fragment fused to the inner surface layer of ZrO_2
ZrO_2 in the prior β layer
Epoxy mounting material
Quench fracture of brittle cladding at a region of wall thinning
Etched, bright field

Figure 7
Fuel/Sheath
Contact/Fusing
In RIA 1-1

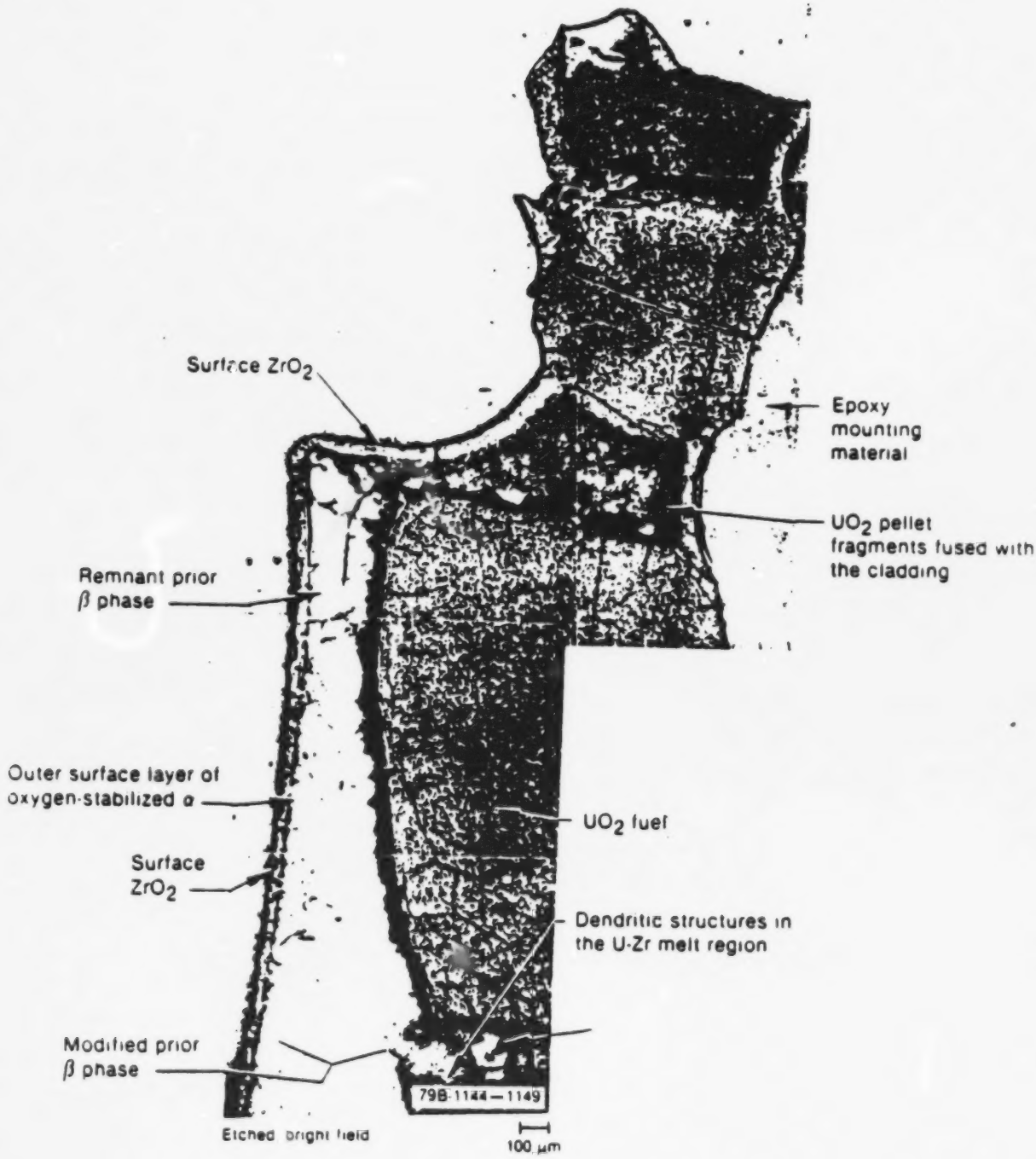

Figure 8
Molten Sheath/Fuel
Intermixing in RIA 1-1

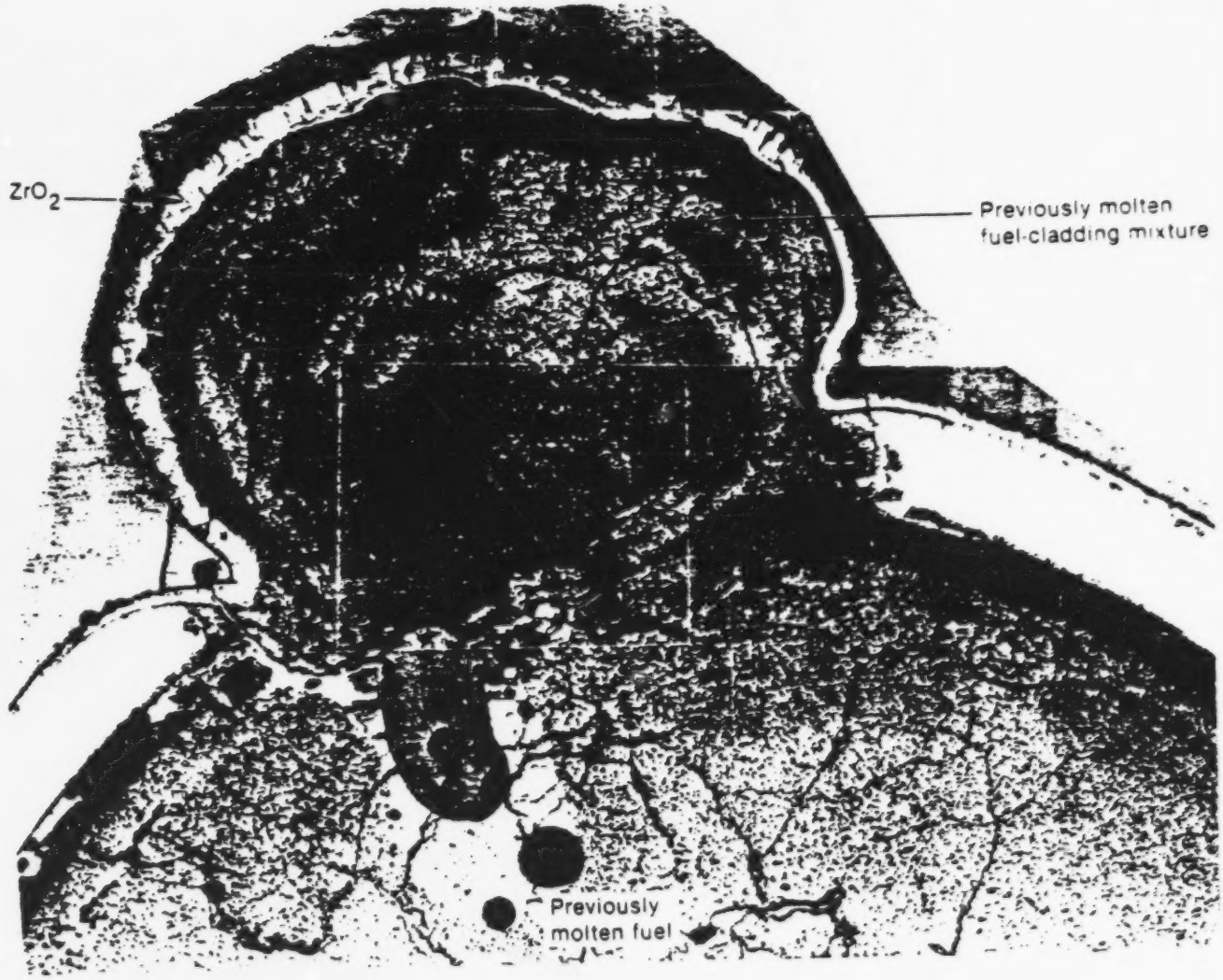

Figure 9
Example of Molten Fuel/Sheath Relocation in Test RIA 1-4

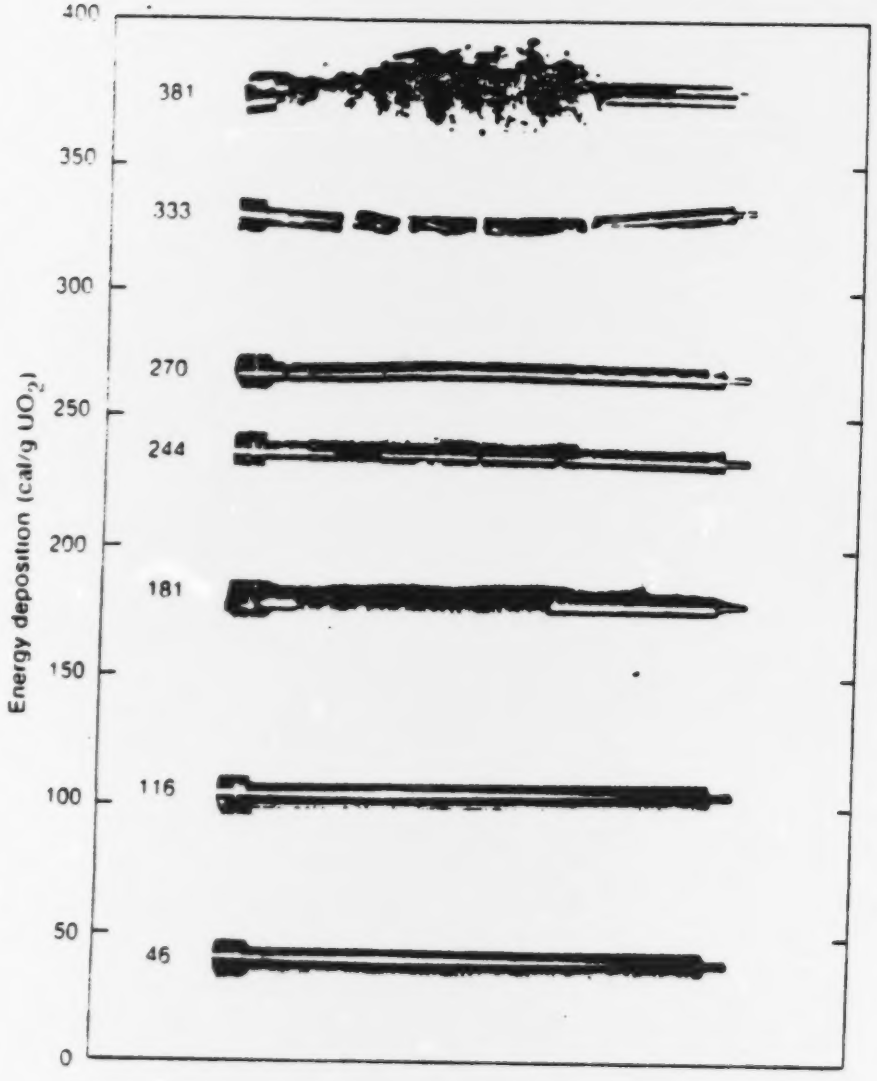

Figure 10
Post-Test Appearance of NSRR Standard Test Elements
As A Function of Total Energy Deposition

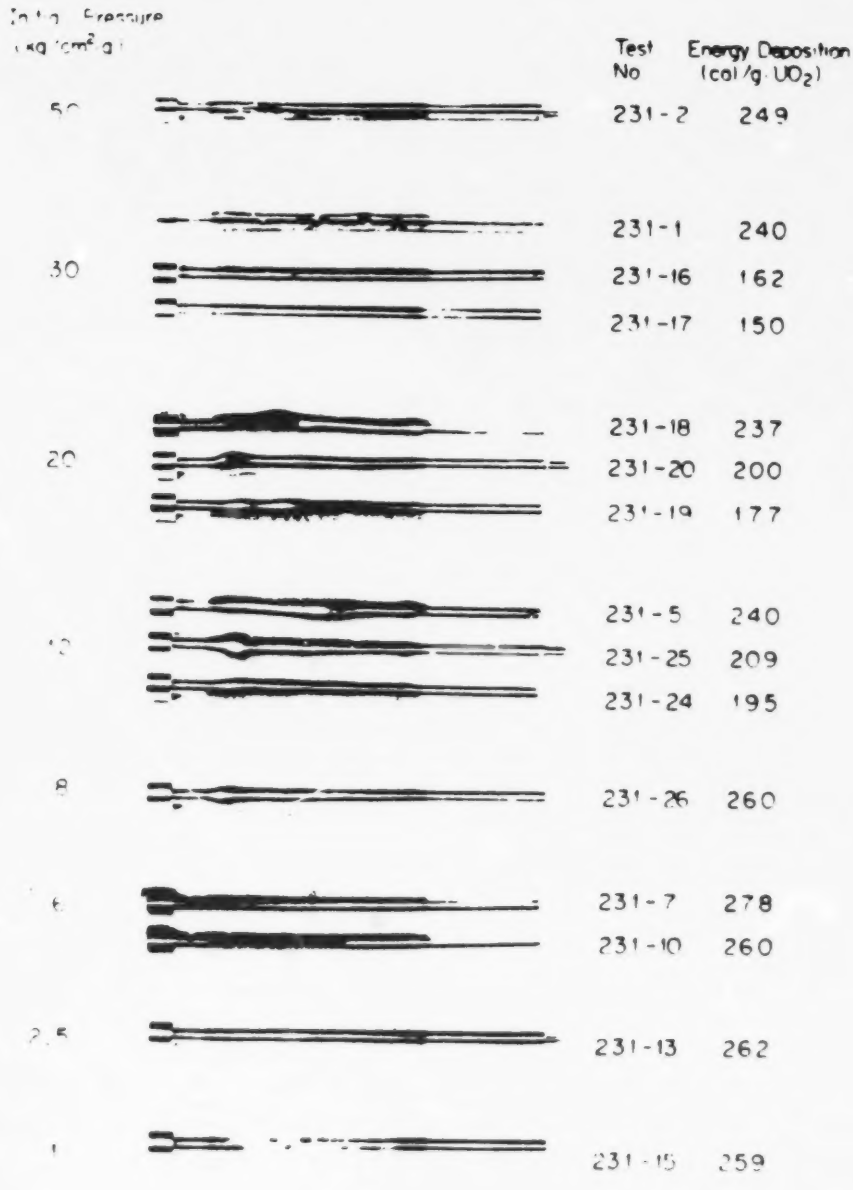

Figure 11
Post-Test Appearance of Pre-Pressurised
Fuel Elements Tested in the NSRR

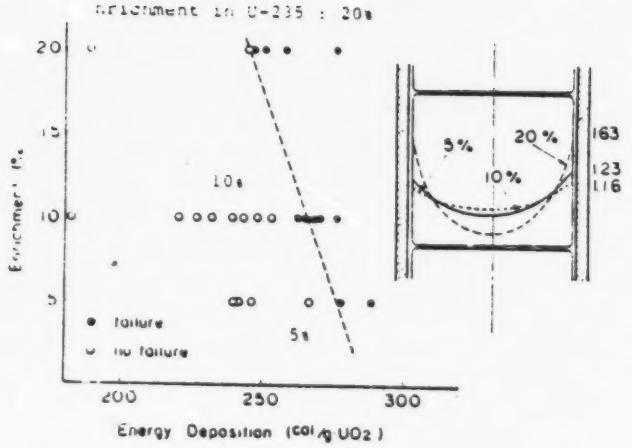

Figure 12
The Effect of Fuel Enrichment on the Energy Deposition Required to Cause Sheath Failure From the NSRR Tests

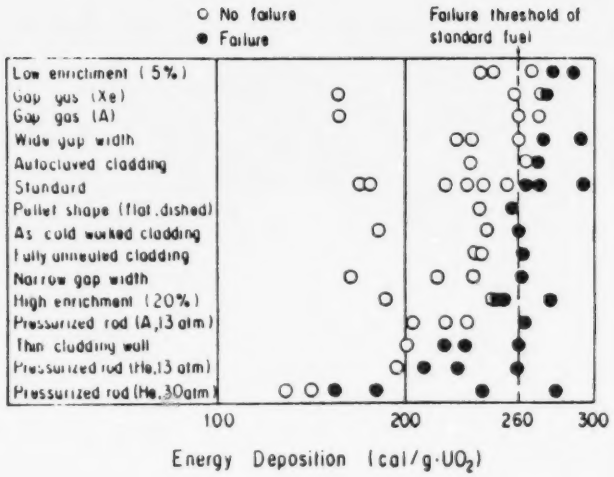

Figure 13
The Effect of Fuel Design Parameters on the Energy Deposition Required to Cause Sheath Failure From the NSRR Tests

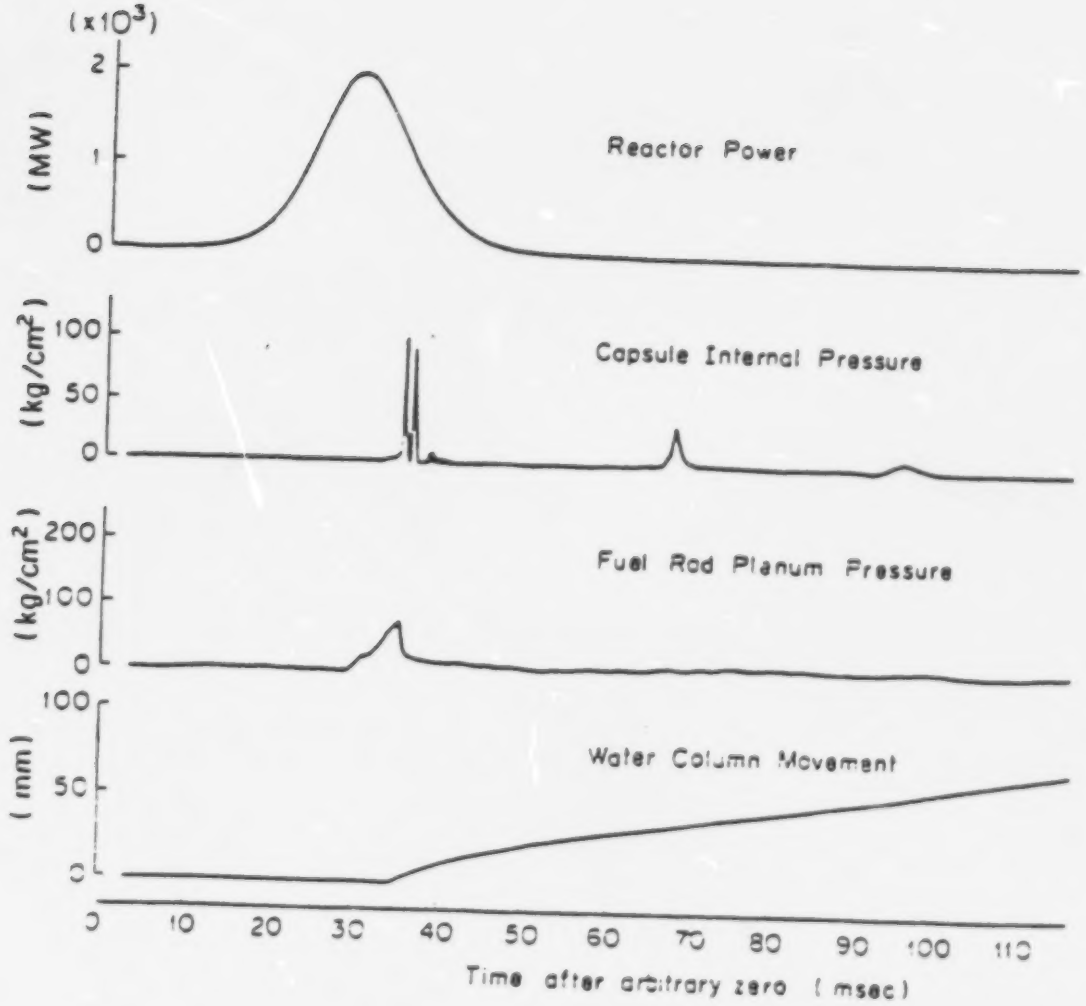

Figure 14
Pressure Pulses Generated by Waterlogged Fuel Failure in the NSRR. Energy Deposition 156 cal/g.

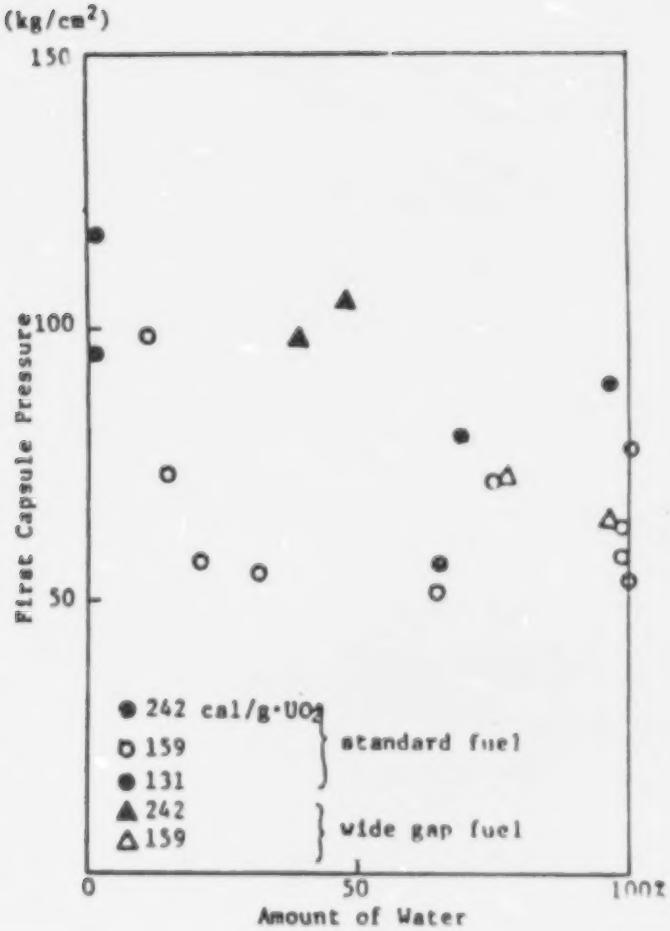

Figure 15
Pressure Pulse Magnitude as a Function of
Water Content in the Fuel-Sheath Gap
In the NSRR Tests

Figure 16
Post-Test Fuel Appearance as a Function of Total Energy Deposition and Axial Peak, Radial Average Fuel Enthalpy. SPXM Fuel Elements Tested in the SPERT-CDC.

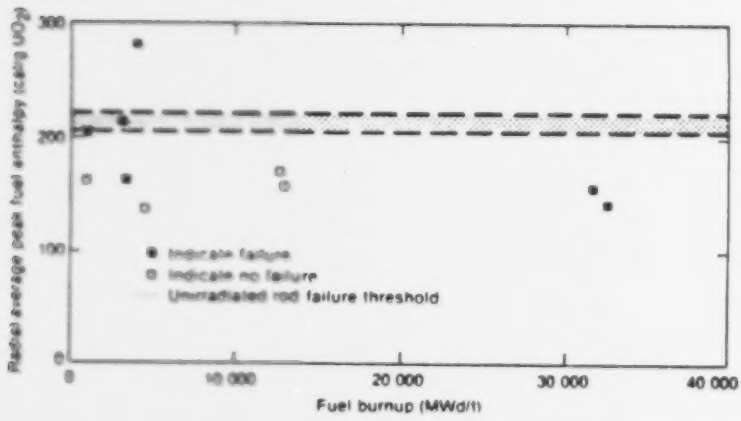

Figure 17
Failure Threshold For Previously Irradiated
Fuel Elements Tested in the SPERT Program

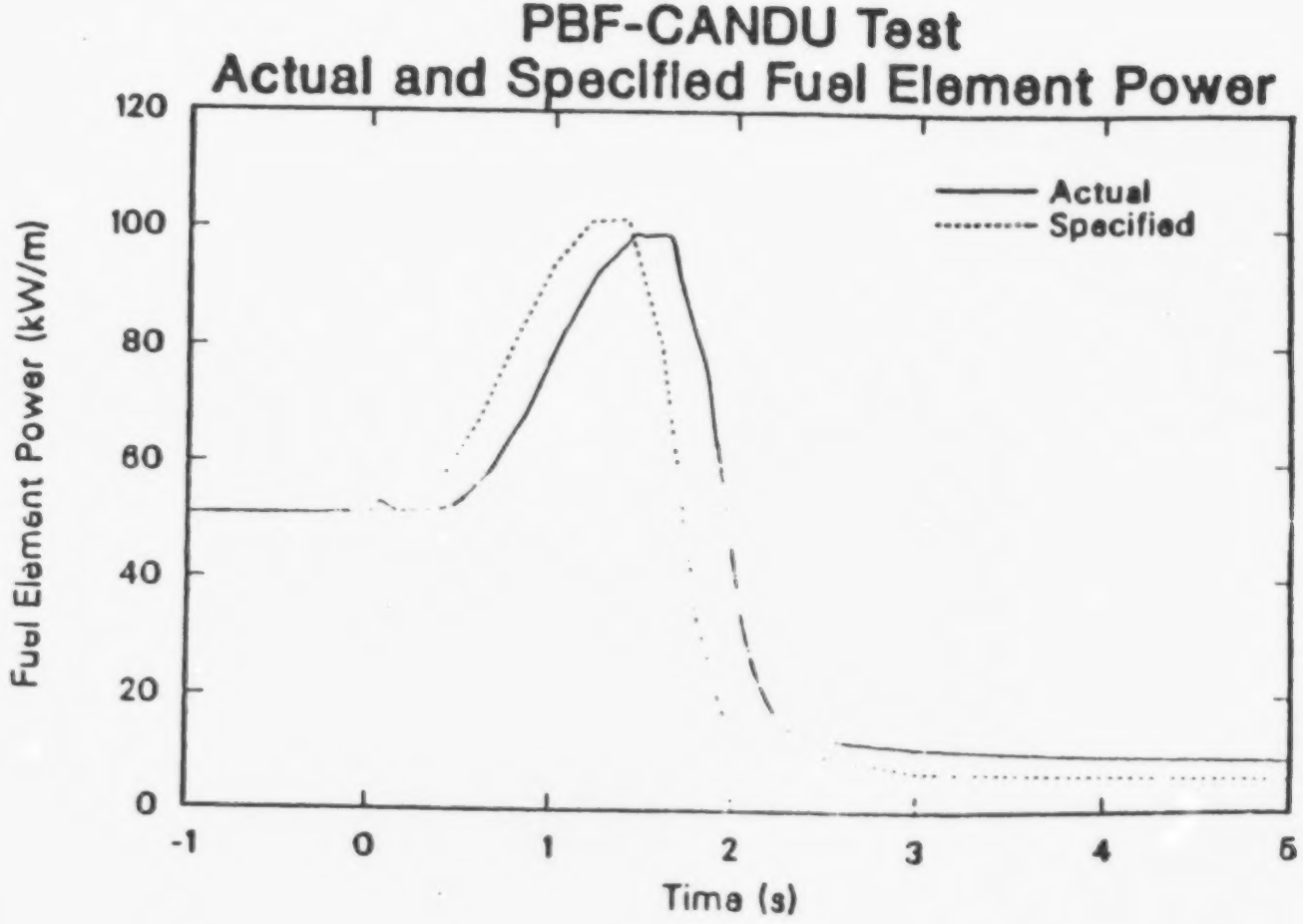

Figure 18
Overpower Transient in the
CANDU LOCA Test in the PBF

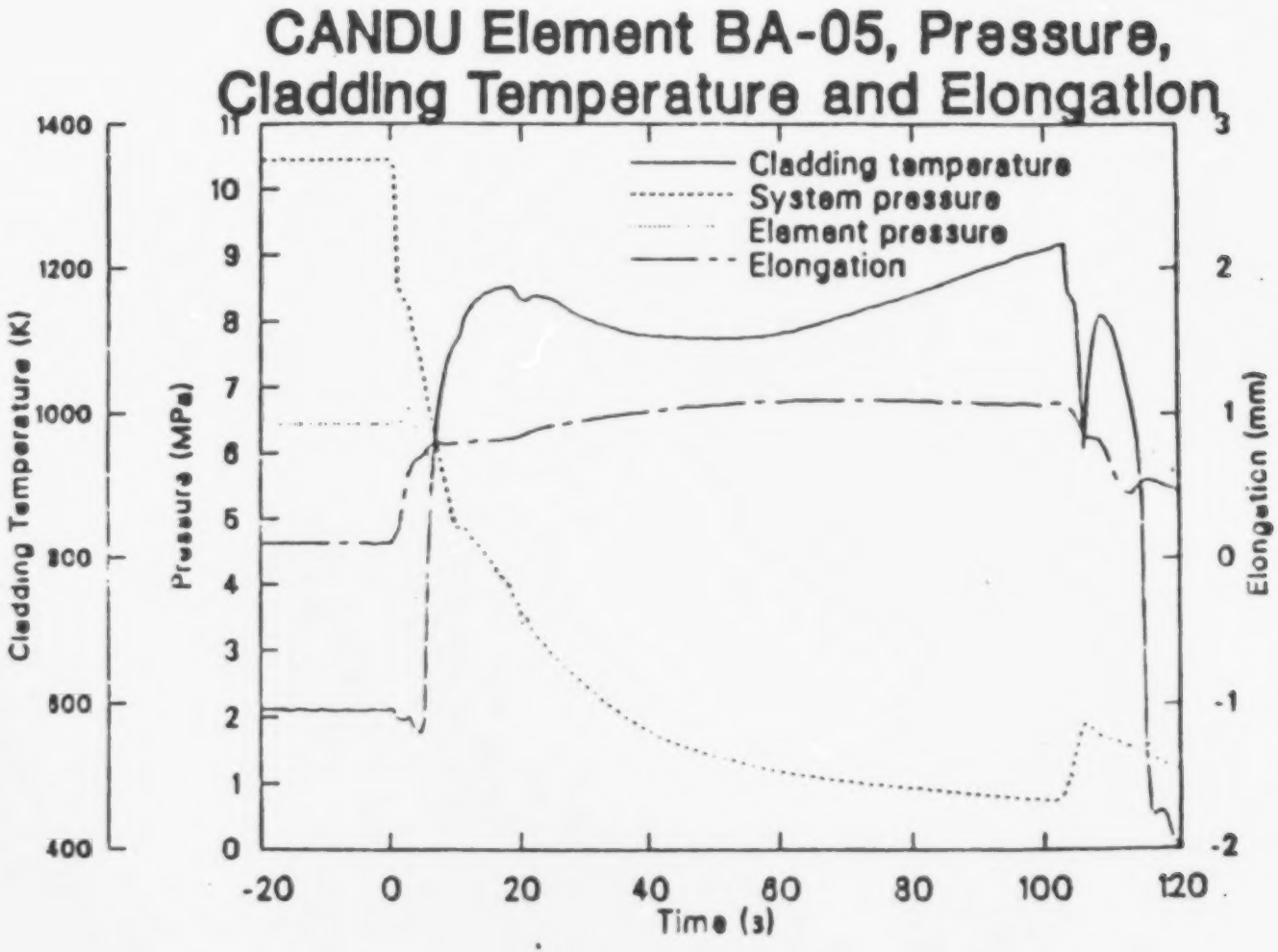

Figure 19
Depressurisation Transient in the
CANDU LOCA Test in the PBF

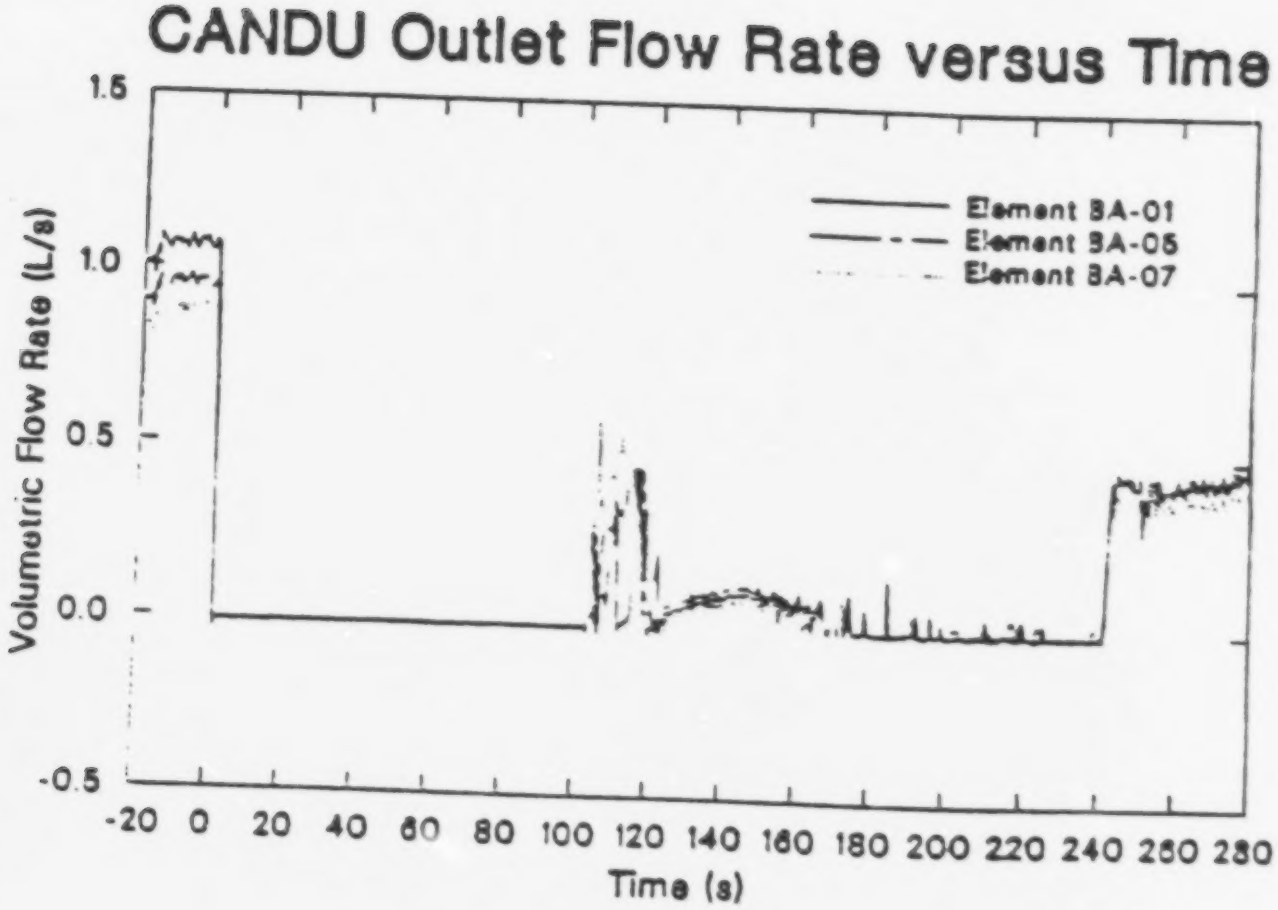

Figure 20
Coolant Flow in the
CANDU LOCA Test in the PBF

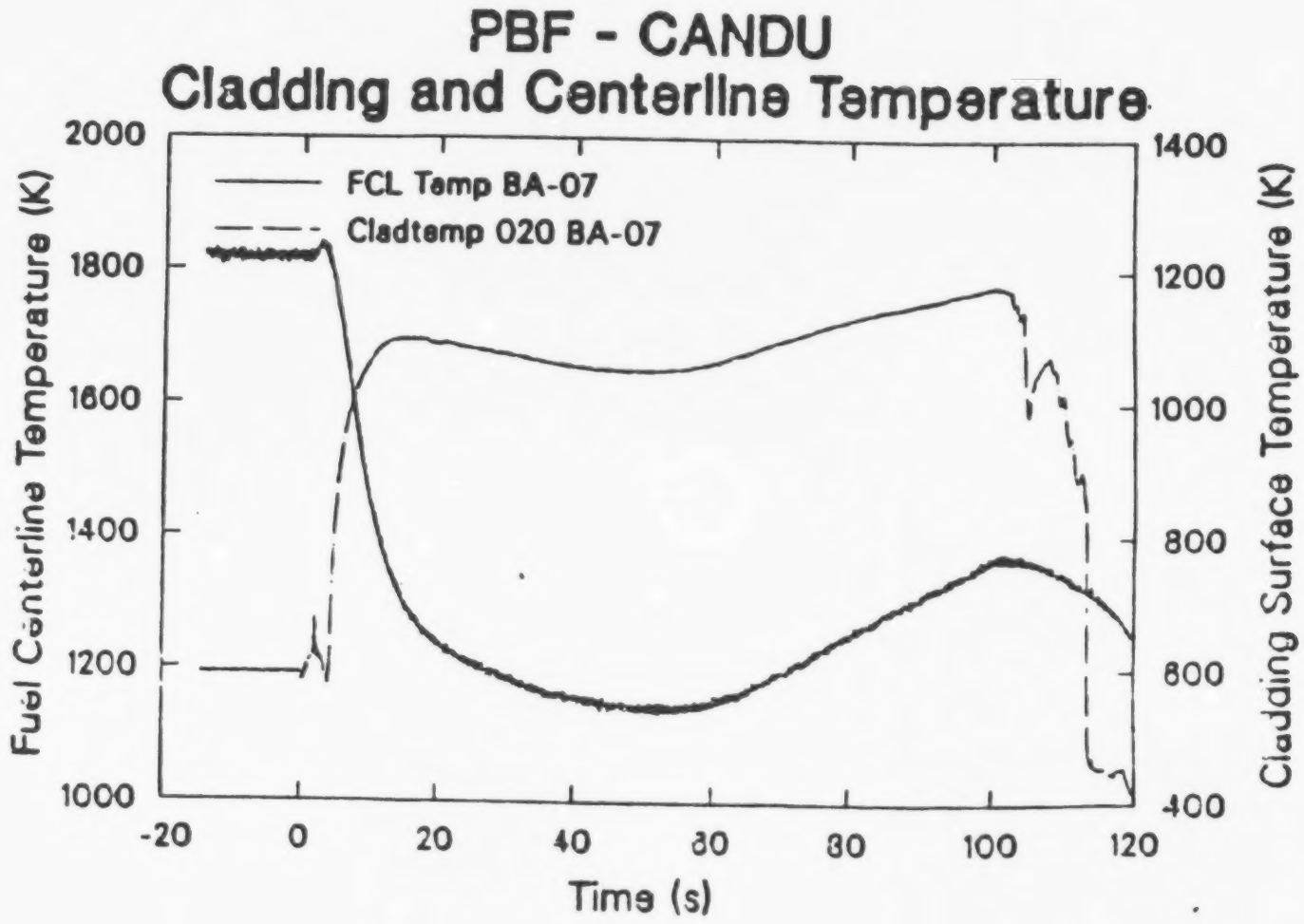

Figure 21
Fuel Centreline and Sheath Temperatures
in the CANDU LOCA Test in the PBF

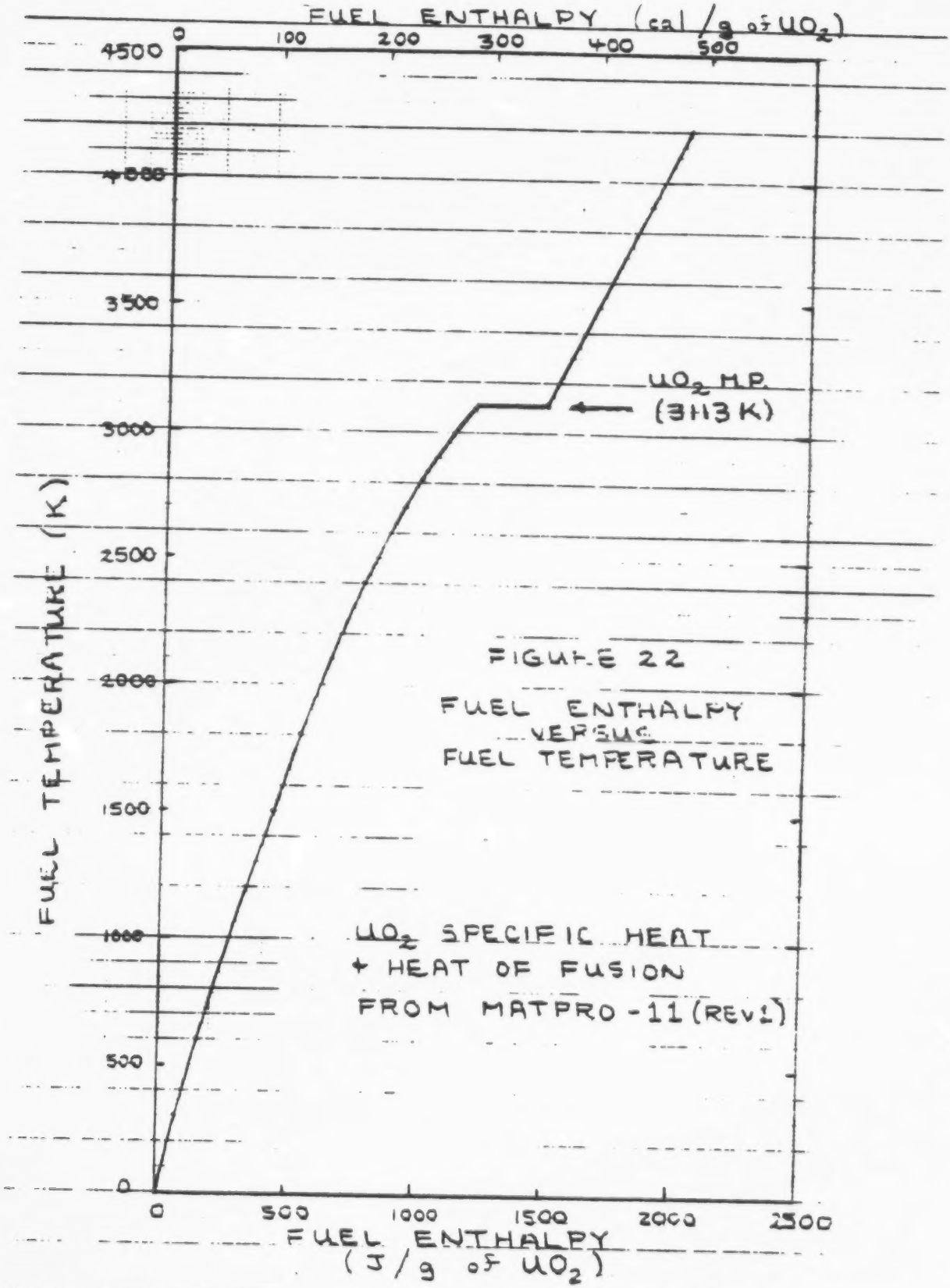
FUEL ENTHALPY (cal / g of UO_2)
0
100
200
300
400
500
4500
4000
3500
3000
2500
2000
1500
1000
500
0
UO_2 M.P.
(3113 K)
FUEL TEMPERATURE (K)
FIGURE 22
FUEL ENTHALPY
VERSUS
FUEL TEMPERATURE
UO_2 SPECIFIC HEAT
+ HEAT OF FUSION
FROM MATPRO-11 (REV 2)
0
500
1000
1500
2000
2500
FUEL ENTHALPY
(J / g of UO_2)

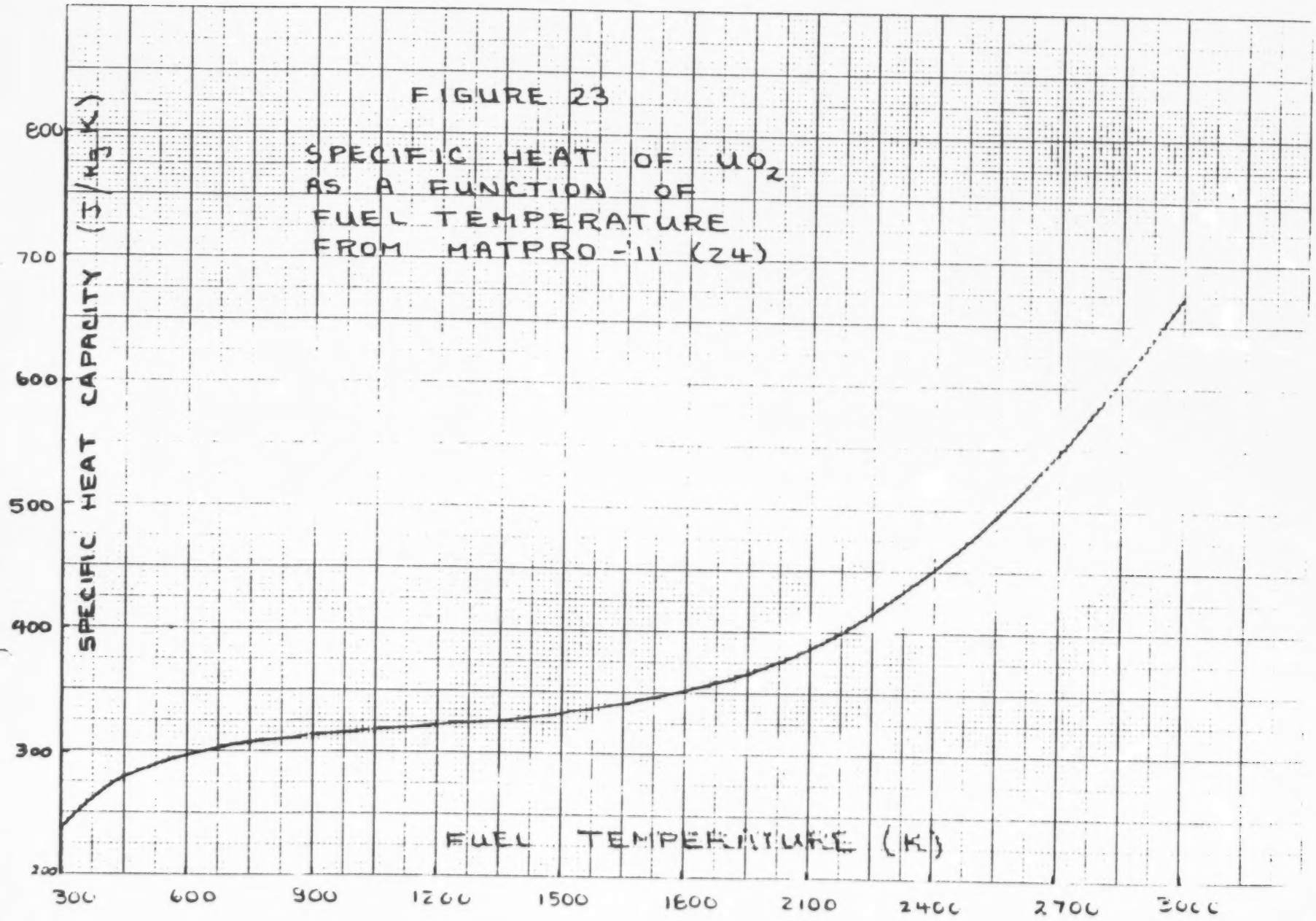
FIGURE 23
SPECIFIC HEAT OF UO_2 AS A FUNCTION OF FUEL TEMPERATURE FROM MATPRO-11 (24)
SPECIFIC HEAT CAPACITY (J/kg K)
800
700
600
500
400
300
200
FUEL TEMPERATURE (K)
300
600
900
1200
1500
1800
2100
2400
2700
3000

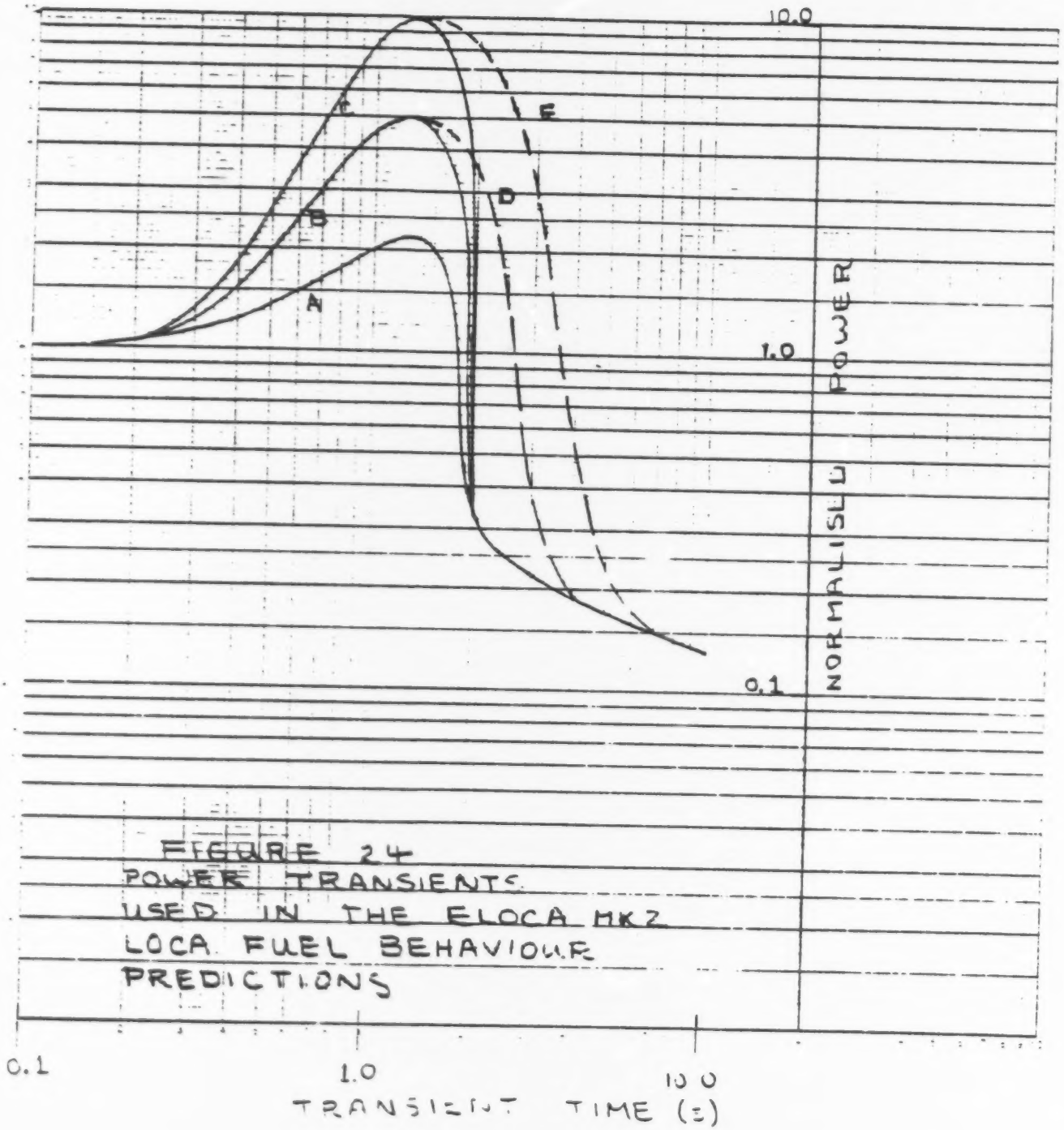

FIGURE 24
POWER TRANSIENTS USED IN THE ELOCA MK2 LOCA FUEL BEHAVIOUR PREDICTIONS

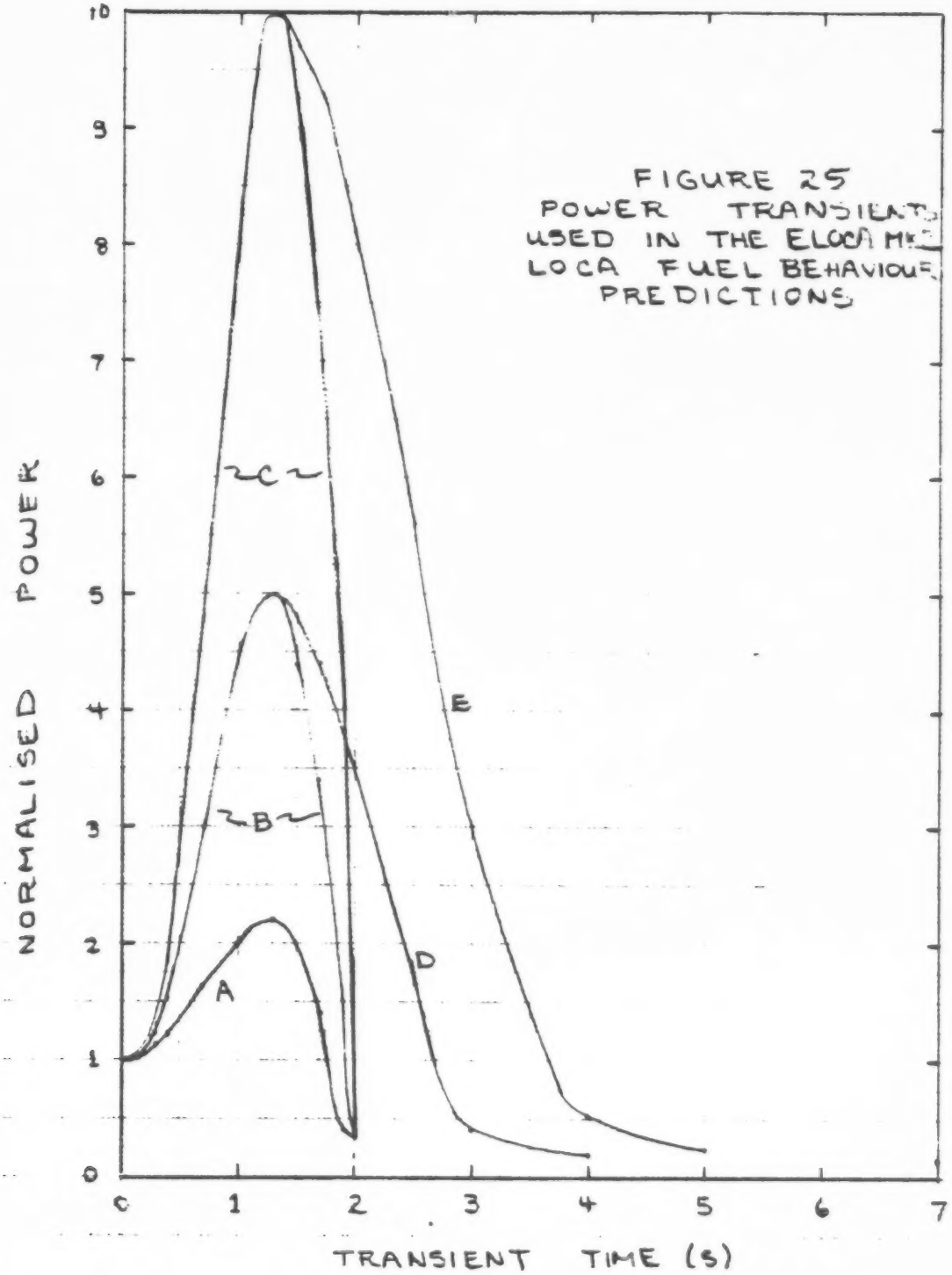

FIGURE 25
POWER TRANSIENTS USED IN THE ELOCA MK. LOCA FUEL BEHAVIOUR PREDICTIONS

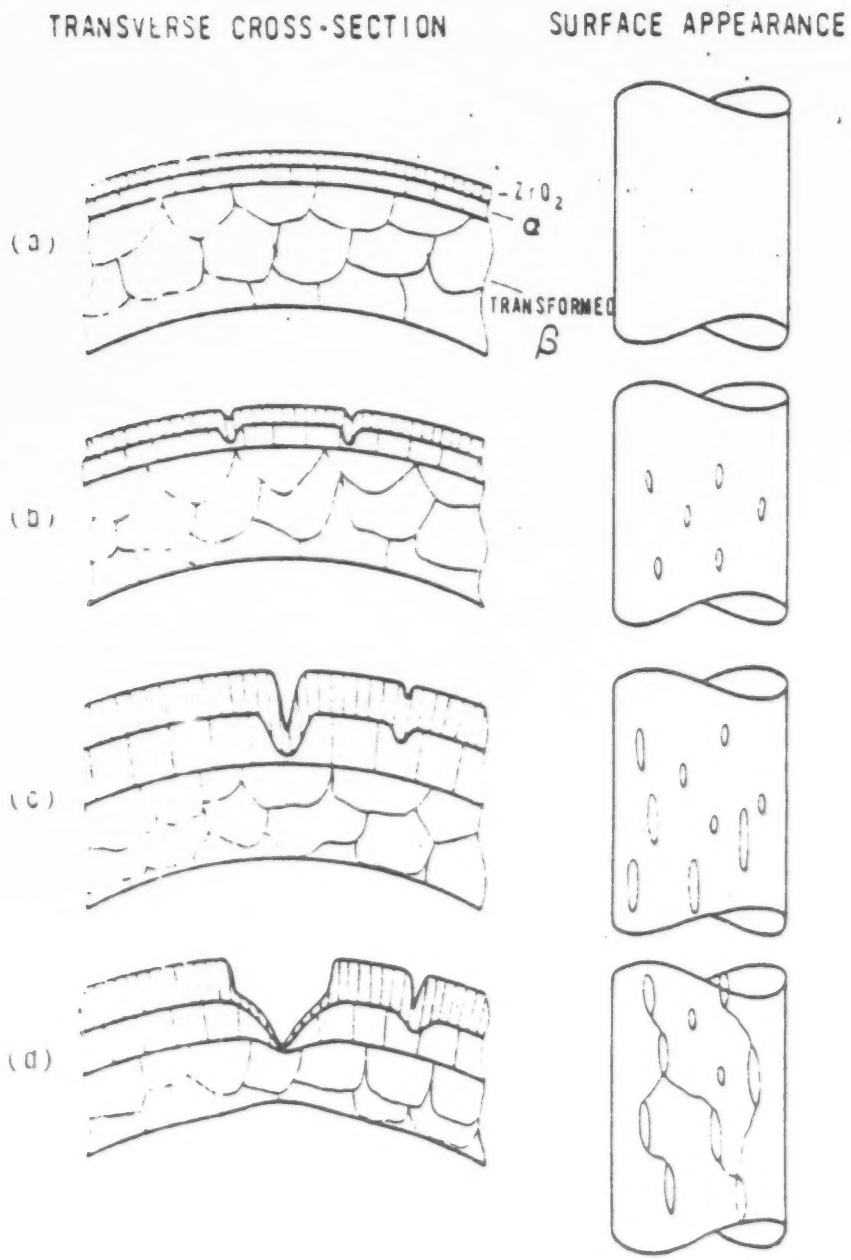

Figure 26
Schematic of the Deformation of Pressurised Zircaloy Fuel Sheath in Steam Under Temperature Ramp Conditions

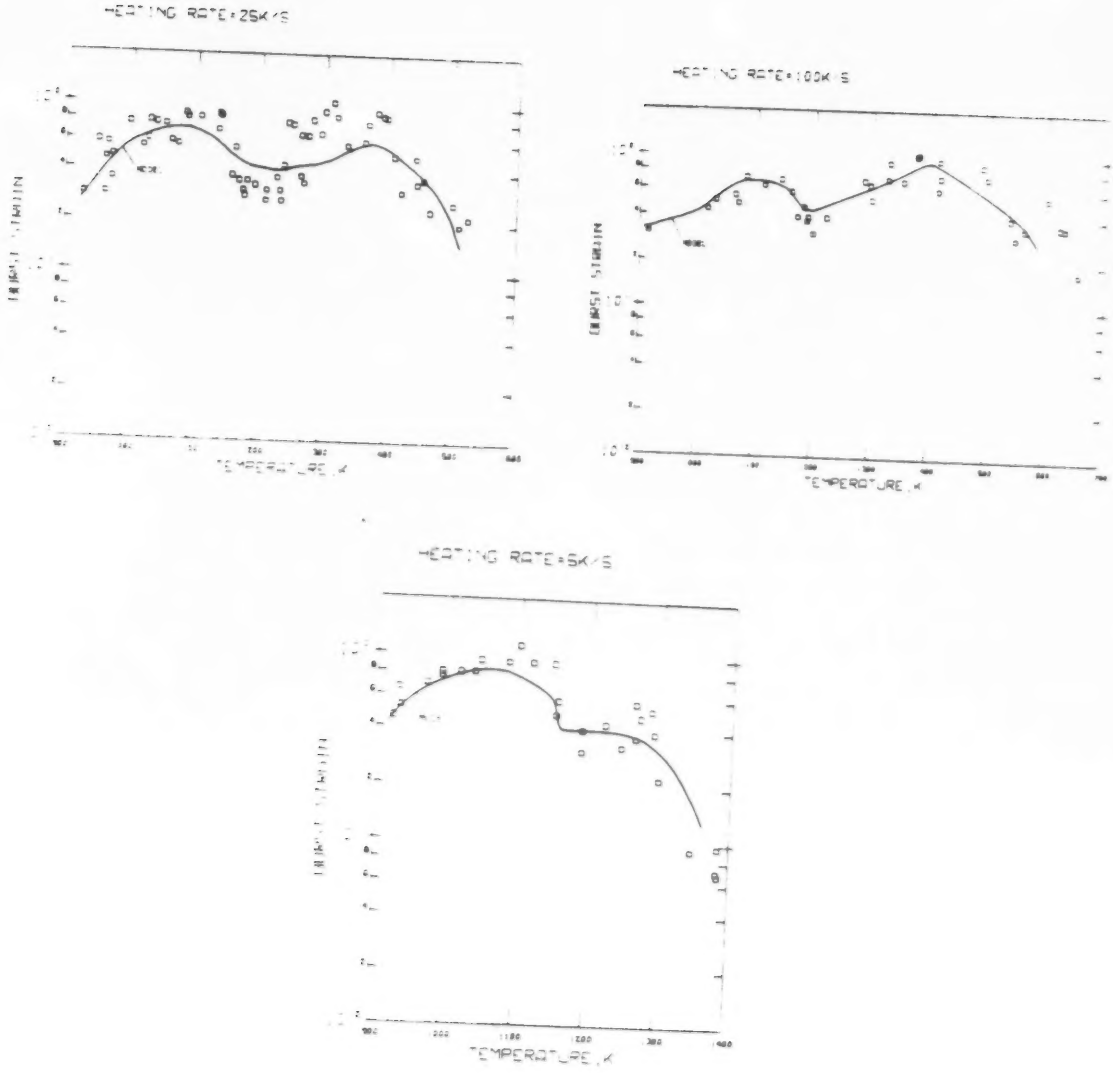

Figure 27
Engineering Burst Strain as a Function of Burst Temperature for Sheaths Tested in Steam at Different Heating Rates and Internal Pressures

Figure 28
Sequence of the Zr/UO_2 Reaction Layers

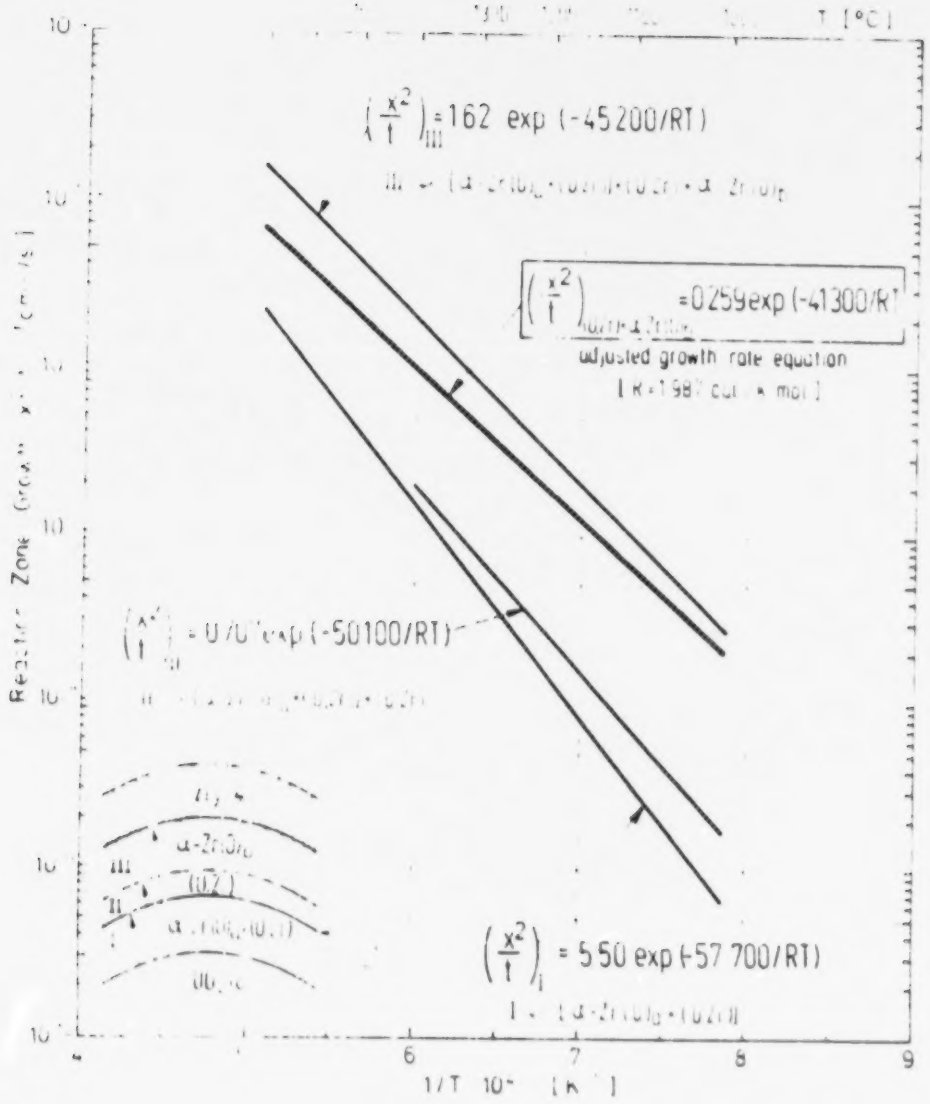

Figure 29
Zr/UO_2 Reaction Layer Growth as a Function of Reciprocal Temperature

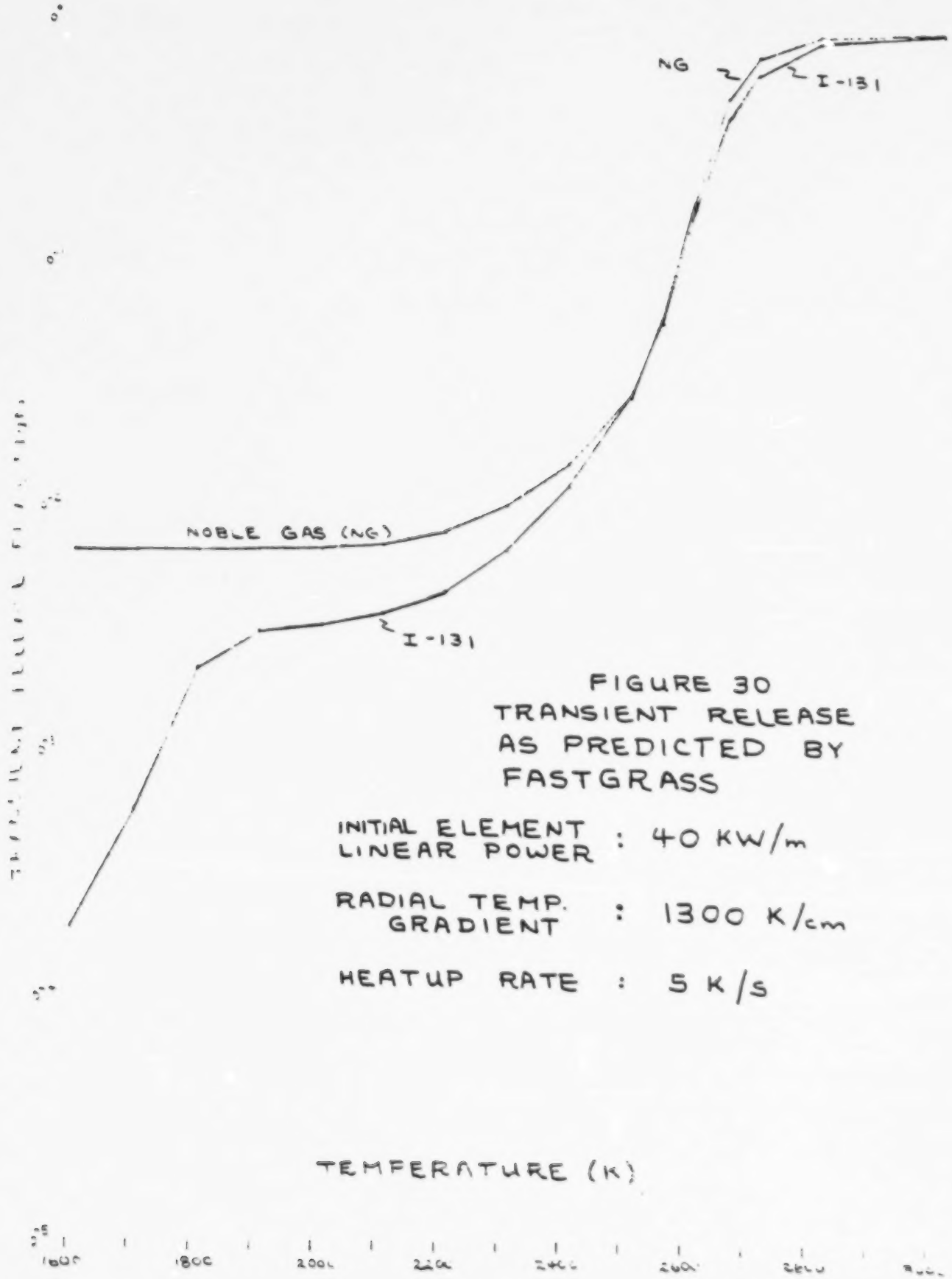

FIGURE 30
TRANSIENT RELEASE
AS PREDICTED BY
FASTGRASS

INITIAL ELEMENT LINEAR POWER : 40 KW/m

RADIAL TEMP. GRADIENT : 1300 K/cm

HEATUP RATE : 5 K/s

CANDU FUEL BEHAVIOUR DURING LARGE BREAK LOSS-OF-COOLANT POWER TRANSIENTS

APPENDIX I

ELOCA MK2 Fuel Behaviour Predictions

APPENDIX I : ELOCA MK2 Fuel Behaviour Predictions

Case 101

The initial element linear power is 55 kW/m at a burnup of 170 MWh/kgU. The element internal gas pressure is 7.3 MPa. The initial centre, average and surface fuel temperatures are 2026K, 1304K and 721K respectively. Therefore, from Figure 22 the initial centre, average and surface fuel enthalpies are 630, 370 and 185 J/g of UO_2 respectively.

The fuel element experiences power transient 'A' with a peak overpower factor of 2.2 at 1.3 seconds and an adiabatic heat addition of 201 J/g of UO_2 for a 55 kW/m element. The coolant boundary conditions are those of heat removal transient '5' with a constant sheath-to-coolant heat transfer coefficient of 1.5 kW/m^2K starting at 0.1 seconds and a peak coolant temperature of 1050K at 5.0 seconds.

The maximum centre, average and surface fuel temperatures are 2136K, 1564K and 1389K respectively. Therefore, the transient results in an increase in the centre, average and surface fuel temperatures of 110K, 260K and 668K respectively. This corresponds to an increase in centre, average and surface fuel enthalpies of 30, 85 and 215 J/g of UO_2 respectively. The sheath temperature increases to 1198K by 7 seconds. The centre and average fuel temperatures peak relatively early in the transient at approximately 2 seconds. The surface fuel temperature peaks later in the transient at approximately 10 seconds.

The internal element gas pressure reaches a maximum of 9.8 MPa at 1.8 seconds. Fuel temperatures are not high enough to result in transient gas release which would further increase the maximum internal gas pressure. The sheath is predicted to lift off the fuel at about 1.8 seconds. The total sheath strain reaches a maximum of 0.97% at 10 seconds. The ZrO_2 layer reaches a maximum thickness of 5.5 microns at 10 seconds. These conditions are not expected to result in sheath failure. The extent of oxidation is not great enough to significantly affect sheath deformation. The sheath temperature is not high enough for the Zr/UO_2 interaction to occur on the inner sheath surface. Also fuel/sheath contact is localised after sheath lift-off.

An increase in average fuel enthalpy from 370 to 455 J/g of UO_2 for conditions of moderate heat transfer from the fuel to the coolant (i.e. 1.5 kW/m^2K) is not expected to result in sheath failure for a high power, high burnup fuel element during the first 10 seconds of a large break LOCA transient.

APPENDIX I : ELOCA MK2 Fuel Behaviour Predictions

Case 102

The initial element linear power is 50 kW/m at a burnup of 170 MWh/kgU. The element internal gas pressure is 3.5 MPa. The initial centre, average and surface fuel temperatures are 1811K, 1192K and 688K respectively. Therefore, from Figure 22 the initial centre, average and surface fuel enthalpies are 540, 340 and 180 J/g of UO_2 respectively.

The fuel element experiences power transient 'A' with a peak overpower factor of 2.2 at 1.3 seconds and an adiabatic heat addition of 183 J/g of UO_2 for a 50 kW/m element. The coolant boundary conditions are those of heat removal transient '5' with a constant sheath-to-coolant heat transfer coefficient of 1.5 kW/m^2K starting at 0.1 seconds and a peak coolant temperature of 1050K at 5.0 seconds.

The maximum centre, average and surface fuel temperatures are 1922K, 1434K and 1227K respectively. Therefore, the transient results in an increase in the centre, average and surface fuel temperatures of 111K, 242K and 539K respectively. This corresponds to an increase in centre, average and surface fuel enthalpies of 35, 75 and 165 J/g of UO_2 respectively. The sheath temperature increases to 1215K by 9 seconds. The centre and average fuel temperatures peak relatively early in the transient at approximately 2 seconds. The surface fuel temperature peaks later in the transient at approximately 9 seconds.

The internal element gas pressure reaches a maximum of 4.8 MPa at 2.0 seconds. Fuel temperatures are not high enough to result in transient gas release which would further increase the maximum internal gas pressure. The sheath does not lift off the fuel during the first 10 seconds of the transient. The total sheath strain reaches a maximum of 0.48% at 1.8 seconds. The ZrO_2 layer reaches a maximum thickness of 5.9 microns at 10^2 seconds. These conditions are not expected to result in sheath failure. The extent of oxidation is not great enough to significantly affect sheath deformation. The sheath temperature is not high enough for the Zr/UO_2 interaction to occur to any extent on the inner sheath surface even though complete fuel/sheath contact is maintained.

An increase in average fuel enthalpy from 340 to 415 J/g of UO_2 for conditions of moderate heat transfer from the fuel to the coolant (i.e. 1.5 kW/m^2K) is not expected to result in sheath failure for a moderate power, high burnup fuel element during the first 10 seconds of a large break LOCA transient.

APPENDIX I : ELOCA MK2 Fuel Behaviour Predictions

Case 103

The initial element linear power is 55 kW/m at a burnup of 170 MWh/kgU. The element internal gas pressure is 7.3 MPa. The initial centre, average and surface fuel temperatures are 2026K, 1304K and 721K respectively. Therefore, from Figure 22 the initial centre, average and surface fuel enthalpies are 630, 370 and 185 J/g of UO_2 respectively.

The fuel element experiences power transient 'A' with a peak overpower factor of 2.2 at 1.3 seconds and an adiabatic heat addition of 201 J/g of UO_2 for a 55 kW/m element. The coolant boundary conditions are those of heat removal transient '3' with a constant sheath-to-coolant heat transfer coefficient of 0.5 kW/m^2K starting at 0.1 seconds and a peak coolant temperature of 1050K at 5.0 seconds.

The maximum centre, average and surface fuel temperatures are 2136K, 1642K and 1528K respectively. Therefore, the transient results in an increase in the centre, average and surface fuel temperatures of 110K, 338K and 807K respectively. This corresponds to an increase in centre, average and surface fuel enthalpies of 30, 110 and 260 J/g of UO_2 respectively. The sheath temperature increases to 1374K by 10 seconds. The centre fuel temperature peaks relatively early in the transient at approximately 2 seconds. The average and surface fuel temperatures peak later in the transient after 10 seconds.

The internal element gas pressure reaches a maximum of 9.6 MPa at 1.5 seconds. Fuel temperatures are not high enough to result in transient gas release which would further increase the maximum internal gas pressure. The sheath is predicted to lift off the fuel at about 1.1 seconds. The total sheath strain reaches a maximum of 1.24% at 10 seconds. The ZrO_2 layer reaches a maximum thickness of 5.4 microns at 10 seconds. These conditions are not expected to result in sheath failure. The extent of oxidation is not great enough to significantly affect sheath deformation. The sheath temperature is just high enough for the Zr/UO_2 interaction to occur on the inner sheath surface. However, fuel/sheath contact is light and localised after sheath lift-off and the extent of the Zr/UO_2 interaction will probably be negligible.

An increase in average fuel enthalpy from 370 to 480 J/g of UO_2 for conditions of degraded heat transfer from the fuel to the coolant (i.e. 0.5 kW/m^2K) is not expected to result in sheath failure for a high power, high burnup fuel element during the first 10 seconds of a large break LOCA transient.

APPENDIX I : ELOCA MK2 Fuel Behaviour Predictions

Case 104

The initial element linear power is 50 kW/m at a burnup of 170 MWh/kgU. The element internal gas pressure is 3.5 MPa. The initial centre, average and surface fuel temperatures are 1811K, 1192K and 688K respectively. Therefore, from Figure 22 the initial centre, average and surface fuel enthalpies are 540, 340 and 180 J/g of UO_2 respectively.

The fuel element experiences power transient 'A' with a peak overpower factor of 2.2 at 1.3 seconds and an adiabatic heat addition of 183 J/g of UO_2 for a 50 kW/m element. The coolant boundary conditions are those of heat removal transient '3' with a constant sheath-to-coolant heat transfer coefficient of 0.5 kW/m^2K starting at 0.1 seconds and a peak coolant temperature of 1050K at 5.0 seconds.

The maximum centre, average and surface fuel temperatures are 1922K, 1490K and 1388K respectively. Therefore, the transient results in an increase in the centre, average and surface fuel temperatures of 111K, 298K and 700K respectively. This corresponds to an increase in centre, average and surface fuel enthalpies of 35, 95 and 220 J/g of UO_2 respectively. The sheath temperature increases to 1382K by 10 seconds. The centre fuel temperature peaks relatively early in the transient at approximately 2 seconds. The average and surface fuel temperatures peak later in the transient after 10 seconds.

The internal element gas pressure reaches a maximum of 5.0 MPa at 10.0 seconds. Fuel temperatures are not high enough to result in transient gas release which would further increase the maximum internal gas pressure. The sheath does not lift off the fuel during the first 10 seconds of the transient. The total sheath strain reaches a maximum of 0.51% at 1.9 seconds. The ZrO_2 layer reaches a maximum thickness of 12.6 microns at 10 seconds. These conditions are not expected to result in sheath failure. The extent of oxidation is not great enough to significantly affect sheath deformation. The sheath temperature is just high enough for the Zr/UO_2 interaction to occur on the inner sheath surface. However, even though complete fuel/sheath contact is maintained the time at temperature is too short for the Zr/UO_2 interaction to occur to any extent during the first 10 seconds of the transient.

An increase in average fuel enthalpy from 340 to 435 J/g of UO_2 for conditions of degraded heat transfer from the fuel to the coolant (i.e. 0.5 kW/m^2K) is not expected to result in sheath failure for a moderate power, high burnup fuel element during the first 10 seconds of a large break LOCA transient.

APPENDIX I : ELOCA MK2 Fuel Behaviour Predictions

Case 105

The initial element linear power is 55 kW/m at a burnup of 170 MWh/kgU. The element internal gas pressure is 7.3 MPa. The initial centre, average and surface fuel temperatures are 2026K, 1304K and 721K respectively. Therefore, from Figure 22 the initial centre, average and surface fuel enthalpies are 630, 370 and 185 J/g of UO_2 respectively.

The fuel element experiences power transient 'A' with a peak overpower factor of 2.2 at 1.3 seconds and an adiabatic heat addition of 201 J/g of UO_2 for a 55 kW/m element. The coolant boundary conditions are those of heat removal transient '4' with a constant sheath-to-coolant heat transfer coefficient of 0.1 kW/m^2K starting at 0.1 seconds and a peak coolant temperature of 1550K at 5.0 seconds.

The maximum centre, average and surface fuel temperatures are 2136K, 1773K and 1749K respectively. Therefore, the transient results in an increase in the centre, average and surface fuel temperatures of 110K, 469K and 1028K respectively. This corresponds to an increase in centre, average and surface fuel enthalpies of 30, 155 and 330 J/g of UO_2 respectively. The sheath temperature increases to 1755K by 10 seconds. The centre fuel temperature peaks relatively early in the transient at approximately 2 seconds. The average and surface fuel temperatures peak later in the transient after 10 seconds.

The internal element gas pressure reaches a maximum of 9.3 MPa at 1.4 seconds. Fuel temperatures are not high enough to result in transient gas release which would further increase the maximum internal gas pressure. The sheath is predicted to lift off the fuel at about 1.4 seconds. The total sheath strain reaches a maximum of 1.59% at 10 seconds. The ZrO_2 layer reaches a maximum thickness of 40.1 microns at 10 seconds. These conditions will probably not result in sheath failure even though the extent of oxidation is great enough to affect sheath deformation. The sheath temperature is high enough for the Zr/UO_2 interaction to occur on the inner sheath surface. However, fuel/sheath contact is light and localised after sheath lift-off and the extent of the Zr/UO_2 interaction will probably be negligible.

An increase in average fuel enthalpy from 370 to 525 J/g of UO_2 for conditions of severely degraded heat transfer from the fuel to the coolant (i.e. 0.1 kW/m^2K) will probably not result in sheath failure for a high power, high burnup fuel element during the first 10 seconds of a large break LOCA transient.

APPENDIX I : ELOCA MK2 Fuel Behaviour Predictions

Case 106

The initial element linear power is 50 kW/m at a burnup of 170 MWh/kgU. The element internal gas pressure is 3.5 MPa. The initial centre, average and surface fuel temperatures are 1811K, 1192K and 688K respectively. Therefore, from Figure 22 the initial centre, average and surface fuel enthalpies are 540, 340 and 180 J/g of UO_2 respectively.

The fuel element experiences power transient 'A' with a peak overpower factor of 2.2 at 1.3 seconds and an adiabatic heat addition of 183 J/g of UO_2 for a 50 kW/m element. The coolant boundary conditions are those of heat removal transient '4' with a constant sheath-to-coolant heat transfer coefficient of 0.1 kW/m^2K starting at 0.1 seconds and a peak coolant temperature of 1550K at 5.0 seconds.

The maximum centre, average and surface fuel temperatures are 1922K, 1628K and 1615K respectively. Therefore, the transient results in an increase in the centre, average and surface fuel temperatures of 111K, 436K and 927K respectively. This corresponds to an increase in centre, average and surface fuel enthalpies of 35, 135 and 290 J/g of UO_2 respectively. The sheath temperature increases to 1615K by 10 seconds. The centre fuel temperature peaks relatively early in the transient at approximately 2 seconds. The average and surface fuel temperatures peak later in the transient after 10 seconds.

The internal element gas pressure reaches a maximum of 5.3 MPa at 10.0 seconds. Fuel temperatures are not high enough to result in transient gas release which would further increase the maximum internal gas pressure. The sheath does not lift off the fuel during the first 10 seconds of the transient. The total sheath strain reaches a maximum of 0.57% at 10.0 seconds. The ZrO_2 layer reaches a maximum thickness of 26.4 microns at 10 seconds. These conditions will probably not result in sheath failure even though the extent of oxidation is great enough to affect sheath deformation. The sheath temperature is high enough for the Zr/UO_2 interaction to occur on the inner sheath surface.

An increase in average fuel enthalpy from 340 to 475 J/g of UO_2 for conditions of severely degraded heat transfer from the fuel to the coolant (i.e. 0.1 kW/m^2K) will probably not result in sheath failure for a moderate power, high burnup fuel element during the first 10 seconds of a large break LOCA transient.

APPENDIX I : ELOCA MK2 Fuel Behaviour Predictions

Case 107

The initial element linear power is 30 kW/m at a burnup of 170 MWh/kgU. The element internal gas pressure is 0.6 MPa. The initial centre, average and surface fuel temperatures are 1129K, 851K and 600K respectively. Therefore, from Figure 22 the initial centre, average and surface fuel enthalpies are 310, 225 and 150 J/g of UO_2 respectively.

The fuel element experiences power transient 'A' with a peak overpower factor of 2.2 at 1.3 seconds and an adiabatic heat addition of 110 J/g of UO_2 for a 30 kW/m element. The coolant boundary conditions are those of heat removal transient '4' with a constant sheath-to-coolant heat transfer coefficient of 0.1 kW/m^2K starting at 0.1 seconds and a peak coolant temperature of 1550K at 5.0 seconds.

The maximum centre, average and surface fuel temperatures are 1207K, 1153K and 1161K respectively. Therefore, the transient results in an increase in the centre, average and surface fuel temperatures of 78K, 302K and 561K respectively. This corresponds to an increase in centre, average and surface fuel enthalpies of 30, 95 and 175 J/g of UO_2 respectively. The sheath temperature increases to 1162K by 10 seconds. The centre fuel temperature peaks relatively early in the transient at approximately 2 seconds. The average and surface fuel temperatures peak later in the transient after 10 seconds.

The internal element gas pressure reaches a maximum of 0.7 MPa at 2.9 seconds. Fuel temperatures are not high enough to result in transient gas release which would further increase the maximum internal gas pressure. The sheath does not lift off the fuel during the transient. The total sheath strain reaches a maximum of 0.05% at 10 seconds. The ZrO_2 layer reaches a maximum thickness of 3.7 microns at 10 seconds. These conditions are not expected to result in sheath failure. The extent of oxidation is not great enough to significantly affect sheath deformation. The sheath temperature is not high enough for the Zr/UO_2 interaction to occur on the inner sheath surface.

An increase in average fuel enthalpy from 225 to 320 J/g of UO_2 for conditions of severely degraded heat transfer from the fuel to the coolant (i.e. 0.1 kW/m^2K) is not expected to result in sheath failure for a low power, high burnup fuel element during the first 10 seconds of a large break LOCA transient.

APPENDIX I : ELOCA MK2 Fuel Behaviour Predictions

Case 108

The initial element linear power is 55 kW/m at a burnup of 170 MWh/kgU. The element internal gas pressure is 7.3 MPa. The initial centre, average and surface fuel temperatures are 2026K, 1304K and 721K respectively. Therefore, from Figure 22 the initial centre, average and surface fuel enthalpies are 630, 370 and 185 J/g of UO_2 respectively.

The fuel element experiences power transient 'B' with a peak overpower factor of 5.0 at 1.3 seconds and an adiabatic heat addition of 336 J/g of UO_2 for a 55 kW/m element. The coolant boundary conditions are those of heat removal transient '2' with a constant sheath-to-coolant heat transfer coefficient of 5.0 kW/m^2K starting at 0.1 seconds and a peak coolant temperature of 1050K at 5.0 seconds.

The maximum centre, average and surface fuel temperatures are 2397K, 1811K and 1415K respectively. Therefore, the transient results in an increase in the centre, average and surface fuel temperatures of 371K, 507K and 694K respectively. This corresponds to an increase in centre, average and surface fuel enthalpies of 140, 170 and 225 J/g of UO_2 respectively. The sheath temperature increases to 1126K by 6 seconds. The centre and average fuel temperatures peak relatively early in the transient at approximately 2 seconds. The surface fuel temperature peaks later in the transient at approximately 10 seconds.

The internal element gas pressure reaches a maximum of 12.0 MPa at 1.9 seconds. The maximum central fuel temperature is high enough to result in a small amount of transient gas release which could further increase the maximum internal gas pressure. The sheath is predicted to lift off the fuel at 2.0 seconds. The total sheath strain reaches a maximum of 1.23% at 10 seconds. The ZrO_2 layer reaches a maximum thickness of 3.6 microns at 10 seconds. These conditions are not expected to result in sheath failure. The extent of oxidation is not great enough to significantly affect sheath deformation. The sheath temperature is not high enough for the Zr/UO_2 interaction to occur on the inner sheath surface. Also fuel/sheath contact is localised after sheath lift-off.

An increase in average fuel enthalpy from 370 to 540 J/g of UO_2 for conditions of moderate heat transfer from the fuel to the coolant (i.e. 5.0 kW/m^2K) is not expected to result in sheath failure for a high power, high burnup fuel element during the first 10 seconds of a large break LOCA transient.

APPENDIX I : ELOCA MK2 Fuel Behaviour Predictions

Case 109

The initial element linear power is 50 kW/m at a burnup of 170 Mwh/kgU. The element internal gas pressure is 3.5 MPa. The initial centre, average and surface fuel temperatures are 1811K, 1192K and 688K respectively. Therefore, from Figure 22 the initial centre, average and surface fuel enthalpies are 540, 340 and 180 J/g of UO_2 respectively.

The fuel element experiences power transient 'B' with a peak overpower factor of 5.0 at 1.3 seconds and an adiabatic heat addition of 305 J/g of UO_2 for a 50 kW/m element. The coolant boundary conditions are those of heat removal transient '2' with a constant sheath-to-coolant heat transfer coefficient of 5.0 kW/m^2K starting at 0.1 seconds and a peak coolant temperature of 1050K at 5.0 seconds.

The maximum centre, average and surface fuel temperatures are 2187K, 1666K and 1102K respectively. Therefore, the transient results in an increase in the centre, average and surface fuel temperatures of 376K, 474K and 414K respectively. This corresponds to an increase in centre, average and surface fuel enthalpies of 140, 150 and 120 J/g of UO_2 respectively. The sheath temperature increases to 1143K by 6.3 seconds. The centre, average and surface fuel temperatures peak relatively early in the transient at approximately 2 seconds.

The internal element gas pressure reaches a maximum of 5.8 MPa at 1.9 seconds. Fuel temperatures are not high enough to result in transient gas release which would further increase the maximum internal gas pressure. The sheath does not lift off the fuel during the first 10 seconds of the transient. The total sheath strain reaches a maximum of 0.88% at 1.9 seconds. The ZrO_2 layer reaches a maximum thickness of 3.9 microns at 10 seconds. These conditions are not expected to result in sheath failure. The extent of oxidation is not great enough to significantly affect sheath deformation. The sheath temperature is not high enough for the Zr/UO_2 interaction to occur to any extent on the inner sheath surface even though complete fuel/sheath contact is maintained.

An increase in average fuel enthalpy from 340 to 490 J/g of UO_2 for conditions of moderate heat transfer from the fuel to the coolant (i.e. 5.0 kW/m^2K) is not expected to result in sheath failure for a moderate power, high burnup fuel element during the first 10 seconds of a large break LOCA transient.

APPENDIX I : ELOCA MK2 Fuel Behaviour Predictions

Case 110

The initial element linear power is 55 kW/m at a burnup of 170 MWh/kgU. The element internal gas pressure is 7.3 MPa. The initial centre, average and surface fuel temperatures are 2026K, 1304K and 721K respectively. Therefore, from Figure 22 the initial centre, average and surface fuel enthalpies are 630, 370 and 185 J/g of UO_2 respectively.

The fuel element experiences power transient 'B' with a peak overpower factor of 5.0 at 1.3 seconds and an adiabatic heat addition of 336 J/g of UO_2 for a 55 kW/m element. The coolant boundary conditions are those of heat removal transient '3' with a constant sheath-to-coolant heat transfer coefficient of 0.5 kW/m^2K starting at 0.1 seconds and a peak coolant temperature of 1050K at 5.0 seconds.

The maximum centre, average and surface fuel temperatures are 2397K, 1934K and 1761K respectively. Therefore, the transient results in an increase in the centre, average and surface fuel temperatures of 371K, 630K and 1040K respectively. This corresponds to an increase in centre, average and surface fuel enthalpies of 140, 215 and 335 J/g of UO_2 respectively. The sheath temperature increases to 1547K by 10 seconds. The centre fuel temperature peaks relatively early in the transient at approximately 2 seconds. The average and surface fuel temperatures peak later in the transient at 7 and after 10 seconds respectively.

The internal element gas pressure reaches a maximum of 9.8 MPa at 1.1 seconds. The central fuel temperature is high enough to result in a small amount of transient gas release which could further increase the maximum internal gas pressure. The sheath is predicted to lift off the fuel at about 1.2 seconds. The total sheath strain reaches a maximum of 1.94% at 10 seconds. The ZrO_2 layer reaches a maximum thickness of 28.0 microns at 10^2 seconds. These conditions will probably not result in sheath failure. The extent of oxidation is enough to significantly affect sheath deformation. The sheath temperature is high enough for the Zr/UO_2 interaction to occur on the inner sheath surface. However, fuel/sheath contact is light and localised after sheath lift-off and the extent of the Zr/UO_2 interaction will probably be negligible.

An increase in average fuel enthalpy from 370 to 585 J/g of UO_2 for conditions of degraded heat transfer from the fuel to the coolant (i.e. 0.5 kW/m^2K) will probably not result in sheath failure for a high power, high burnup fuel element during the first 10 seconds of a large break LOCA transient.

APPENDIX I : ELOCA MK2 Fuel Behaviour Predictions

Case 111

The initial element linear power is 50 kW/m at a burnup of 170 MWh/kgU. The element internal gas pressure is 3.5 MPa. The initial centre, average and surface fuel temperatures are 1811K, 1192K and 688K respectively. Therefore, from Figure 22 the initial centre, average and surface fuel enthalpies are 540, 340 and 180 J/g of UO_2 respectively.

The fuel element experiences power transient 'B' with a peak overpower factor of 5.0 at 1.3 seconds and an adiabatic heat addition of 305 J/g of UO_2 for a 50 kW/m element. The coolant boundary conditions are those of heat removal transient '3' with a constant sheath-to-coolant heat transfer coefficient of 0.5 kW/m^2K starting at 0.1 seconds and a peak coolant temperature of 1050K at 5.0 seconds.

The maximum centre, average and surface fuel temperatures are 2187K, 1765K and 1579K respectively. Therefore, the transient results in an increase in the centre, average and surface fuel temperatures of 376K, 573K and 891K respectively. This corresponds to an increase in centre, average and surface fuel enthalpies of 140, 180 and 280 J/g of UO_2 respectively. The sheath temperature increases to 1561K at 6.9 seconds. The centre and average fuel temperatures peak relatively early in the transient at approximately 2.5 seconds. The surface fuel temperature peaks later in the transient at 9.8 seconds.

The internal element gas pressure reaches a maximum of 5.9 MPa at 2.0 seconds. Fuel temperatures are not high enough to result in transient gas release which would further increase the maximum internal gas pressure. The sheath lifts off the fuel at 7.2 seconds. The total sheath strain reaches a maximum of 0.97% at 2.0 seconds. The ZrO_2 layer reaches a maximum thickness of 29.6 microns at 10 seconds. These conditions will probably not result in sheath failure. The extent of oxidation is enough to affect sheath deformation. The sheath temperature is high enough for the Zr/UO_2 interaction to occur on the inner sheath surface.

An increase in average fuel enthalpy from 340 to 520 J/g of UO_2 for conditions of degraded heat transfer from the fuel to the coolant (i.e. 0.5 kW/m^2K) is not expected to result in sheath failure for a moderate power, high burnup fuel element during the first 10 seconds of a large break LOCA transient.

APPENDIX I : ELOCA MK2 Fuel Behaviour Predictions

Case 112

The initial element linear power is 55 kW/m at a burnup of 170 MWh/kgU. The element internal gas pressure is 7.3 MPa. The initial centre, average and surface fuel temperatures are 2026K, 1304K and 721K respectively. Therefore, from Figure 22 the initial centre, average and surface fuel enthalpies are 630, 370 and 185 J/g of UO_2 respectively.

The fuel element experiences power transient '8' with a peak overpower factor of 5.0 at 1.3 seconds and an adiabatic heat addition of 336 J/g of UO_2 for a 55 kW/m element. The coolant boundary conditions are those of heat removal transient '4' with a constant sheath-to-coolant heat transfer coefficient of 0.1 kW/m^2K starting at 0.1 seconds and a peak coolant temperature of 1550K at 5.0 seconds.

The maximum centre, average and surface fuel temperatures are 2397K, 2023K and 1954K respectively. Therefore, the transient results in an increase in the centre, average and surface fuel temperatures of 371K, 719K and 1233K respectively. This corresponds to an increase in centre, average and surface fuel enthalpies of 140, 250 and 405 J/g of UO_2 respectively. The sheath temperature increases to 2086K by 5.1 seconds. The centre fuel temperature peaks relatively early in the transient at approximately 2 seconds. The average and surface fuel temperatures peak at 5.1 seconds which was when the ELOCA MK2 calculation terminated.

The internal element gas pressure reaches a maximum of 9.6 MPa at 1.3 seconds. The central fuel temperature is high enough to result in a small amount of transient gas release which could further increase the maximum internal gas pressure. The sheath is predicted to lift off the fuel at about 1.4 seconds. The total sheath strain reaches a maximum of 1.75% at 5.1 seconds. The sheath temperature exceeds the melting point of beta phase Zircaloy-4 and absorbed hydrogen and oxygen will affect the deformation behaviour of the sheath. The Zr/UO_2 interaction will occur at least locally on the inner sheath surface.

An increase in average fuel enthalpy from 370 to 620 J/g of UO_2 for conditions of severely degraded heat transfer from the fuel to the coolant (i.e. 0.1 kW/m^2K) will probably result in sheath failure due to localised melting or overstrain beneath an oxide crack for a high power, high burnup fuel element during the first 10 seconds of a large break LOCA transient.

APPENDIX I : ELOCA MK2 Fuel Behaviour Predictions

Case 113

The initial element linear power is 50 kW/m at a burnup of 170 MWh/kgU. The element internal gas pressure is 3.5 MPa. The initial centre, average and surface fuel temperatures are 1611K, 1192K and 688K respectively. Therefore, from Figure 22 the initial centre, average and surface fuel enthalpies are 540, 340 and 180 J/g of UO_2 respectively.

The fuel element experiences power transient '8' with a peak overpower factor of 5.0 at 1.3 seconds and an adiabatic heat addition of 305 J/g of UO_2 for a 50 kW/m element. The coolant boundary conditions are those of heat removal transient '4' with a constant sheath-to-coolant heat transfer coefficient of 0.1 kW/m^2K starting at 0.1 seconds and a peak coolant temperature of 1550K at 5.0 seconds.

The maximum centre, average and surface fuel temperatures are 2187K, 1970K and 2023K respectively. Therefore, the transient results in an increase in the centre, average and surface fuel temperatures of 376K, 778K and 1335K respectively. This corresponds to an increase in centre, average and surface fuel enthalpies of 140, 260 and 440 J/g of UO_2 respectively. The sheath temperature increases to 2047K by 10 seconds. The centre fuel temperature peaks relatively early in the transient at approximately 2 seconds. The average and surface fuel temperatures peak later in the transient after 10 seconds.

The internal element gas pressure reaches a maximum of 6.0 MPa at 6.7 seconds. Fuel temperatures are not high enough to result in transient gas release which would further increase the maximum internal gas pressure. The sheath lifts off the fuel at 6.8 seconds. The total sheath strain reaches a maximum of 1.24% at 10.0 seconds. The ZrO_2 layer reaches a maximum thickness of 95.3 microns at 10 seconds. These conditions will probably result in sheath failure due to localised melting or overstrain at an oxide crack. The extent of oxidation is great enough to affect sheath deformation. The sheath temperature is high enough for the Zr/UO_2 interaction to occur on the inner sheath surface.

An increase in average fuel enthalpy from 340 to 600 J/g of UO_2 for conditions of severely degraded heat transfer from the fuel to the coolant (i.e. 0.1 kW/m^2K) will probably result in sheath failure for a moderate power, high burnup fuel element during the first 10 seconds of a large break LOCA transient.

APPENDIX I : ELOCA MK2 Fuel Behaviour Predictions

Case 114

The initial element linear power is 55 kW/m at a burnup of 170 MWh/kgU. The element internal gas pressure is 7.3 MPa. The initial centre, average and surface fuel temperatures are 2026K, 1304K and 721K respectively. Therefore, from Figure 22 the initial centre, average and surface fuel enthalpies are 630, 370 and 185 J/g of UO_2 respectively.

The fuel element experiences power transient 'D' with a peak overpower factor of 5.0 at 1.3 seconds and an adiabatic heat addition of 437 J/g of UO_2 for a 55 kW/m element. The coolant boundary conditions are those of heat removal transient '1' with a constant sheath-to-coolant heat transfer coefficient of 50.0 kW/m^2K and a constant coolant temperature of 550K throughout the transient.

The maximum centre, average and surface fuel temperatures are 2540K, 1792K and 849K respectively. Therefore, the transient results in an increase in the centre, average and surface fuel temperatures of 514K, 488K and 128K respectively. This corresponds to an increase in centre, average and surface fuel enthalpies of 210, 160 and 40 J/g of UO_2 respectively. The sheath temperature increases to 639K by 1.8 seconds. The centre, average and surface fuel temperatures peak relatively early in the transient by approximately 3 seconds.

The internal element gas pressure reaches a maximum of 11.4 MPa at 2.2 seconds. The central fuel temperature is high enough to result in a small amount of transient gas release which could further increase the maximum internal gas pressure. The sheath is predicted to lift off the fuel at about 5.1 seconds. However, by 2.3 seconds 0.44% athermal strain has occurred. Therefore, non-ductile, PCI-type sheath failure could occur at this time. The total sheath strain reaches a maximum of 1.22% at 2.6 seconds. The ZrO_2 layer does not grow during the transient. The extent of oxidation is not great enough to significantly affect sheath deformation. The sheath temperature is not high enough for the Zr/UO_2 interaction to occur on the inner sheath surface.

An increase in average fuel enthalpy from 370 to 530 J/g of UO_2 for conditions of good heat transfer from the fuel to the coolant (i.e. 50.0 kW/m^2K) could result in non-ductile, PCI-type sheath failure for a high power, high burnup fuel element during the first 10 seconds of a large break LOCA transient.

APPENDIX I : ELOCA MK2 Fuel Behaviour Predictions

Case 115

The initial element linear power is 50 kW/m at a burnup of 170 MWh/kgU. The element internal gas pressure is 3.5 MPa. The initial centre, average and surface fuel temperatures are 1811K, 1192K and 688K respectively. Therefore, from Figure 22 the initial centre, average and surface fuel enthalpies are 540, 340 and 180 J/g of UO_2 respectively.

The fuel element experiences power transient 'D' with a peak overpower factor of 5.0 at 1.3 seconds and an adiabatic heat addition of 397 J/g of UO_2 for a 50 kW/m element. The coolant boundary conditions are those of heat removal transient '1' with a constant sheath-to-coolant heat transfer coefficient of 50.0 kW/m^2K and a constant coolant temperature of 550K throughout the transient.

The maximum centre, average and surface fuel temperatures are 2337K, 1645K and 802K respectively. Therefore, the transient results in an increase in the centre, average and surface fuel temperatures of 526K, 453K and 114K respectively. This corresponds to an increase in centre, average and surface fuel enthalpies of 205, 140 and 30 J/g of UO_2 respectively. The sheath temperature increases to 633K by 1.7 seconds. The centre, average and surface fuel temperatures peak relatively early in the transient by approximately 3 seconds.

The internal element gas pressure reaches a maximum of 5.5 MPa at 2.2 seconds. The central fuel temperature is high enough to result in a small amount of transient gas release which could further increase the maximum internal gas pressure. The sheath is predicted to lift off the fuel at about 5.7 seconds. However, by 2.3 seconds 0.32% athermal strain has occurred. Therefore, non-ductile, PCI-type sheath failure could occur at this time. The total sheath strain reaches a maximum of 1.00% at 2.6 seconds. The ZrO_2 layer does not grow during the transient. The extent of oxidation is not great enough to significantly affect sheath deformation. The sheath temperature is not high enough for the Zr/UO_2 interaction to occur on the inner sheath surface.

An increase in average fuel enthalpy from 340 to 480 J/g of UO_2 for conditions of good heat transfer from the fuel to the coolant (i.e. 50.0 kW/m^2K) could result in non-ductile, PCI-type sheath failure for a moderate power, high burnup fuel element during the first 10 seconds of a large break LOCA transient.

APPENDIX I : ELOCA MK2 Fuel Behaviour Predictions

Case 116

The initial element linear power is 55 kW/m at a burnup of 170 MWh/kgU. The element internal gas pressure is 7.3 MPa. The initial centre, average and surface fuel temperatures are 2026K, 1304K and 721K respectively. Therefore, from Figure 22 the initial centre, average and surface fuel enthalpies are 630, 370 and 185 J/g of UO_2 respectively.

The fuel element experiences power transient 'D' with a peak overpower factor of 5.0 at 1.3 seconds and an adiabatic heat addition of 437 J/g of UO_2 for a 55 kW/m element. The coolant boundary conditions are those of heat removal transient '5' with a constant sheath-to-coolant heat transfer coefficient of 1.5 kW/m^2K starting at 0.1 seconds and a peak coolant temperature of 1050K at 5.0 seconds.

The maximum centre, average and surface fuel temperatures are 2543K, 2120K and 1732K respectively. Therefore, the transient results in an increase in the centre, average and surface fuel temperatures of 517K, 717K and 1011K respectively. This corresponds to an increase in centre, average and surface fuel enthalpies of 210, 285 and 325 J/g of UO_2 respectively. The sheath temperature increases to 1360K by 5.5 seconds. The centre and average fuel temperatures peak relatively early in the transient at approximately 3 seconds. The surface fuel temperature peaks later in the transient at 8.3 seconds.

The internal element gas pressure reaches a maximum of 10.4 MPa at 1.3 seconds. Fuel temperatures are high enough to result in transient gas release which would further increase the maximum internal gas pressure. The sheath is predicted to lift off the fuel at about 1.3 seconds. The total sheath strain reaches a maximum of 2.10% at 8.0 seconds. The ZrO_2 layer reaches a maximum thickness of 12.1 microns at 10 seconds. These conditions are not expected to result in sheath failure. The extent of oxidation is not great enough to significantly affect sheath deformation. The sheath temperature is just high enough for the Zr/UO_2 interaction to occur on the inner sheath surface. However, fuel/sheath contact is light and localised after sheath lift-off and the extent of the Zr/UO_2 interaction will probably be negligible.

An increase in average fuel enthalpy from 370 to 655 J/g of UO_2 for conditions of moderate heat transfer from the fuel to the coolant (i.e. 1.5 kW/m^2K) is not expected to result in sheath failure for a high power, high burnup fuel element during the first 10 seconds of a large break LOCA transient.

APPENDIX I : ELOCA MK2 Fuel Behaviour Predictions

Case 117

The initial element linear power is 50 kW/m at a burnup of 170 MWh/kgU. The element internal gas pressure is 3.5 MPa. The initial centre, average and surface fuel temperatures are 1811K, 1192K and 688K respectively. Therefore, from Figure 22 the initial centre, average and surface fuel enthalpies are 540, 340 and 180 J/g of UO_2 respectively.

The fuel element experiences power transient 'D' with a peak overpower factor of 5.0 at 1.3 seconds and an adiabatic heat addition of 397 J/g of UO_2 for a 50 kW/m element. The coolant boundary conditions are those of heat removal transient '5' with a constant sheath-to-coolant heat transfer coefficient of 1.5 kW/m^2K starting at 0.1 seconds and a peak coolant temperature of 1050K at 5.0 seconds.

The maximum centre, average and surface fuel temperatures are 2341K, 1916K and 1451K respectively. Therefore, the transient results in an increase in the centre, average and surface fuel temperatures of 530K, 724K and 763K respectively. This corresponds to an increase in centre, average and surface fuel enthalpies of 210, 235 and 240 J/g of UO_2 respectively. The sheath temperature increases to 1435K by 2.8 seconds. The centre, average and surface fuel temperatures also peak at 2.8 seconds

The internal element gas pressure reaches a maximum of 6.7 MPa at 2.8 seconds. The central fuel temperature is high enough to result in a small amount of transient gas release which would further increase the maximum internal gas pressure. The sheath is predicted to lift off the fuel at about 6.7 seconds. The total sheath strain reaches a maximum of 1.25% at 2.8 seconds. The ZrO_2 layer reaches a maximum thickness of 17.0 microns at 10 seconds. These conditions are not expected to result in sheath failure. The extent of oxidation is not great enough to significantly affect sheath deformation. The sheath temperature is just high enough for the Zr/UO_2 interaction to occur on the inner sheath surface. However, fuel/sheath contact is light and localised after sheath lift-off and the extent of the Zr/UO_2 interaction will probably be negligible.

An increase in average fuel enthalpy from 340 to 575 J/g of UO_2 for conditions of moderate heat transfer from the fuel to the coolant (i.e. 1.5 kW/m^2K) is not expected to result in sheath failure for a moderate power, high burnup fuel element during the first 10 seconds of a large break LOCA transient.

APPENDIX I : ELOCA MK2 Fuel Behaviour Predictions

Case 118

The initial element linear power is 55 kW/m at a burnup of 170 MWh/kgU. The element internal gas pressure is 7.3 MPa. The initial centre, average and surface fuel temperatures are 2026K, 1304K and 721K respectively. Therefore, from Figure 22 the initial centre, average and surface fuel enthalpies are 630, 370 and 185 J/g of UO_2 respectively.

The fuel element experiences power transient 'D' with a peak overpower factor of 5.0 at 1.3 seconds and an adiabatic heat addition of 437 J/g of UO_2 for a 55 kW/m element. The coolant boundary conditions are those of heat removal transient '4' with a constant sheath-to-coolant heat transfer coefficient of 0.1 kW/m^2K starting at 0.1 seconds and a peak coolant temperature of 1550K at 5.0 seconds.

The maximum centre, average and surface fuel temperatures are 2543K, 2211K and 2023K respectively. Therefore, the transient results in an increase in the centre, average and surface fuel temperatures of 517K, 907K and 1302K respectively. This corresponds to an increase in centre, average and surface fuel enthalpies of 210, 325 and 435J/g of UO_2 respectively. The sheath temperature increases to 2063K by 2.9 seconds. The centre, average and surface fuel temperatures are at their maximums at 2.9 seconds when the ELOCA MK2 calculation terminates.

The internal element gas pressure reaches a maximum of 9.5 MPa at 1.3 seconds. Fuel temperatures are high enough to result in transient gas release which could further increase the maximum internal gas pressure. The sheath is predicted to lift off the fuel at about 1.1 seconds. The total sheath strain reaches a maximum of 2.05% at 2.9 seconds. The ZrO_2 layer reaches a thickness of 30.9 microns at 2.9 seconds. These conditions will probably result in sheath failure due to localised melting or overstrain under an oxide crack. The extent of oxidation is great enough to affect sheath deformation. The sheath temperature is high enough for the Zr/UO_2 interaction to occur on the inner sheath surface wherever fuel/sheath contact exists.

An increase in average fuel enthalpy from 370 to 695 J/g of UO_2 for conditions of severely degraded heat transfer from the fuel to the coolant (i.e. 0.1 kW/m^2K) will probably result in sheath failure for a high power, high burnup fuel element during the first 10 seconds of a large break LOCA transient.

APPENDIX I : ELOCA MK2 Fuel Behaviour Predictions

Case 119

The initial element linear power is 50 kW/m at a burnup of 170 MWh/kgU. The element internal gas pressure is 3.5 MPa. The initial centre, average and surface fuel temperatures are 1811K, 1192K and 688K respectively. Therefore, from Figure 22 the initial centre, average and surface fuel enthalpies are 540, 340 and 180 J/g of UO_2 respectively.

The fuel element experiences power transient 'D' with a peak overpower factor of 5.0 at 1.3 seconds and an adiabatic heat addition of 397 J/g of UO_2 for a 55 kW/m element. The coolant boundary conditions are those of heat removal transient '4' with a constant sheath-to-coolant heat transfer coefficient of 0.1 kW/m^2K starting at 0.1 seconds and a peak coolant temperature of 1550K at 5.0 seconds.

The maximum centre, average and surface fuel temperatures are 2341K, 2122K and 2125K respectively. Therefore, the transient results in an increase in the centre, average and surface fuel temperatures of 530K, 930K and 1437K respectively. This corresponds to an increase in centre, average and surface fuel enthalpies of 210, 315 and 475J/g of UO_2 respectively. The sheath temperature increases to 2126K by 4.6 seconds. The central fuel temperature peaks at 2.8 seconds. The average and surface fuel temperatures are at their maximums at 4.6 seconds when the ELOCA MK2 calculation terminates.

The internal element gas pressure reaches a maximum of 6.4 MPa at 4.6 seconds. Fuel temperatures are high enough to result in transient gas release which could further increase the maximum internal gas pressure. The sheath is predicted not to lift off the fuel. The total sheath strain reaches a maximum of 1.44% at 4.6 seconds. The ZrO_2 layer reaches a thickness of 80.0 microns at 4.6 seconds. These conditions will probably result in sheath failure due to localised melting or overstrain under an oxide crack. The extent of oxidation is great enough to affect sheath deformation. The sheath temperature is high enough for the Zr/UO_2 interaction to occur on the inner sheath surface wherever fuel/sheath contact exists.

An increase in average fuel enthalpy from 340 to 655 J/g of UO_2 for conditions of severely degraded heat transfer from the fuel to the coolant (i.e. 0.1 kW/m^2K) will probably result in sheath failure for a moderate power, high burnup fuel element during the first 10 seconds of a large break LOCA transient.

APPENDIX I : ELOCA MK2 Fuel Behaviour Predictions

Case 120

The initial element linear power is 55 kW/m at a burnup of 170 MWh/kgU. The element internal gas pressure is 7.3 MPa. The initial centre, average and surface fuel temperatures are 2026K, 1304K and 721K respectively. Therefore, from Figure 22 the initial centre, average and surface fuel enthalpies are 630, 370 and 185 J/g of UO_2 respectively.

The fuel element experiences power transient 'C' with a peak overpower factor of 10.0 at 1.3 seconds and an adiabatic heat addition of 559 J/g of UO_2 for a 55 kW/m element. The coolant boundary conditions are those of heat removal transient '2' with a constant sheath-to-coolant heat transfer coefficient of 5.0 kW/m^2K starting at 0.1 seconds and a peak coolant temperature of 1050K at 5.0 seconds.

The maximum centre, average and surface fuel temperatures are 2762K, 2301K and 1666K respectively. Therefore, the transient results in an increase in the centre, average and surface fuel temperatures of 736K, 997K and 945K respectively. This corresponds to an increase in centre, average and surface fuel enthalpies of 330, 360 and 305 J/g of UO_2 respectively. The sheath temperature increases to 1169K by 6 seconds. The centre, average and surface fuel temperatures peak relatively early in the transient at approximately 2 seconds.

The internal element gas pressure reaches a maximum of 12.8 MPa at 1.4 seconds. Fuel temperatures are high enough to result in transient gas release which would further increase the maximum internal gas pressure. The sheath is predicted to lift off the fuel at about 1.4 seconds. The total sheath strain reaches a maximum of 2.26% at 8.1 seconds. The ZrO_2 layer reaches a maximum thickness of 4.5 microns at 10 seconds. These conditions are not expected to result in sheath failure. The extent of oxidation is not great enough to significantly affect sheath deformation. The sheath temperature is not high enough for the Zr/UO_2 interaction to occur on the inner sheath surface. Also fuel/sheath contact is localised after sheath lift-off.

An increase in average fuel enthalpy from 370 to 730 J/g of UO_2 for conditions of moderate heat transfer from the fuel to the coolant (i.e. 5.0 kW/m^2K) is not expected to result in sheath failure for a high power, high burnup fuel element during the first 10 seconds of a large break LOCA transient.

APPENDIX I : ELOCA MK2 Fuel Behaviour Predictions

Case 121

The initial element linear power is 50 kW/m at a burnup of 170 MWh/kgU. The element internal gas pressure is 3.5 MPa. The initial centre, average and surface fuel temperatures are 1811K, 1192K and 688K respectively. Therefore, from Figure 22 the initial centre, average and surface fuel enthalpies are 540, 340 and 180 J/g of UO_2 respectively.

The fuel element experiences power transient 'C' with a peak overpower factor of 10.0 at 1.3 seconds and an adiabatic heat addition of 508 J/g of UO_2 for a 50 kW/m element. The coolant boundary conditions are those of heat removal transient '2' with a constant sheath-to-coolant heat transfer coefficient of 5.0 kW/m^2K starting at 0.1 seconds and a peak coolant temperature of 1050K at 5.0 seconds.

The maximum centre, average and surface fuel temperatures are 2567K, 2091K and 1306K respectively. Therefore, the transient results in an increase in the centre, average and surface fuel temperatures of 756K, 899K and 618K respectively. This corresponds to an increase in centre, average and surface fuel enthalpies of 315, 305 and 190 J/g of UO_2 respectively. The sheath temperature increases to 1219K by 2 seconds. The centre, average and surface fuel temperatures also peak by 2.0 seconds.

The internal element gas pressure reaches a maximum of 8.0 MPa at 1.9 seconds. Fuel temperatures are high enough to result in transient gas release which would further increase the maximum internal gas pressure. The sheath is predicted to lift off the fuel at about 6.8 seconds. The total sheath strain reaches a maximum of 1.63% at 2 seconds. The ZrO_2 layer reaches a maximum thickness of 5.7 microns at 10 seconds. These conditions are not expected to result in sheath failure. The extent of oxidation is not great enough to significantly affect sheath deformation. The sheath temperature is not high enough for the Zr/UO_2 interaction to occur on the inner sheath surface. Also fuel/sheath contact is localised after sheath lift-off.

An increase in average fuel enthalpy from 340 to 645 J/g of UO_2 for conditions of moderate heat transfer from the fuel to the coolant (i.e. 1.5 kW/m^2K) is not expected to result in sheath failure for a moderate power, high burnup fuel element during the first 10 seconds of a large break LOCA transient.

APPENDIX I : ELOCA MK2 Fuel Behaviour Predictions

Case 122

The initial element linear power is 55 kW/m at a burnup of 170 MWh/kgU. The element internal gas pressure is 7.3 MPa. The initial centre, average and surface fuel temperatures are 2026K, 1304K and 721K respectively. Therefore, from Figure 22 the initial centre, average and surface fuel enthalpies are 630, 370 and 185 J/g of UO_2 respectively.

The fuel element experiences power transient 'C' with a peak overpower factor of 10.0 at 1.3 seconds and an adiabatic heat addition of 559 J/g of UO_2 for a 55 kW/m element. The coolant boundary conditions are those of heat removal transient '3' with a constant sheath-to-coolant heat transfer coefficient of 0.5 kW/m^2K starting at 0.1 seconds and a peak coolant temperature of 1050K at 5.0 seconds.

The maximum centre, average and surface fuel temperatures are 2762K, 2417K and 2169K respectively. Therefore, the transient results in an increase in the centre, average and surface fuel temperatures of 736K, 1113K and 1448K respectively. This corresponds to an increase in centre, average and surface fuel enthalpies of 330, 410 and 490 J/g of UO_2 respectively. The sheath temperature increases to 2076K by 3.4 seconds. The centre and average fuel temperatures peak relatively early in the transient at approximately 2 seconds. The surface fuel temperature is at a maximum when the ELOCA MK2 calculation terminates at 3.4 seconds.

The internal element gas pressure reaches a maximum of 10.2 MPa at 1.0 seconds. Fuel temperatures are high enough to result in transient gas release which would further increase the maximum internal gas pressure. The sheath is predicted to lift off the fuel at about 1.0 seconds. The total sheath strain reaches a maximum of 2.51% at 3.4 seconds. The ZrO_2 layer reaches a maximum thickness of 50.5 microns at 3.4 seconds. These conditions will result in sheath failure due to localised melting or overstrain under an oxide crack. The extent of oxidation is great enough to significantly affect sheath deformation. The sheath temperature is high enough for the Zr/UO_2 interaction to occur on the inner sheath surface.

An increase in average fuel enthalpy from 370 to 780 J/g of UO_2 for conditions of degraded heat transfer from the fuel to the coolant (i.e. 0.5 kW/m^2K) is not expected to result in sheath failure for a high power, high burnup fuel element during the first 10 seconds of a large break LOCA transient.

APPENDIX I : ELOCA MK2 Fuel Behaviour Predictions

Case 123

The initial element linear power is 50 kW/m at a burnup of 170 MWh/kgU. The element internal gas pressure is 3.5 MPa. The initial centre, average and surface fuel temperatures are 1811K, 1192K and 688K respectively. Therefore, from Figure 22 the initial centre, average and surface fuel enthalpies are 540, 340 and 180 J/g of UO_2 respectively.

The fuel element experiences power transient 'C' with a peak overpower factor of 10.0 at 1.3 seconds and an adiabatic heat addition of 508 J/g of UO_2 for a 50 kW/m element. The coolant boundary conditions are those of heat removal transient '3' with a constant sheath-to-coolant heat transfer coefficient of 0.5 kW/m^2K starting at 0.1 seconds and a peak coolant temperature of 1050K at 5.0 seconds.

The maximum centre, average and surface fuel temperatures are 2567K, 2244K and 2035K respectively. Therefore, the transient results in an increase in the centre, average and surface fuel temperatures of 756K, 1052K and 1347K respectively. This corresponds to an increase in centre, average and surface fuel enthalpies of 315, 365 and 445 J/g of UO_2 respectively. The sheath temperature increases to 2025K by 4.2 seconds. The centre fuel temperature peaks relatively early in the transient at approximately 2 seconds. The average and surface fuel temperatures peak later in the transient at 3.3 and 5.6 seconds respectively.

The internal element gas pressure reaches a maximum of 7.5 MPa at 1.9 seconds. Fuel temperatures are high enough to result in transient gas release which would further increase the maximum internal gas pressure. The sheath is predicted to lift off the fuel at about 4.7 seconds. The total sheath strain reaches a maximum of 1.91% at 7.7 seconds. The ZrO_2 layer reaches a maximum thickness of 144 microns at 10 seconds. These conditions will probably result in sheath failure due to localised melting or overstrain beneath an oxide crack. The extent of oxidation is great enough to significantly affect sheath deformation. The sheath temperature is high enough for the Zr/UO_2 interaction to occur on the inner sheath surface.

An increase in average fuel enthalpy from 370 to 705 J/g of UO_2 for conditions of degraded heat transfer from the fuel to the coolant (i.e. 0.5 kW/m^2K) will probably result in sheath failure for a moderate power, high burnup fuel element during the first 10 seconds of a large break LOCA transient.

APPENDIX I : ELOCA MK2 Fuel Behaviour Predictions

Case 124

The initial element linear power is 30 kW/m at a burnup of 170 MWh/kgU. The element internal gas pressure is 0.6 MPa. The initial centre, average and surface fuel temperatures are 1129K, 851K and 600K respectively. Therefore, from Figure 22 the initial centre, average and surface fuel enthalpies are 310, 225 and 150 J/g of UO_2 respectively.

The fuel element experiences power transient 'C' with a peak overpower factor of 10.0 at 1.3 seconds and an adiabatic heat addition of 305 J/g of UO_2 for a 30 kW/m element. The coolant boundary conditions are those of heat removal transient '3' with a constant sheath-to-coolant heat transfer coefficient of 0.5 kW/m^2K starting at 0.1 seconds and a peak coolant temperature of 1050K at 5.0 seconds.

The maximum centre, average and surface fuel temperatures are 1718K, 1542K and 1406K respectively. Therefore, the transient results in an increase in the centre, average and surface fuel temperatures of 589K, 691K and 806K respectively. This corresponds to an increase in centre, average and surface fuel enthalpies of 195, 225 and 255 J/g of UO_2 respectively. The sheath temperature increases to 1403K by 7.1 seconds. The centre and average fuel temperatures peak relatively early in the transient at approximately 2 seconds. The surface fuel temperature peaks later at 7.1 seconds .

The internal element gas pressure reaches a maximum of 1.2 MPa at 2.0 seconds. Fuel temperatures are not high enough to result in transient gas release which would further increase the maximum internal gas pressure. The sheath is predicted not to lift off the fuel. The total sheath strain reaches a maximum of 0.46% at 2.0 seconds. The ZrO_2 layer reaches a maximum thickness of 16.7 microns at 10 seconds. These conditions are not expected to result in sheath failure. The extent of oxidation is not great enough to significantly affect sheath deformation. The sheath temperature is high enough for the Zr/UO_2 interaction to occur on the inner sheath surface.

An increase in average fuel enthalpy from 370 to 450 J/g of UO_2 for conditions of degraded heat transfer from the fuel to the coolant (i.e. 0.5 kW/m^2K) will probably not result in sheath failure for a low power, high burnup fuel element during the first 10 seconds of a large break LOCA transient.

APPENDIX I : ELOCA MK2 Fuel Behaviour Predictions

Case 125

The initial element linear power is 55 kW/m at a burnup of 170 MWh/kgU. The element internal gas pressure is 7.3 MPa. The initial centre, average and surface fuel temperatures are 2026K, 1304K and 721K respectively. Therefore, from Figure 22 the initial centre, average and surface fuel enthalpies are 630, 370 and 185 J/g of UO_2 respectively.

The fuel element experiences power transient 'E' with a peak overpower factor of 10.0 at 1.3 seconds and an adiabatic heat addition of 946 J/g of UO_2 for a 55 kW/m element. The coolant boundary conditions are those of heat removal transient '1' with a constant sheath-to-coolant heat transfer coefficient of 50.0 kW/m^2K and a constant coolant temperature of 550K throughout the transient.

The maximum centre, average and surface fuel temperatures are 3113K, 2440K and 1040K respectively. Therefore, the transient results in an increase in the centre, average and surface fuel temperatures of 1087K, 1136K and 319K respectively. This corresponds to an increase in centre, average and surface fuel enthalpies of 570, 425 and 100 J/g of UO_2 respectively. The sheath temperature increases to 694K by 1.9 seconds. The centre, average and surface fuel temperatures peak relatively early in the transient by approximately 3 seconds.

The internal element gas pressure reaches a maximum of 14.5 MPa at 1.8 seconds. The fuel temperatures are high enough to result in transient gas release which could further increase the maximum internal gas pressure. The sheath is predicted to lift off the fuel at about 6.7 seconds. However, by 3.1 seconds 1.91% athermal strain has occurred. Therefore, non-ductile, PCI-type sheath failure could occur at this time. The total sheath strain reaches a maximum of 2.58% at 3.4 seconds. The ZrO_2 layer does not grow during the transient. Therefore, oxidation does not affect sheath deformation. The sheath temperature is not high enough for the Zr/UO_2 interaction to occur on the inner sheath surface.

An increase in average fuel enthalpy from 370 to 795 J/g of UO_2 for conditions of good heat transfer from the fuel to the coolant (i.e. 50.0 kW/m^2K) could result in non-ductile, PCI-type sheath failure for a high power, high burnup fuel element during the first 10 seconds of a large break LOCA transient.

APPENDIX I : ELOCA MK2 Fuel Behaviour Predictions

Case 126

The initial element linear power is 50 kW/m at a burnup of 170 MWh/kgU. The element internal gas pressure is 3.5 MPa. The initial centre, average and surface fuel temperatures are 1811K, 1192K and 688K respectively. Therefore, from Figure 22 the initial centre, average and surface fuel enthalpies are 540, 340 and 180 J/g of UO_2 respectively.

The fuel element experiences power transient 'E' with a peak overpower factor of 10.0 at 1.3 seconds and an adiabatic heat addition of 860 J/g of UO_2 for a 50 kW/m element. The coolant boundary conditions are those of heat removal transient '1' with a constant sheath-to-coolant heat transfer coefficient of 50.0 kW/m^2K and a constant coolant temperature of 550K throughout the transient.

The maximum centre, average and surface fuel temperatures are 2996K, 2272K and 967K respectively. Therefore, the transient results in an increase in the centre, average and surface fuel temperatures of 1185K, 1080K and 279K respectively. This corresponds to an increase in centre, average and surface fuel enthalpies of 570, 380 and 85 J/g of UO_2 respectively. The sheath temperature increases to 684K by 2.0 seconds. The centre, average and surface fuel temperatures peak relatively early in the transient at 3.9, 2.9 and 2.1 seconds respectively.

The internal element gas pressure reaches a maximum of 7.4 MPa at 2.1 seconds. The central fuel temperature is high enough to result in transient gas release which could further increase the maximum internal gas pressure. The sheath is predicted to lift off the fuel at about 5.7 seconds. However, by 3.0 seconds 1.46% athermal strain has occurred. Therefore, non-ductile, PCI-type sheath failure could occur at this time. The total sheath strain reaches a maximum of 2.25% at 3.2 seconds. The ZrO_2 layer does not grow during the transient. The extent of oxidation is not great enough to significantly affect sheath deformation. The sheath temperature is not high enough for the Zr/UO_2 interaction to occur on the inner sheath surface.

An increase in average fuel enthalpy from 340 to 720 J/g of UO_2 for conditions of good heat transfer from the fuel to the coolant (i.e. 50.0 kW/m^2K) could result in non-ductile, PCI-type sheath failure for a moderate power, high burnup fuel element during the first 10 seconds of a large break LOCA transient.

APPENDIX I : ELOCA MK2 Fuel Behaviour Predictions

Case 127

The initial element linear power is 30 kW/m at a burnup of 170 MWh/kgU. The element internal gas pressure is 0.6 MPa. The initial centre, average and surface fuel temperatures are 1129K, 851K and 600K respectively. Therefore, from Figure 22 the initial centre, average and surface fuel enthalpies are 310, 225 and 150 J/g of UO_2 respectively.

The fuel element experiences power transient 'E' with a peak overpower factor of 10.0 at 1.3 seconds and an adiabatic heat addition of 516 J/g of UO_2 for a 30 kW/m element. The coolant boundary conditions are those of heat removal transient '1' with a constant sheath-to-coolant heat transfer coefficient of 50.0 kW/m^2K and a constant coolant temperature of 550K throughout the transient.

The maximum centre, average and surface fuel temperatures are 2154K, 1554K and 724K respectively. Therefore, the transient results in an increase in the centre, average and surface fuel temperatures of 1025K, 703K and 124K respectively. This corresponds to an increase in centre, average and surface fuel enthalpies of 360, 230 and 40 J/g of UO_2 respectively. The sheath temperature increases to 644K by 2.0 seconds. The centre, average and surface fuel temperatures peak relatively early in the transient at 3.9, 2.9 and 2.0 seconds respectively.

The internal element gas pressure reaches a maximum of 1.3 MPa at 2.5 seconds. The fuel temperatures are is not high enough to result in transient gas release which could further increase the maximum internal gas pressure. The fuel is predicted to thermally contract away from the fuel at 6.7 seconds. However, by 2.8 seconds 0.40% athermal strain has occurred. Therefore, non-ductile, PCI-type sheath failure could occur at this time. The total sheath strain reaches a maximum of 0.75% at 3.2 seconds. The ZrO_2 layer does not grow during the transient. The extent of oxidation is not great enough to significantly affect sheath deformation. The sheath temperature is not high enough for the Zr/UO_2 interaction to occur on the inner sheath surface.

An increase in average fuel enthalpy from 340 to 455 J/g of UO_2 for conditions of good heat transfer from the fuel to the coolant (i.e. 50.0 kW/m^2K) could result in non-ductile, PCI-type sheath failure for a low power, high burnup fuel element during the first 10 seconds of a large break LOCA transient.

APPENDIX I : ELOCA MK2 Fuel Behaviour Predictions

Case 128

The initial element linear power is 55 kW/m at a burnup of 170 MWh/kgU. The element internal gas pressure is 7.3 MPa. The initial centre, average and surface fuel temperatures are 2026K, 1304K and 721K respectively. Therefore, from Figure 22 the initial centre, average and surface fuel enthalpies are 630, 370 and 185 J/g of UO_2 respectively.

The fuel element experiences power transient 'E' with a peak overpower factor of 10.0 at 1.3 seconds and an adiabatic heat addition of 946 J/g of UO_2 for a 55 kW/m element. The coolant boundary conditions are those of heat removal transient '5' with a constant sheath-to-coolant heat transfer coefficient of 1.5 kW/m^2K starting at 0.1 seconds and a peak coolant temperature of 1050K at 5.0 seconds.

The maximum centre, average and surface fuel temperatures are 3113K, 2918K and 2554K respectively. Therefore, the transient results in an increase in the centre, average and surface fuel temperatures of 1087K, 1614K and 1833K respectively. This corresponds to an increase in centre, average and surface fuel enthalpies of 570, 690 and 660 J/g of UO_2 respectively. The sheath temperature increases to 1744K by 5.1 seconds. The centre, average and surface fuel temperatures peak relatively early in the transient at approximately 4 seconds.

The internal element gas pressure reaches a maximum of 10.6 MPa at 1.1 seconds. Fuel temperatures are high enough to result in a large amount transient gas release which would further increase the maximum internal gas pressure and possibly cause fuel swelling. The sheath is predicted to lift off the fuel at about 1.1 seconds. The total sheath strain reaches a maximum of 4.19% at 7.7 seconds. The ZrO_2 layer reaches a maximum thickness of 46.0 microns at 10^{-2} seconds. These conditions will probably result in sheath failure due to localised overstrain beneath an oxide crack. The extent of oxidation is great enough to significantly affect sheath deformation. The sheath temperature is high enough for the Zr/UO_2 interaction to occur on the inner sheath surface. However, fuel/sheath contact is light and localised after sheath lift-off and the extent of the Zr/UO_2 interaction will probably be negligible.

An increase in average fuel enthalpy from 370 to 1060 J/g of UO_2 for conditions of moderate heat transfer from the fuel to the coolant (i.e. 1.5 kW/m^2K) will probably result in sheath failure for a high power, high burnup fuel element during the first 10 seconds of a large break LOCA transient.

APPENDIX I : ELOCA MK2 Fuel Behaviour Predictions

Case 129

The initial element linear power is 50 kW/m at a burnup of 170 MWh/kgU. The element internal gas pressure is 3.5 MPa. The initial centre, average and surface fuel temperatures are 1811K, 1192K and 688K respectively. Therefore, from Figure 22 the initial centre, average and surface fuel enthalpies are 540, 340 and 180 J/g of UO_2 respectively.

The fuel element experiences power transient 'E' with a peak overpower factor of 10.0 at 1.3 seconds and an adiabatic heat addition of 360 J/g of UO_2 for a 50 kW/m element. The coolant boundary conditions are those of heat removal transient '5' with a constant sheath-to-coolant heat transfer coefficient of 1.5 kW/m^2K starting at 0.1 seconds and a peak coolant temperature of 1050K at 5.0 seconds.

The maximum centre, average and surface fuel temperatures are 2944K, 2651K and 2182K respectively. Therefore, the transient results in an increase in the centre, average and surface fuel temperatures of 1133K, 1459K and 1494K respectively. This corresponds to an increase in centre, average and surface fuel enthalpies of 530, 560 and 500 J/g of UO_2 respectively. The sheath temperature increases to 2015K[2] by 2.9 seconds. The centre, average and surface fuel temperatures are also at their maximums at this time which is when the ELOCA MK2 calculation terminates.

The internal element gas pressure reaches a maximum of 8.9 MPa at 2.2 seconds. Fuel temperatures are high enough to result in transient gas release which would further increase the maximum internal gas pressure. The sheath is predicted to lift off the fuel at about 2.2 seconds. The total sheath strain reaches a maximum of 2.74% at 2.9 seconds. The ZrO_2 layer reaches a maximum thickness of 40.6 microns at 2.9 seconds. These conditions will probably result in sheath failure due to localised melting or overstrain beneath an oxide crack. The extent of oxidation is great enough to significantly affect sheath deformation. The sheath temperature is high enough for the Zr/UO_2 interaction to occur on the inner sheath surface.

An increase in average fuel enthalpy from 340 to 900 J/g of UO_2 for conditions of moderate heat transfer from the fuel to the coolant (i.e. 1.5 kW/m^2K) will probably result in sheath failure for a moderate power, high burnup fuel element during the first 10 seconds of a large break LOCA transient.

APPENDIX I : ELOCA MK2 Fuel Behaviour Predictions

Case 130

The initial element linear power is 30 kW/m at a burnup of 170 MWh/kgU. The element internal gas pressure is 0.6 MPa. The initial centre, average and surface fuel temperatures are 1129K, 851K and 600K respectively. Therefore, from Figure 22 the initial centre, average and surface fuel enthalpies are 310, 225 and 150 J/g of UO_2 respectively.

The fuel element experiences power transient 'E' with a peak overpower factor of 10.0 at 1.3 seconds and an adiabatic heat addition of 516 J/g of UO_2 for a 30 kW/m element. The coolant boundary conditions are those of heat removal transient '5' with a constant sheath-to-coolant heat transfer coefficient of 1.5 kW/m^2K starting at 0.1 seconds and a peak coolant temperature of 1050K at 5.0 seconds.

The maximum centre, average and surface fuel temperatures are 2175K, 1923K and 1525K respectively. Therefore, the transient results in an increase in the centre, average and surface fuel temperatures of 1046K, 1072K and 925K respectively. This corresponds to an increase in centre, average and surface fuel enthalpies of 365, 350 and 295 J/g of UO_2 respectively. The sheath temperature increases to 1517K by 3.4 seconds. The centre, average and surface fuel temperatures peak at 4.5, 3.5 and 3.4 seconds respectively.

The internal element gas pressure reaches a maximum of 1.6 MPa at 3.4 seconds. Fuel temperatures are not high enough to result in transient gas release which would further increase the maximum internal gas pressure. The sheath is predicted not to lift off the fuel. The total sheath strain reaches a maximum of 1.21% at 3.7 seconds. The ZrO_2 layer reaches a maximum thickness of 21.2 microns at 10 seconds. These conditions will probably not result in sheath failure. The extent of oxidation maybe great enough to significantly affect sheath deformation. The sheath temperature is high enough for the Zr/UO_2 interaction to occur on the inner sheath surface.

An increase in average fuel enthalpy from 340 to 575 J/g of UO_2 for conditions of moderate heat transfer from the fuel to the coolant (i.e. 1.5 kW/m^2K) will probably not result in sheath failure for a moderate power, high burnup fuel element during the first 10 seconds of a large break LOCA transient. The sheath may be embrittled and fail upon rewet.